

Effects of Riociguat and Sildenafil in a  
murine model of chronic right ventricular  
pressure overload

Inaugural Dissertation  
submitted to the  
Faculty of Medicine  
in partial fulfillment of the requirements  
for the PhD-Degree  
of the Faculties of Veterinary Medicine and Medicine  
of the Justus Liebig University Giessen

by  
Schymura, Yves  
of  
Frankfurt am Main

Giessen (2012)

From the Max-Planck-Institute of Heart and Lung Research

Director / Chairman: Prof. Dr. Stefan Offermanns

First Supervisor and Committee Member: Prof. Dr. Ralph T. Schermuly

Second Supervisor and Committee Member: Prof. Dr. Siebert

Committee Members: Prof. Dr. Dr. Gerald Reiner

Prof. Dr. Ralf Middendorff

Prof. Dr. Michaela Kuhn

Date of Doctoral Defense: 2013/02/07

# Abstract

Right heart failure is a prevalent mechanism of cardiovascular collapse and distinctly different from left heart failure. Conventionally, afterload reduction has been the main focus to treat right ventricular (RV) dysfunction, but it cannot be achieved in many cases. A new strategy is to directly target RV remodelling. Pulmonary artery banding (PAB) in mice is used to induce a chronic pressure overload on the RV, without any changes in the pulmonary vasculature.

This work addressed two questions: a) the time-course of effects of PAB on right- and left-ventricular (LV) hypertrophy and function, assessed non-invasively via magnetic resonance imaging (MRI). b) Stimulation of the nitric oxide pathway was shown to ameliorate maladaptive changes in murine models of chronic LV pressure overload. Therefore, the effects of the sGC stimulator Riociguat and the PDE5 inhibitor Sildenafil on RV function and fibrosis were investigated.

Chronic RV pressure overload was induced by PAB in male C57Bl/6 wild-type mice. For the time-course study, 1, 3, 7, 14, 28, 56 and 105 days after PAB, the functional and morphological consequences of sustained pressure overload on the RV and LV were assessed non-invasively using MRI. Additionally, the time-course of the effects of PAB on cardiomyocyte size and fibrosis was investigated.

For the pharmacological intervention study, drug treatment was started seven days after surgery for 2 weeks. Animals received either 30 mg/kg/d Riociguat per os, Sildenafil 100 mg/kg/d per drinking water, or placebo. The consequences of the sustained pressure overload on RV fibrosis, cardiomyocyte size and function were assessed using Picrosirius red staining, WGA-FITC staining and Magnetic Resonance Imaging.

PAB led to RV dilatation, indicated by an increase in end-diastolic volume. RV mass, cardiomyocyte size, as well as the collagen content of the RV increased in banded animals. The ejection fraction and the stroke volume (SV) of the RV decreased, as well as the LV SV and the cardiac output (CO). Whilst RV mass increased continually over the time-course of the study, the RV performance declined initially, followed by a weak compensatory phase. In the course of the study, the heart continued to decompensate, which finally resulted in heart failure of the animals.

Treatment with both Riociguat and Sildenafil led to significant improvements in RV ejection fraction ( $35.4 \pm 1.7\%$  vs.  $43.7 \pm 2.2\%$  vs.  $48.2 \pm 3.3\%$  [Placebo vs. Riociguat vs. Sildenafil]), but only Riociguat significantly reduced the collagen content of the RV ( $5.6 \pm 0.3\%$  vs.  $3.0 \pm 0.8\%$  vs.  $5.4 \pm 0.2\%$ ). Neither drug had effects on RV hypertrophy ( $62.3 \pm 3.1$  mg vs.  $59.6 \pm 2.5$  mg vs.  $57.1 \pm 2.2$  mg), on the RV/(LV+S) ratio ( $0.84 \pm 0.04$  mg/mg vs.  $0.91 \pm 0.04$  mg/mg vs.  $0.83 \pm 0.03$  mg/mg), nor on cardiomyocyte size ( $20.7 \pm 0.6$   $\mu$ m vs.  $19.8 \pm 0.3$   $\mu$ m vs.  $19.7 \pm 0.6$   $\mu$ m).

It was shown, that chronic pressure overload in C57Bl/6 mice induced RV dilatation, hypertrophy and contractile dysfunction. Furthermore, LV performance was negatively affected by intraventricular interaction, resulting in decreased LV SV and CO. Riociguat and Sildenafil both led to significant improvements in RV function, without any changes in RV mass or cardiomyocyte size. One reason for the functional improvement of the RV under Riociguat treatment is the decrease in collagen content, making the RV more apt to deal with the pressure overload. Further experiments will be needed to determine the mechanism of the functional improvement with Sildenafil treatment, and the reason for the differential effects of the drugs.

# Zusammenfassung

Rechtsherzversagen ist ein vorherrschender Mechanismus des kardiovaskulären Kollapses und unterscheidet sich deutlich vom Linksherzversagen. Die konventionelle Methode, um rechtsventrikuläre (RV) Dysfunktion zu behandeln, ist eine Reduktion der Nachlast. Dies ist jedoch in vielen Fällen nicht möglich. Eine neue Strategie stellt die Behandlung der RV Hypertrophie dar. Pulmonal-arterielles Banding (PAB) in Mäusen wird verwendet, um RV Hypertrophie auszulösen, ohne eine Veränderung des pulmonalen Gefäßsystems zu induzieren.

In dieser Arbeit wurden zwei Fragestellungen behandelt: a) der zeitliche Verlauf der Effekte des PAB auf die rechts- und linksventrikuläre (LV) Hypertrophie und Funktion mittels Magnetresonanztomographie (MRT) zu untersuchen. b) Es wurde gezeigt, dass der Stickstoffmonoxid (NO)-Signalweg an der Entwicklung der LV Hypertrophie entscheidend beteiligt ist. Daher wurden die Effekte des löslichen Guanylatzyklase-Stimulators (sGC-Stimulator) Riociguat, sowie des Phosphodiesterase 5-Hemmers Sildenafil, auf die RV Hypertrophie und Funktion untersucht.

Bei C57Bl6-Mäusen wurde eine chronische Druckbelastung für den rechten Ventrikel durch eine PAB-Operation erzeugt. Für die Langzeitstudie wurden die Folgen der anhaltenden Drucküberlastung auf RV und LV Morphologie und Funktion 1, 3, 7, 14, 28, 56 und 105 Tage nach der PAB-Operation nicht-invasiv mit MRT untersucht. Zusätzlich wurden der zeitliche Verlauf der Effekte des PAB auf die Kardiomyozytengröße, sowie den Grad der Fibrosierung untersucht.

In der pharmakologischen Interventionsstudie, wurde die Behandlung mit Riociguat (30 mg/kg/d p.o.), resp. Sildenafil (100 mg/kg/d p.o.), 7 Tage nach der Operation für eine Dauer von 14 Tagen durchgeführt. Nach 21 Tagen wurden die Auswirkungen einer dauerhaften Druckbelastung auf die RV Morphologie und Funktion unter Verwendung von Magnetresonanztomographie untersucht. Desweiteren wurde der Grad der Fibrosierung, sowie die Kardiomyozytengröße durch eine histologische Untersuchung analysiert.

PAB-operierte Mäuse zeigten etliche Merkmale der RV Dysfunktion. PAB führte zu RV Dilatation verglichen mit Sham-operierten Tieren, gemessen als eine Zunahme des end-diastolischen Volumens. Sowohl RV Masse als auch Kardiomyozytengröße

und Fibrosierungsgrad nahmen in PAB-Mäusen zu. Die Ejektionsfraktion (EF) und das Schlagvolumen (SV) des RV nahmen ab. Das LV-SV und das Herzzeitvolumen nahmen ab. Während die RV Masse über den Versuchszeitraum zunahm, fiel die RV Leistung initial stark ab, woraufhin eine zunächst kompensatorische Phase folgte. Mit Fortschritt der Studie dekompensierte das Herz zusehends, was schlussendlich im Herzversagen der Tiere mündete.

Sowohl die Behandlung der Tiere mit Riociguat, als auch mit Sildenafil, führte zu signifikanten Verbesserungen der RV EF ( $35.4 \pm 1.7\%$  vs.  $43.7 \pm 2.2\%$  vs.  $48.2 \pm 3.3\%$  [Placebo vs. Riociguat vs. Sildenafil]), aber nur Riociguat reduzierte signifikant den Fibrosierungsgrad des RV ( $5.6 \pm 0.3\%$  vs.  $3.0 \pm 0.8\%$  vs.  $5.4 \pm 0.2\%$ ). Weder Riociguat, noch Sildenafil, hatten einen Effekt auf die RV Hypertrophie ( $62.3 \pm 3.1$  mg vs.  $59.6 \pm 2.5$  mg vs.  $57.1 \pm 2.2$  mg), auf den RV/(LV+S) Quotienten ( $0.84 \pm 0.04$  mg/mg vs.  $0.91 \pm 0.04$  mg/mg vs.  $0.83 \pm 0.03$  mg/mg), oder auf die Kardiomyozytengröße ( $20.7 \pm 0.6$   $\mu\text{m}$  vs.  $19.8 \pm 0.3$   $\mu\text{m}$  vs.  $19.7 \pm 0.6$   $\mu\text{m}$ ).

Es wurde gezeigt, dass die chronische Drucküberlastung in C57Bl/6 Wildtyp-Mäusen zu RV Dilatation, Hypertrophie und kontraktile Dysfunktion führt. Zusätzlich wurde die LV Leistung durch interventrikuläre Interaktion, d. h. durch eine Reduktion des LV Schlagvolumens und des Herzzeitvolumens, beeinträchtigt. Sowohl Riociguat als auch Sildenafil führten zu signifikanter Verbesserung der RV Funktion, ohne Veränderungen in der RV Masse oder Kardiomyozytengröße ausgelöst zu haben. Ein Grund für die funktionelle Verbesserung unter Riociguat-Behandlung könnte die Reduktion der RV Fibrosierung sein. Weitere Studien sollten durchgeführt werden, um den Mechanismus der funktionellen Verbesserung unter Sildenafil-Gabe, sowie die unterschiedlichen Effekte der Substanzen zu untersuchen.

# Contents

<b>1</b>	<b>Introduction</b>	<b>1</b>
1.1	The Right Ventricle . . . . .	2
1.1.1	History of Research . . . . .	2
1.1.2	Anatomy . . . . .	3
1.1.3	Physiology . . . . .	5
1.1.4	Differences Between the Left and the Right Ventricle . . . . .	6
1.1.5	Cor Pulmonale . . . . .	7
1.1.5.1	Etiology . . . . .	7
1.1.5.2	Pathophysiology . . . . .	9
1.1.5.3	Molecular Mechanisms of Pathological Right Ven- tricular Hypertrophy . . . . .	11
1.1.5.4	Epidemiology . . . . .	12
1.1.6	Reverse Remodeling as a Novel Treatment Strategy . . . . .	13
1.1.7	The Pulmonary Artery Banding (PAB) Model . . . . .	14
1.2	The Nitric Oxide Pathway . . . . .	15
1.2.1	Nitric Oxide . . . . .	16
1.2.2	Soluble Guanylyl Cyclase . . . . .	18
1.2.3	Cyclic Guanosine Monophosphate . . . . .	20
1.2.4	cGMP-dependent Protein Kinase . . . . .	21
1.2.5	Phosphodiesterases . . . . .	23
1.2.6	Riociguat . . . . .	26
1.2.6.1	Discovery . . . . .	26
1.2.6.2	Mechanism of Action . . . . .	26

1.2.7	Sildenafil . . . . .	27
1.2.7.1	Discovery . . . . .	27
1.2.7.2	Mechanism of Action . . . . .	27
1.3	Rationale . . . . .	28
<b>2</b>	<b>Materials and methods</b>	<b>29</b>
2.1	Materials . . . . .	29
2.1.1	Instruments . . . . .	29
2.1.2	Chemicals and reagents . . . . .	30
2.1.3	Mice . . . . .	31
2.2	Methods . . . . .	31
2.2.1	Study plans . . . . .	31
2.2.1.1	Staging study - MRI . . . . .	32
2.2.1.2	Staging study - Histology & Catheterization . . . . .	32
2.2.1.3	Treatment study . . . . .	32
2.2.2	Pulmonary artery banding . . . . .	33
2.2.3	Drug treatment . . . . .	34
2.2.3.1	Sildenafil . . . . .	34
2.2.3.2	Riociguat . . . . .	35
2.2.4	Magnetic Resonance Imaging . . . . .	35
2.2.5	Analysis of MRI images . . . . .	36
2.2.5.1	Calculation of derived parameters . . . . .	37
2.2.6	In vivo hemodynamics . . . . .	39
2.2.7	Tissue processing . . . . .	39
2.2.8	Histology . . . . .	40
2.2.8.1	Picrosirius red staining . . . . .	40
2.2.8.2	WGA-FITC staining . . . . .	41
2.2.9	Statistics . . . . .	43
<b>3</b>	<b>Results</b>	<b>44</b>
3.1	Staging Study . . . . .	44
3.1.1	Time Course of Function and Morphology of the Banded Heart	44

3.1.2	Right Ventricular Pressure . . . . .	45
3.1.3	Right Ventricular Dilatation and Impaired Function . . . . .	47
3.1.4	Right Ventricular Hypertrophy . . . . .	48
3.1.5	Functional Impairment of the Left Ventricle . . . . .	51
3.1.6	Systemic Arterial Pressure . . . . .	53
3.1.7	Heart Rate and Cardiac Output . . . . .	53
3.1.8	Survival . . . . .	55
3.1.9	Timecourse of Fibrosis in the Banded Heart . . . . .	55
3.1.10	Timecourse of Cardiomyocyte Size in the Banded Heart . . . . .	56
3.2	Riociguat and Sildenafil Study . . . . .	60
3.2.1	Right Ventricular Pressure . . . . .	63
3.2.2	Effects on Right Ventricular Volumes and Function . . . . .	63
3.2.3	Effects on Right Ventricular Hypertrophy . . . . .	68
3.2.4	Effects on the Left Heart . . . . .	68
3.2.5	Effects on the Systemic Arterial Pressure . . . . .	70
3.2.6	Effects on Right Ventricular Fibrosis . . . . .	72
3.2.7	Effects on Cardiomyocyte Size . . . . .	74
<b>4</b>	<b>Discussion</b>	<b>76</b>
4.1	Staging Study . . . . .	76
4.2	Treatment Study . . . . .	79
4.2.1	Riociguat . . . . .	82
4.2.2	Sildenafil . . . . .	84
4.3	Benefits and Limitations of the Methods . . . . .	86
4.3.1	Magnetic Resonance Imaging . . . . .	86
4.3.2	Pulmonary Artery Banding . . . . .	88
4.4	Clinical Relevance . . . . .	92
4.5	Further Experiments . . . . .	92
4.6	Conclusion . . . . .	93
<b>A</b>	<b>Tables</b>	<b>94</b>

<b>B Declaration</b>	<b>120</b>
<b>C Acknowledgements</b>	<b>121</b>
<b>D Curriculum vitae</b>	<b>122</b>

# List of Figures

1.1	Coronal section of the heart . . . . .	4
1.2	Heart fields . . . . .	6
1.3	The nitric oxide pathway . . . . .	15
2.1	Staging study - Study plan MRI . . . . .	32
2.2	Staging study - Study plan histology & catheterization; Cat. indicates catheterization; Histo., histology . . . . .	32
2.3	Treatment study - Study plan . . . . .	32
2.4	Weck Hemoclip® . . . . .	33
	(a) Size comparison . . . . .	33
	(b) Applied clip . . . . .	33
2.5	Sildenafil - Chemical structure . . . . .	34
2.6	Riociguat - Chemical structure . . . . .	35
2.7	The MRI and sample images . . . . .	36
	(a) Bruker Pharmascan . . . . .	36
	(b) Scout image in coronal plane . . . . .	36
	(c) End-systole . . . . .	36
	(d) End-diastole . . . . .	36
2.8	Calculation of the LV eccentricity index . . . . .	39
3.1	Mouse heart before/after PAB in coronal/axial plane . . . . .	45
3.2	Three-dimensional reconstruction of mouse heart before/after banding	46
3.3	Staging study - RV systolic pressure . . . . .	47
3.4	Staging study - RV end-diastolic volume + end-systolic volume . . . .	48
3.5	Staging study - RV stroke volume + ejection fraction . . . . .	49

3.6	Staging study - RV mass . . . . .	49
3.7	Staging study - RV/LV mass . . . . .	50
3.8	Staging study - LV mass . . . . .	50
3.9	Staging study - LV end-diastolic volume + end-systolic volume . . . . .	51
3.10	Staging study - LV stroke volume + ejection fraction . . . . .	52
3.11	Staging study - LV eccentricity index . . . . .	53
3.12	Staging study - Systolic blood pressure . . . . .	54
3.13	Staging study - Heart rate . . . . .	54
3.14	Staging study - Cardiac output . . . . .	55
3.15	Staging study - Survival curve . . . . .	56
3.16	Staging study - Fibrosis (Graph) . . . . .	57
3.17	Staging study - Fibrosis (Images) . . . . .	58
3.18	Staging study - Cardiomyocyte size (Graph) . . . . .	60
3.19	Staging study - Cardiomyocyte size (Images) . . . . .	61
3.20	Treatment study - RV systolic pressure . . . . .	63
3.21	Treatment study - RV end-diastolic volume . . . . .	64
3.22	Treatment study - RV end-systolic volume . . . . .	65
3.23	Treatment study - RV stroke volume . . . . .	66
3.24	Treatment study - RV ejection fraction . . . . .	66
3.25	Treatment study - Heartrate . . . . .	67
3.26	Treatment study - Cardiac Output . . . . .	68
3.27	Treatment study - RV mass . . . . .	69
3.28	Treatment study - LV stroke volume . . . . .	69
3.29	Treatment study - LV mass . . . . .	70
3.30	Treatment study - Systolic blood pressure . . . . .	71
3.31	Treatment study - Fibrosis (Graph) . . . . .	72
3.32	Treatment study - Fibrosis (Images) . . . . .	73
	(a) Sham . . . . .	73
	(b) PAB + Placebo . . . . .	73
	(c) PAB + Sildenafil . . . . .	73
	(d) PAB + Riociguat . . . . .	73

3.33 Treatment study - Cardiomyocyte size (Graph) . . . . .	74
3.34 Treatment study - Cardiomyocyte size (Images) . . . . .	75
(a) Sham . . . . .	75
(b) PAB + Placebo . . . . .	75
(c) PAB + Sildenafil . . . . .	75
(d) PAB + Riociguat . . . . .	75

# List of Tables

1.1	NO studies . . . . .	18
1.2	sGC studies . . . . .	20
1.3	cGMP studies . . . . .	21
1.4	cGK studies . . . . .	22
1.5	PDE studies . . . . .	25
2.1	Instruments . . . . .	29
2.2	Chemicals and reagents . . . . .	30
2.3	Picrosirius red staining protocol . . . . .	41
2.4	WGA-FITC staining . . . . .	42
A.1	Staging Study - Results (MRI) . . . . .	95
A.2	Staging Study - Results (Harvest) . . . . .	97
A.3	Treatment Study -Results . . . . .	97

# Abbreviations

---

<b>Abbreviation</b>	<b>Explanation</b>
BP	Blood pressure
BSA	Bovine serum albumin
cGMP	Cyclic Guanosine Monophosphate
CO	Cardiac output
COPD	Chronic Obstructive Pulmonary Disease
dH <sub>2</sub> O	deionized H <sub>2</sub> O
DAPI	4',6-diamidino-2-phenylindole
ED	End-diastole
EDV	End-diastolic volume
EF	Ejection fraction
ES	End-systole
ESV	End-systolic volume
FITC	Fluorescein isothiocyanate
FLASH	Fast-low-angle-shot
FOV	Field of view
i.p.	Intraperitoneal
K <sub>m</sub>	The Michaelis constant
LV	Left ventricle
LVP <sub>sys</sub>	Left ventricular systolic pressure
MCT	Monocrotalin
MRI	Magnetic resonance imaging

---

Continued on next page

Table 1 – continued from previous page

---

<b>Abbreviation</b>	<b>Explanation</b>
MW	Molecular weight
N/A	Not applicable
NO	Nitric oxide
p.o.	Per os
PAB	Pulmonary Artery Banding
PDE	Phosphodiesterase
PFA	Paraformaldehyde
RV	Right ventricle
RVP <sub>sys</sub>	Right ventricular systolic pressure
s.c.	Subcutaneous
SEM	Standard error of the mean
sGC	Soluble Guanylyl Cyclase
SNAP	S-Nitroso-N-acetylpenicillamine
SV	Stroke volume
T	Tesla
TAC	Transverse aortic constriction
V <sub>max</sub>	Maximum reaction rate

---

# Chapter 1

## Introduction

This dissertation is about the role of the nitric oxide (NO) pathway in right ventricular hypertrophy. The introduction is split into two main sections; one about the right ventricle, and one about the NO pathway. I will begin the first section by giving a short outline on why the right ventricle has not been in the centre of research interest so far, followed by a description of the right ventricle's anatomy and physiology, and why we cannot simply translate research findings made in the left ventricle to the right ventricle. Hereafter, I will provide a description of the main form of pathological remodeling of the right ventricle, cor pulmonale, its etiology and pathophysiology, and the importance of finding new treatments. This section will be concluded by a brief description of the pulmonary artery banding (PAB) model, which is a murine model of chronic right ventricular pressure-overload. The next section will deal with the nitric oxide pathway, describing its main constituents, as well as the research that has been done on them so far in the context of cardiac hypertrophy. The introduction will be concluded by a brief description of the history and mechanism of action of riociguat and sildenafil, and a rationale summarizing the purpose of this dissertation.

## 1.1 The Right Ventricle

### 1.1.1 History of Research

Even though William Harvey already in the 16th century experimentally demonstrated that blood flows from the right ventricle to the left ventricle via the lungs,<sup>1</sup> the right ventricle has in the past been scientifically under-investigated because of numerous reasons: it is less muscular than the left ventricle, it is pumping blood only through a single organ and it has been less obviously involved in cardiac diseases of epidemic proportions like myocardial ischemia and cardiomyopathy.<sup>2</sup> Furthermore, in the 1940s studies were carried out in open-pericardium dog models, which showed that virtually complete ablation of the right ventricular free wall hardly decreased cardiac output nor systemic venous pressure and did not result in venous congestion, whilst damage to the left ventricle led to significant changes in pressure and lethal cardiogenic shock.<sup>3-5</sup> It was then suggested that a functional left ventricle is sufficient for pumping blood, and that it is able to transfer its mechanical energy to the right ventricle via the interventricular septum.<sup>3,4</sup>

Additionally, surgical treatments of congenital heart diseases, like tricuspid and pulmonary atresia, were developed which tried to completely circumvent the right heart, of which the best known became the Fontan/Kreutzer procedure.<sup>6,7</sup> In this procedure the right ventricle is bypassed and patients were shown to survive without a functional right ventricle, further questioning the role the right ventricle plays in circulation.<sup>6,8</sup> In 1975 these findings culminated in the proposition of the "dispensable right ventricle",<sup>9</sup> and scientific interest of the workings of the right ventricle in health and disease ceased.

This position was challenged in the mid 1980s by "the essential function of the right ventricle".<sup>10</sup> Furey provided evidence that the essential role of the right ventricle is not to pump blood through the pulmonary circulation, but rather to provide capacitance to the pulmonary circulation to maintain a low pressure, preventing the development of venous distention and peripheral edema.<sup>10</sup>

A final change of thinking occurred after it was shown that isolated right ventricular infarcts negatively affected its hemodynamics,<sup>11</sup> that right ventricular contractile

dysfunction is associated with increased morbidity and mortality in diseases of the left heart, and that right ventricular parameters can be a better prognostic marker than left ventricular readouts.<sup>12,13</sup> This was further corroborated with evidence that right ventricular infarction is an independent predictor of morbidity and mortality in inferior myocardial infarction:<sup>14</sup> in patients with right ventricular infarction, additional to left ventricular infarction, incident mortality increased from 5% to 31% and complications increased from 28% to 64%. The prognostic value of the right ventricle in inferior myocardial infarction was later confirmed in a meta-analysis, which showed that right ventricular dysfunction led to significant increases in mortality, morbidity and serious complications.<sup>15</sup>

Eventually in 2006 the National Heart, Lung and Blood Institute (NHLBI, Bethesda, US) concluded, that right heart failure is distinctly different from left heart failure, and that it is a prevalent mechanism of cardiovascular collapse.<sup>2</sup>

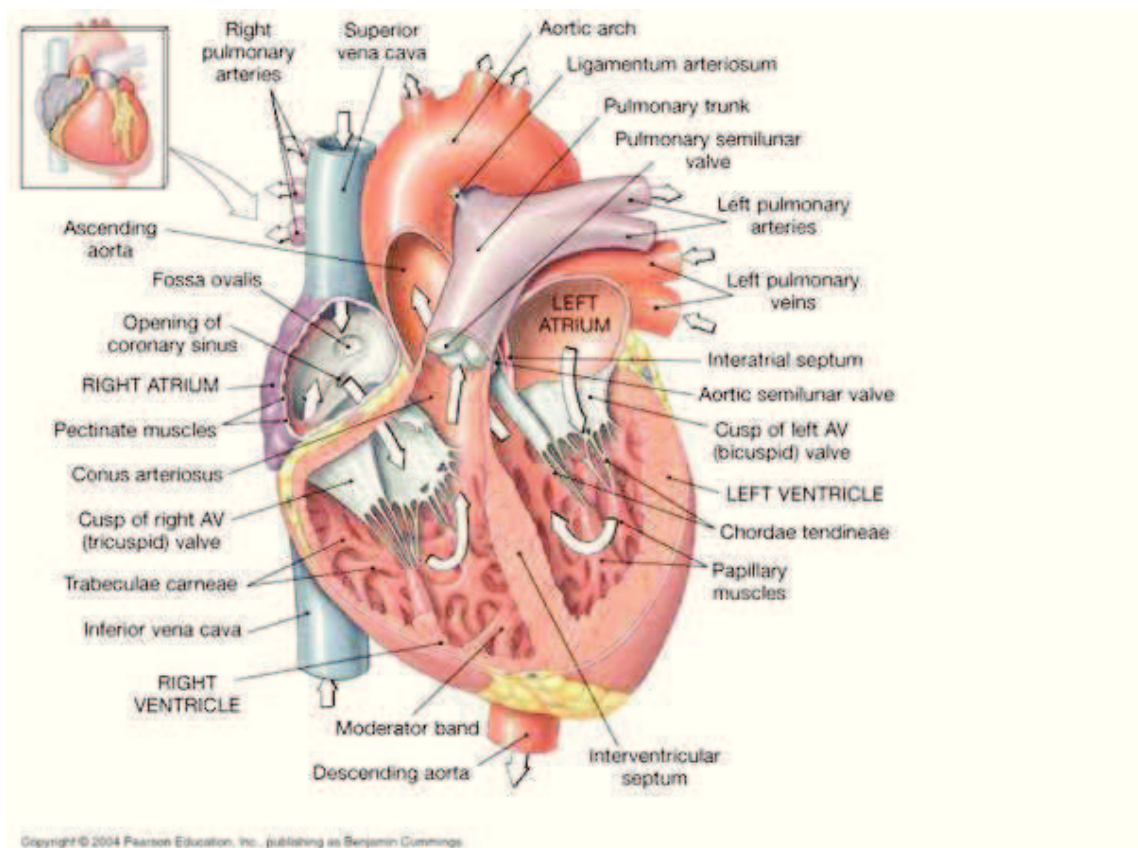
### 1.1.2 Anatomy

The primary role of the right heart is to accept deoxygenated blood from the systemic circulation via the inferior and superior vena cava, and to pump it through the pulmonary circulation for gas exchange.<sup>16</sup> It consists of the right atrium and the right ventricle.

The right ventricle has a complex geometry and is comprised of two functionally and anatomically distinct cavities, which are separated by the crista supraventricularis: the sinus and the conus region (Fig. 1.1, p. 4).<sup>16</sup> The sinus region includes the trabeculated part of the ventricle and accepts the blood from the right atrium via the tricuspid valve.<sup>17</sup> The conus region is free of trabeculations and connects the right ventricle to the pulmonary circulation via the pulmonary valve.<sup>17</sup> The valves prevent regurgitation of blood back into the atrium (tricuspid valve) and into the ventricle (pulmonary valve).

The right heart is separated from the left heart by the septum and they are functionally linked by muscle bundles, allowing the ventricles to hemodynamically influence each other.<sup>18</sup> The left and right heart are surrounded by the pericardium. In the axial plane, the right ventricle appears crescently-shaped at the base and

triangularly-shaped at the apex, whilst it looks triangular from the side-view. This is in stark contrast to the left ventricle, which appears elliptically-shaped in cross-section, and also accounts for the higher compliance of the right ventricle.<sup>18</sup> Under physiological conditions the left ventricle protrudes into the right ventricle, i.e. the septum is shaped concave to the left ventricle. In humans, the volume of the right ventricle is marginally larger than that of the left ventricle (49-101 mL/m<sup>2</sup> vs. 44-89 mL/m<sup>2</sup>). As the stroke volumes of both ventricles are on average the same, the right ventricular ejection fraction is slightly lower than left ventricular ejection fraction.



Copyright © 2004 Pearson Education, Inc., publishing as Benjamin Cummings.

**Figure 1.1 – Coronal section of the heart.** The right atrium receives deoxygenated blood from the systemic circulation via the superior and inferior vena cava, which is then delivered through the tricuspid valve into the right ventricle. The blood is expelled from the right ventricle via the pulmonary artery into the pulmonary circulation for gas exchange. The oxygenated blood leaves the pulmonary circulation via the pulmonary veins into the left atrium, which passes the blood on to the left ventricle via the bicuspid valve. Finally, the blood is pumped out from the left ventricle through the aorta back into the systemic circulation. Copyright © 2004 Pearson Education, Inc., publishing as Benjamin Cummings.

The right ventricle is primarily perfused by the right coronary artery and partially perfused by the left coronary artery.<sup>19</sup> Perfusion takes place during both systole and diastole under physiological conditions; partial occlusion of the coronary arteries might occur under conditions of high afterload and increased filling pressures; this

can result in ischemia.<sup>19</sup>

### 1.1.3 Physiology

The right ventricle contracts by generating pressure in the sinus region with a peristaltic motion that starts at the apex and moves toward the conus.<sup>16</sup> Effectively, this leads to a decrease in the distance between the right ventricular free wall and the septum, and a reduction in the right ventricular free wall, propelling the blood forward.

On the cardiomyocyte level, force is generated by the interaction of actin and myosin, with the energy obtained from the conversion of adenosine triphosphate (ATP) to adenosine diphosphate (ADP). Each myosin heavy chain interacts with two myosin light chains, forming a hexameric structure.<sup>16</sup> The predominantly expressed myosin heavy chain isoform in ventricles is the  $\beta$  isoform, whilst the distinct myosin light chain isoforms are expressed differently in the left and right heart.<sup>16</sup> The localization of actin isoforms has not been well described yet.<sup>16</sup>

The right ventricle has only 1/6 of the mass of the left ventricle, and performs 1/4 of the cardiac stroke work of the left ventricle, making the right ventricle highly compliant.<sup>17,20</sup> This is the result of the right ventricular free wall being relatively thin-walled (1–3 mm) compared to the left ventricular free wall ( $\sim$ 10 mm), as it has to work against a much smaller resistance: the pulmonary circulation is a very compliant "low pressure system" (15–30 mmHg vs 100–140 mmHg [RV systolic pressure vs. LV systolic pressure]), due to the greater diameter and thinner walls of the pulmonary vessels.<sup>18</sup>

The high compliance of the right ventricle allows it to readily adapt to changes in volume, but not to changes in pressure, as its role is to work under low pressure conditions.<sup>19</sup> Therefore volume overload conditions, as in atrial septal defects or with tricuspid regurgitation, can be tolerated for a long time before pumping is impaired. This is in stark contrast to pressure overload conditions, as they often occur in constrictive pulmonary disorders, which can lead to rapid right ventricular functional deterioration.<sup>21</sup>

### 1.1.4 Differences Between the Left and the Right Ventricle

The left and right ventricle differ not only in structure and loading conditions (see above), but also display different cell signaling and calcium handling.<sup>22</sup> These differences have their origins in development, as the right and left ventricle originate from different progenitor cells which are located in different heart fields (Fig. 1.2, p. 6).<sup>16</sup> Whilst the primary heart field gives rise to the atrial chambers and the left ventricle, the secondary heart field gives rise to the right ventricle and its outflow tract.<sup>16</sup> The primary and secondary heart field cells can be discriminated by their differential expression of transcription factors: whilst the cells of the primary heart field express the T-box transcription factor *Tbx5* and the basic helix-loop-helix transcription factor *Hand1*, cells of the secondary heart field express *Hand2*, the LIM-homeodomain transcription factor *Islet-1 (Isl1)* and Fibroblast growth factor 10 (*Fgf10*).<sup>16</sup> Studies with knock-out mice which lacked either *Hand1* or *Hand2* led to recognition of this chamber-specific gene expression, as genetic ablation of one of these transcription factors resulted in impaired right, respectively left, ventricular development.<sup>23</sup>

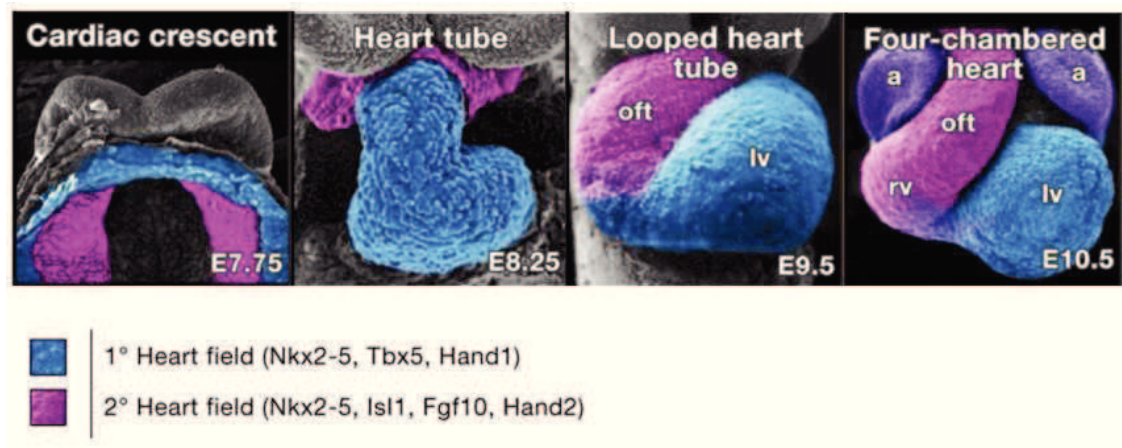


**Figure 1.2 – The heart forms from two heart fields.** Scanning electron micrographs of representative stages of murine heart development. Derivatives of the primary and secondary heart field are depicted in color. a indicates, atrium; lv, left ventricle; oft, outflow tract; rv, right ventricle. Adapted from Garry et al., 2006<sup>24</sup>

These inherent differences between the right and left ventricle allow for the possibility that drugs which can successfully treat disorders in one ventricle, do not necessarily exert the same effects in the other ventricle. A clinical example of this are patients with a systemic right ventricle, who respond worse to drugs which are

used to treat left ventricular dysfunction.<sup>21</sup> As an experimental example, treatment of the hypertrophied left ventricle with sildenafil was shown to a decrease hypertrophy,<sup>25</sup> whilst treatment of the hypertrophied right ventricle with sildenafil actually led to an increase in hypertrophy.<sup>26</sup> Whether these differences actually stem from inherent differences between the left and the right ventricle, their differing structural and loading conditions, the distinct animal models employed, or various drug treatment procedures, is so far unresolved.<sup>27</sup> Summing up, these differences do exist, and carefully designed experiments have to be carried out before conclusions about the efficacy of certain drugs in particular pathological cardiac conditions can be drawn.

### 1.1.5 Cor Pulmonale

Cor pulmonale stems from the Latin *cor* ("heart") and the new Latin *pulmōnāle* ("of the lungs"), and is synonymous with pulmonary heart disease. It was defined by a World Health Organization expert committee in 1963 as "hypertrophy of the right ventricle resulting from diseases affecting the function and/or structure of the lungs, except when these pulmonary alterations are the result of diseases that primarily affect the left side of the heart, as in congenital heart disease".<sup>28</sup> A current definition of chronic cor pulmonale is: "Right ventricular hypertrophy, dilation, or both as a result of pulmonary hypertension caused by pulmonary disorders involving the lung parenchyma, impaired pulmonary bellows function, or altered ventilatory drive".<sup>29</sup> Acute cor pulmonale, as in pulmonary embolism, usually results in dilatation, whereas chronic cor pulmonale, as in pulmonary hypertension, is the result of prolonged pressure overload, and leads to right ventricular hypertrophy. If left untreated, both conditions can eventually culminate in right heart failure and death.

#### 1.1.5.1 Etiology

**Pulmonary hypertension** Pulmonary hypertension (PH) is characterized by a progressively elevated mean pulmonary arterial pressure, which exceeds 25 mmHG at rest or 30 mmHg with exercise.<sup>30</sup> It can be further divided into mild (25–35 mmHg), moderate (35–45 mmHg) and severe (> 45 mmHg) pulmonary hypertension, of which the severe ones are more likely to be pulmonary arterial hypertension and chronic

thromboembolic disease.<sup>18</sup> Pulmonary hypertension was classified by the WHO into 5 groups in 2003, and reclassified in 2009,<sup>31</sup> namely pulmonary arterial hypertension, pulmonary hypertension secondary to left heart disease, pulmonary disease, chronic thromboembolic disease, and miscellaneous causes.

**Group I: Pulmonary Arterial Hypertension (PAH)** Pulmonary arterial hypertension is caused by abnormalities in the pulmonary vasculatures anatomy or physiology. This usually results in mechanical obstruction to blood flow, which is resistant to vasodilator therapy. It includes idiopathic PAH (formerly called primary PH), heritable PAH, and PAH secondary to other conditions including congenital heart disease, connective tissue disease, portal hypertension, HIV infection, and drug or toxin exposure.

**Group II: Pulmonary Hypertension Owing to Left Heart Disease** The second group is PH caused by left heart disease. An impairment of the left ventricle to sufficiently eject blood eventually leads to a backlog of blood into the pulmonary circulation, with the resultant abnormally elevated pulmonary vein pressures being retrogradely transmitted to the right ventricle. Group II PH is very common. It is as yet unknown, to what extent right ventricular failure actually contributes to mortality and to what extent it simply is a marker of left ventricular dysfunction.

**Group III: Pulmonary Hypertension Owing to Lung Diseases and/or Hypoxia** Alterations in pre-capillary arterioles from the third group of PH, which is the by far most common form of PH and includes chronic obstructive pulmonary disorder (COPD). In COPD some areas of the lung are hypoventilated which stimulates the pulmonary vasoconstrictor reflex, effectively increasing pulmonary vascular resistance.<sup>19</sup> These diseases can often be treated with vasodilators, but the severity of the disease may increase and become permanent, resulting in respiratory and/or right ventricular failure.<sup>32</sup>

**Group IV: Chronic Thromboembolic Pulmonary Hypertension (CTEPH)** CTEPH is a mechanical obstruction of pulmonary arteries or arterioles secondary

to pulmonary emboli. Pulmonary embolism is the most common cause of acute right ventricular pressure overload and acute cor pulmonale.<sup>8</sup> The sudden increase in afterload leads to a dilatation of the right heart as a compensatory mechanism to maintain stroke volume despite decreased ejection fraction (Frank-Starling mechanism).<sup>18</sup> Even though acute cor pulmonale is often associated with dilatation, studies in patients with massive pulmonary embolism have shown that hypertrophy can occur in the right heart during the acute phase.<sup>33</sup>

**Group V: Pulmonary Hypertension With Unclear Multifactorial Mechanisms** The fifth group is a collection of PH disorders with unclear multifactorial mechanisms.

#### 1.1.5.2 Pathophysiology

The progressive increase in pulmonary vascular resistance seen in pulmonary hypertension leads to right ventricular hypertrophy, dilatation and eventually right ventricular failure. The progression from right ventricular hypertrophy to right ventricular failure can be divided into three phases, namely compensatory, intermediate, and decompensated phase.

**Compensatory Right Ventricular Hypertrophy** In the compensatory phase, concentric hypertrophy develops and right ventricular function is preserved. There are no changes in chamber volume nor any clinical signs of heart failure. Elevated right ventricular pressure leads to an increase in wall stress, and the compensatory myocardial hypertrophy is believed to reduce wall stress and oxygen consumption to maintain cardiac output.<sup>34</sup> This can be concluded from the Law of Laplace, which describes wall stress as a ratio of intraluminal pressure times internal chamber radius to the chambers wall thickness.<sup>34</sup> Following from this law, one can see that an increase in chamber wall thickness leads to a decrease in wall stress:

$$\sigma = \frac{P \times r}{h} \quad (1.1)$$

$\sigma$  = wall stress

P = intraluminal pressure

r = chamber internal radius

h = chamber wall thickness

**Intermediate Right Ventricular Hypertrophy** Sustained increases in filling pressures eventually lead to a progressive contractile dysfunction owing to functional and structural changes, as well as cardiomyocyte apoptosis.<sup>35</sup> The right ventricular wall continues to grow; this process is paralleled by eccentric hypertrophy, that is an elongation of the myocardial sarcomeres, leading to ventricular dilatation.<sup>16</sup> Chamber dilatation is thought to occur to allow a compensatory increase in preload to maintain stroke volume in face of a progressive contractile dysfunction. In time, diastolic dysfunction occurs, which is reflected by a reduced compliance of the right ventricle. The reduced compliance is caused by progressive stiffening of the ventricular wall because of an increase in interstitial collagen content and a thickening of the ventricular wall.<sup>35</sup> Progressive chamber dilatation leads to tricuspid regurgitation, as the tricuspid leaflets are unable to close any longer sufficiently due to annular dilation, and to a displacement of the septum towards, and eventually protruding into, the left ventricle. This also impairs left ventricular function, as the left ventricle is hindered to distend sufficiently to maintain an adequate end-diastolic filling, resulting in a decreased cardiac output.

**Decompensated Right Ventricular Hypertrophy** The decreased cardiac output and the increased right ventricular pressure and wall tension finally lead to the decompensated phase. The decreased cardiac output leads to systemic hypotension, which, in combination with the increased right ventricular wall tension, results in reduced right ventricular tissue perfusion pressure, culminating in a reduced coronary blood flow to the right ventricular myocardium and eventually right ventricular ischemia.<sup>35</sup> This mismatch between increased oxygen demand and decreased oxygen delivery leads to further contractile weakening of the right ventricle. Recently, it was also shown that angiogenesis is reduced and cannot keep up with the elevated oxygen

demand.<sup>35</sup> On the cell level, an increased formation of reactive oxygen (ROS) and nitrogen species (RNS), as well as increased inflammation can be observed. ROS and RNS have the potential to induce cell damage, which can lead to apoptosis, as well as to inhibition of enzymes and impaired intracellular signaling, which can lead to impaired excitation-contraction coupling, hindering the heart from successfully functioning as a syncytium.<sup>35</sup>

Eventually the heart becomes incapable to adequately pump blood in response to systemic demands, leading to deficient end-organ perfusion, premature fatigue, dyspnoea, lower extremity edema, congestive hepatomegaly, and possibly cardiovascular collapse due to arrhythmia and ischemia.<sup>2,16,36</sup>

### 1.1.5.3 Molecular Mechanisms of Pathological Right Ventricular Hypertrophy

For now, the right heart remains relatively under-investigated and not much is known about the protein and cellular alterations which underlie maladaptive right ventricular hypertrophy, as research in the past has mostly focused on the hypertrophied left ventricle.<sup>35</sup>

It is known that protein synthesis in the right ventricle is induced by stretch-sensitive integrins and ion channels, via autocrine and paracrine signaling mechanisms, as well as neurohormonal influences.<sup>35</sup> One of the hallmarks of maladaptive cardiac hypertrophy is the  $\alpha$ - to  $\beta$ -isotype switch of myosin heavy chain in cardiac myocytes. The  $\alpha$ -myosin heavy chain usually accounts for 23–34% of the myosin heavy chain content in the right ventricle, and goes down to 5% in pathological right ventricular hypertrophy.<sup>37</sup> As the  $\beta$ -isoform has a decreased ATPase activity, this results in an impaired systolic function. Moreover, there is a decrease in  $\alpha$ -cardiac actin, and a concomitant increase in  $\alpha$ -smooth muscle and  $\alpha$ -skeletal muscle actin; the functional consequences of this are unclear so far.<sup>35</sup> Another decrease in systolic function comes about by the proteolytic degradation, as well as phosphorylation, of the regulatory protein troponin, which impairs its binding to tropomyosin.<sup>35</sup> Lastly, the right ventricle switches from fatty acid to carbohydrate metabolism, and the fetal contractile gene expression program is re-induced.<sup>38</sup>

#### 1.1.5.4 Epidemiology

Chronic cor pulmonale is responsible for 5–10 % of all diseases of the heart and has the highest prevalence after hypertensive heart diseases and coronary heart diseases in patients over the age of 50.<sup>39</sup> Right ventricular performance is an important prognostic determinant in chronic heart failure,<sup>40,41</sup> and it is estimated that 10–30 % of all hospital admissions for heart failure in the US yearly are owing to cor pulmonale.<sup>42</sup>

A low cardiac index, a high mean right atrial pressure, an increased diastolic eccentricity index, as well as pericardial effusion have all been associated with increased mortality in pulmonary arterial hypertension.<sup>43–45</sup> The mortality rate of pulmonary arterial hypertension is estimated to be 20–40 % 3 years after diagnosis,<sup>35</sup> and it is estimated that 47 % of patients with idiopathic pulmonary arterial hypertension die of right ventricular failure.<sup>43</sup>

Pulmonary embolism has a high mortality rate and is strongly related to right ventricular dysfunction.<sup>46</sup> there are more than 600000 cases of pulmonary embolism in the US each year, and around 50000 deaths in pulmonary embolism are attributed to right ventricular failure.<sup>21</sup> But also in patients with hemodynamically stable pulmonary embolism, right ventricular dysfunction, as assessed by computed tomography, echocardiography, or cardiac biomarkers, is associated with an increased risk of mortality.<sup>47,48</sup>

It is difficult to estimate the actual prevalence of cor pulmonale in COPD, as it is challenging to catheterize the right heart in large scale, and non-invasive techniques are not investigated enough yet or not widely available. Nonetheless, there are several indicators, that right ventricular dysfunction plays a major role in COPD. In the 1966 Veterans Administration trial, patients with COPD and cor pulmonale had a 4-year mortality rate of 73 %.<sup>49,50</sup> It is thought that around 80 % of cor pulmonale cases stem from COPD.<sup>39</sup> Autopsy studies in patients with chronic lung disease have shown that in more than 40 % of patients examined, there was evidence of cor pulmonale.<sup>51,52</sup> Additionally, 59 % of end-stage COPD patients have right ventricular dysfunction.<sup>53</sup> COPD was world-wide ranked as the 6th leading cause of death in 1990 and is projected to increase to be the 5th leading cause of death in 2020 and the 4th leading cause in 2030, as a result of the rise in smoking rates and

the demographic changes in many countries.<sup>54,55</sup>

Additionally, the right ventricle appears to play a crucial role in cardiac diseases, e.g. myocardial infarction, congenital heart disease, as well as in cardiac transplantation. In this line, right ventricular ejection fraction was shown to predict mortality after myocardial infarction.<sup>56</sup> Furthermore there are about 100000 adults in the US with congenital heart disease,<sup>57</sup> and about the same number in Europe,<sup>58</sup> and a correct right ventricular function was shown to be important for long-term survival after congenital heart disease correction.<sup>59</sup> Lastly, acute right ventricular failure accounts for 50 % of all cardiac complications in cardiac transplant patients, and is responsible for 19 % of early deaths.<sup>60</sup>

Taking all of this into account, it becomes evident that there is already a large proportion of people affected by a dysfunctional right ventricle, and the number is likely to increase in the future. Therefore it is crucial to develop effective treatments to alleviate the burdens of this disease.

### **1.1.6 Reverse Remodeling as a Novel Treatment Strategy**

Afterload reduction is the mainstay to alleviate the right ventricle of its increased afterload, but unfortunately this cannot be achieved in many cases.<sup>2</sup> Drugs which have commonly been employed to decrease afterload include loop diuretics and angiotensin-converting-enzyme (ACE) inhibitors. Loop diuretics are used to get rid of excess fluid accumulation to reduce blood pressure, whilst ACE inhibitors directly promote vasodilation and reduce afterload. The problem with loop diuretics is that they also decrease the preload of the heart, which can result in diminished cardiac output.<sup>16</sup> Moreover, afterload reduction cannot be achieved in many cases. A new treatment strategy is to directly target the right heart and its pathological remodeling process.

Recent studies call into question the long held belief that compensatory hypertrophy indeed is compensatory and that normalization of wall stress is essential, and rather propose that hypertrophy might be detrimental from the outset.<sup>34</sup> So is an increase in left ventricular mass associated with decreased survival in virtually all forms of heart failure.<sup>61</sup> Furthermore, studies with ACE inhibitors demonstrated

that even though they reduce cardiac hypertrophy, they also increase survival.<sup>62,63</sup> Also, in an experimental model of left ventricular hypertrophy, a reduction of myocardial mass was shown to have positive effects on left heart function.<sup>25</sup> That the hypertrophied right heart has the capability to regress, can be witnessed in patients undergoing treatment of the underlying cause of their right ventricular dysfunction: so does lung transplantation or pulmonary endarterectomy in CTEPH lead to a disappearance of acute cor pulmonale.<sup>64</sup>

Therefore a reduction of right ventricular hypertrophy forms a potential new treatment target, which could be employed to enhance right ventricular function and reduce mortality.

### 1.1.7 The Pulmonary Artery Banding (PAB) Model

Most animal models of right ventricular hypertrophy and failure involve a direct modification of the pulmonary (vascular) structure, so as to increase the resistance the right heart has to work against (e.g. hypoxia mouse model, monocrotaline rat model).<sup>65,66</sup> These models make it difficult to assess whether drug treatment effects on the right heart are caused by a secondary effect due to right ventricular unloading, or a potential primary effect on the right heart. Here, I employ the pulmonary artery banding (PAB) model in mice, which results in a constant afterload and resistance the right ventricle has to work against. This allows to elucidate the effects of treatment on the right heart independently of the pulmonary vasculature. Experimentally the PAB model was first employed in piglets,<sup>67</sup> advances in microsurgical approaches to create a graded constriction allowed the model to be extended to rodents.<sup>68</sup> A comprehensive description of this procedure was published by Tarnavski et al.<sup>69</sup> Briefly, a clip with a predefined diameter is placed around the pulmonary artery which is thereby constricted by a certain amount. The right ventricle has to work against an increased vascular resistance that leads to chronic pressure overload and subsequent pathological right ventricular remodeling. Pharmacological or genetic manipulation of chosen signaling pathways can then be carried out to assess the direct effects they have on the right heart.

## 1.2 The Nitric Oxide Pathway

This section describes the major players of the nitric oxide (NO) signaling cascade, that is NO, soluble guanylyl cyclase (sGC), cyclic guanosine monophosphate (cGMP), cGMP-dependent protein kinase (cGK) and phosphodiesterase 5 (PDE5). Each constituent of the pathway will be briefly described and the role it plays in the pathway explained. Subsequently, experimental *in vitro* and *in vivo* studies will be presented, which assessed their role in left and right ventricular hypertrophy, as well as in fibroblast growth. The results of these studies will be summarized in tables.

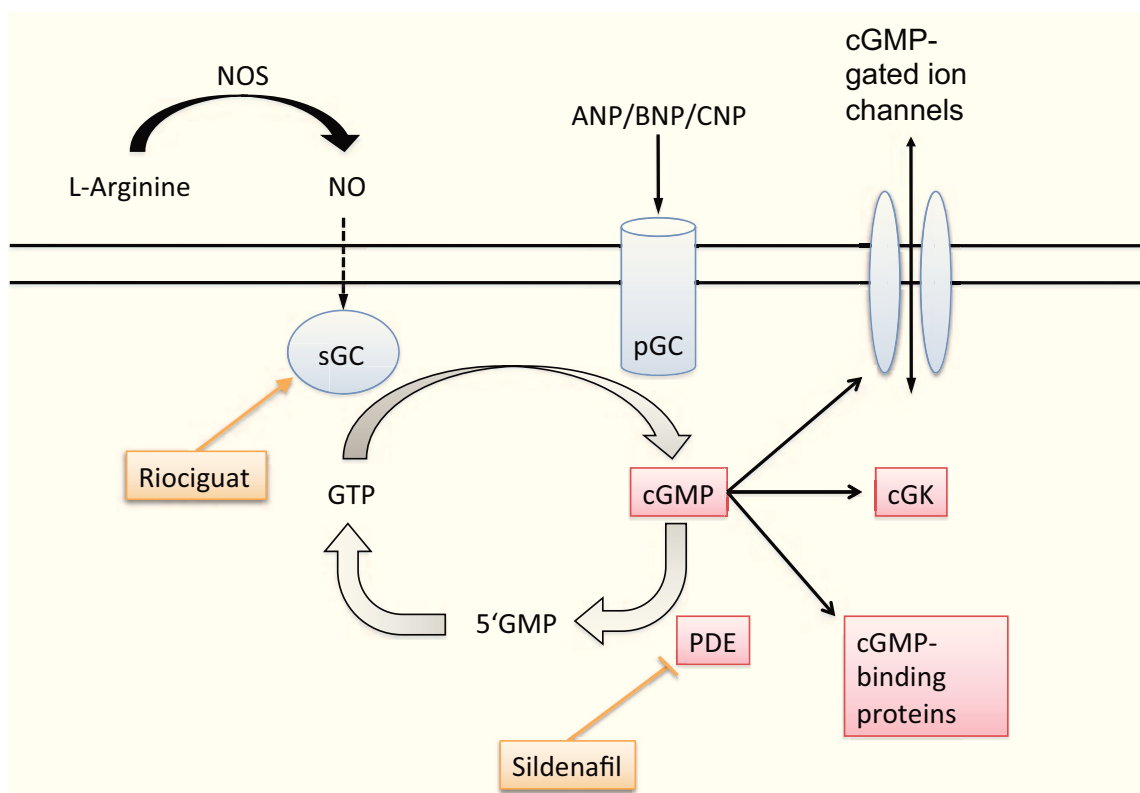


**Figure 1.3** – Schematic drawing of the nitric oxide (NO) pathway. L-Arginine is converted to NO by nitric oxide synthase (NOS). NO freely diffuses into its target cell, where it activates soluble guanylyl cyclase (sGC), leading to the formation of cyclic guanosine monophosphate (cGMP) from guanosine-5'-triphosphate (GTP). cGMP exerts its various effects via regulating the activity of cGMP-gated ion channels, cyclic guanosine kinase (cGK) and cGMP-binding proteins. Another pathway, which leads to the generation of cGMP, is the natriuretic peptide pathway: atrial natriuretic peptide (ANP), brain natriuretic peptide (BNP) and C-type natriuretic peptide (CNP) bind to and activate particulate guanylyl cyclase (pGC), which in turn leads to the production of cGMP. cGMP is broken down to 5'GMP by the enzyme phosphodiesterase (PDE). Riociguat is a drug which activates sGC, and sildenafil is a drug which inhibits PDE.

### 1.2.1 Nitric Oxide

Nitric oxide (NO) was first identified as endothelial-derived relaxing factor (EDRF) by Furchgott in 1980,<sup>70</sup> for which he received the Nobel prize in 1998.<sup>71</sup> NO is a key signaling molecule, which is involved in the regulation of a plethora of physiological processes in mammals, amongst which are vasodilation,<sup>72</sup> inhibition of platelet aggregation,<sup>72</sup> inhibition of smooth muscle proliferation,<sup>72</sup> anti-apoptotic<sup>73</sup> and anti-inflammatory effects.<sup>73</sup>

NO is generated by the conversion of L-Arginine to L-Citrulline by various nitric oxide synthases (NOS).<sup>74</sup> In the vascular system, NO is produced by endothelial nitric oxide synthase (eNOS) in endothelial cells, after which it diffuses across cell membranes into target cells, acting as a paracrine and autocrine signaling molecule.<sup>74</sup> NO activates sGC, increasing its activity ~200- to 400-fold, resulting in the accumulation of cyclic guanosine monophosphate (cGMP).<sup>75,76</sup> Apart from activating sGC, NO is able to exert effects independently of cGMP production, e.g. modification of intracellular proteins by S-nitrosylation of cysteine residues.<sup>77</sup>

Reduced levels of, or responsiveness to, NO is implied in diseases of the cardiovascular, pulmonary, endothelial, renal and hepatic system, as well as in erectile dysfunction. Decreased levels of NO, either owing to impaired production, excessive degradation, or chemical interaction with oxidants like superoxide, leads to disrupted sGC-cGMP-signaling, which has been implicated in heart failure.<sup>73,76</sup> Traditionally, organic nitrates, like glycerol trinitrate, or NO-donors like molsidomine, have been used to treat diseases with impaired NO-signaling. Glycerol trinitrate and other organic nitrates have been successfully used for treating coronary artery disease for more than 100 years. Nonetheless, several problems are inherent in using these drugs: their effects are of short duration,<sup>76</sup> a lack of response can occur,<sup>76</sup> development of tolerance following prolonged administration can arise,<sup>78</sup> and NO and its metabolites can have non-specific interactions with several biological molecules.<sup>79</sup> This is by way of NO showing reactivity with iron-containing catalytic sites, thereby affecting the functioning of various enzymes, which can lead to potentially negative consequences.<sup>79</sup> Tolerance can occur, as sGC desensitizes after chronic exposure to NO, without any changes in sGC expression levels.<sup>80</sup> Indeed, it was shown that eNOS-

/- mice, which have decreased endogenous NO production, have a more sensitive sGC towards exogenously applied NO, and pharmacological inhibition of NO production has been shown to restore sGC sensitivity in formerly desensitized sGC.<sup>80</sup> Furthermore, even though symptomatic improvements can be achieved in patients with cardiovascular disease, evidence for a decrease in mortality is pending.<sup>75</sup>

The inference from all of this is, that drugs, which are able to activate sGC directly, like sGC stimulators, could have the beneficial effects of NO, whilst circumventing the negative side-effects associated with increased NO levels mentioned above.

In vitro studies carried out in models of cardiomyocyte<sup>81,82</sup> and fibroblast<sup>81,83,84</sup> hypertrophy have shown that NO donors, like S-Nitroso-N-acetylpenicillamine (SNAP), have the potential to reduce cell growth. Additionally, in in vivo models of right ventricular hypertrophy, NO inhalation,<sup>85</sup> i.p. application of L-Arginine<sup>86,87</sup>, and Molsidomine delivered in drinking-water<sup>88</sup> during chronic hypoxia exposure, were shown to reduce right ventricular hypertrophy. In contrast, continuous NO inhalation following hypoxia exposure,<sup>89</sup> and L-Arginine delivered in drinking water,<sup>90</sup> did not have any effects on right ventricular hypertrophy. The limitation of these studies regarding the effects on right ventricular hypertrophy is that by using chronic hypoxia or monocrotaline-injection as a model, the effects on the right ventricle are afterload-dependent; this prevents the inference of a direct effect on the right ventricle. A study carried out in spontaneously hypertensive rats treated with L-Arginine p.o.<sup>91</sup> showed a reduction in hypertrophy, and this time independent of the effects on blood pressure. However, the model used was a model of left ventricular hypertrophy, and not of right.

In conclusion it can be said that there is good in vitro evidence that NO application has the potential to reduce cardiac hypertrophy. The in vivo evidence is less clear: whether the effects on the right ventricle are a direct one cannot be judged from the above-mentioned studies, because of the afterload-dependence of these models. The effects observed in the left ventricle cannot be outrightly translated to the right ventricle, owing to the inherent differences between the left and the right ventricle.

**Table 1.1** – In vitro and in vivo studies of NO donors in experimental models of cardiac hypertrophy

Reference	Experimental model	Intervention	Effect on hypertrophy	Afterload-dependency
<i>In vitro studies</i>				
Cao & Gardner, <sup>83</sup> 1995	Cultured rat cardiac fibroblasts, agonist and stretch-stimulated	Application of nitroprusside	↓ growth	
Fujisaki et al., <sup>84</sup> 1995	Cultured rat neonatal fibroblasts, agonist stimulated	Application of nitroprusside,	↓ growth	
Calderone et al., <sup>81</sup> 1998	Cultured rat ventricular myocytes and fibroblasts, agonist stimulated	Application of SNAP	↓ growth	
Wollert et al., <sup>82</sup> 2002	Neonatal rat cardiomyocytes stimulated with PE	Application of SNAP	↓ hypertrophy	
<i>In vivo studies</i>				
Roberts et al., <sup>85</sup> 1995	Rat hypoxia	Continuous inhalation of NO during exposure	↓ RV hypertrophy	dependent
Matsuoka et al., <sup>91</sup> 1996	Spontaneously hypertensive rats	L-Arginine p.o. in drinking water	↓ Heart/BW	independent
Mitani et al., <sup>87</sup> 1997	Rat hypoxia, rat MCT	L-Arginine i.p. during exposure	↓ RV hypertrophy	dependent
Fagan et al., <sup>86</sup> 1999	Rat hypoxia	L-Arginine i.p. during exposure	↓ RV hypertrophy	dependent
Jiang et al., <sup>89</sup> 2004	Rat hypoxia	Continuous NO inhalation following exposure	No effect	dependent
Elmedal et al., <sup>88</sup> 2004	Rat hypoxia	Molsidomine delivered in drinking water during exposure	↓ RV hypertrophy	dependent
Laursen et al., <sup>90</sup> 2008	Rat hypoxia	L-Arginine delivered in drinking water during exposure	No effect	dependent

SNAP indicates S-Nitroso-N-acetylpenicillamine; PE, phenylephrine; NO, nitric oxide; RV, right ventricular; p.o., per os; BW, body weight; MCT, monocrotaline; i.p., intraperitoneal

## 1.2.2 Soluble Guanylyl Cyclase

Soluble guanylyl cyclases (sGCs) are intracellular receptors which convert guanosine triphosphate (GTP) to cGMP upon binding of NO or carbon monoxide (CO).<sup>75</sup> Two subunits can be found in humans, which both can exist in two different isoforms:  $\alpha 1$  and  $\alpha 2$  (molecular weight (MW) 73 kDa), and  $\beta 1$  and  $\beta 2$  (MW 70 kDa).<sup>92</sup>  $\alpha$ -subunits cannot form dimers by themselves and are dependent on the presence of a  $\beta$ -subunit to form a functional enzyme.<sup>93</sup> Even though  $\beta$ -homodimers are possible, sGCs are usually found as heterodimers.<sup>94</sup> The best characterized sGC isoforms are the  $\alpha 2\beta 1$  isoform, and the  $\alpha 1\beta 1$  isoform; the  $\alpha 1\beta 1$  isoform is also the most abundant one.<sup>92</sup> To form an active catalytic centre, the catalytic domains of both subunits

are needed.<sup>95</sup>

sGC subunits are made up of three functional domains: an N-terminal, a central domain, and a C-terminal domain. The  $\beta$ -subunit contains the evolutionary conserved N-terminal heme-binding domain, which is ligated to the prosthetic heme moiety via His105, which in turn binds gaseous ligands.<sup>96,97</sup> Important for activation of sGC is the redox-state of the heme moiety: in its native, i.e. reduced, state,  $\text{Fe}^{2+}$  binds NO, forming an  $\text{Fe}^{2+}$ -nitrosyl-heme complex, activating sGC. If the prosthetic heme group gets oxidized to  $\text{Fe}^{3+}$ , NO is unable to activate sGC any longer.<sup>76</sup> This has implications under conditions of increased oxidative stress, as reactive oxygen and nitrogen species can render sGC insensitive to NO.<sup>98</sup>

A plethora of studies employing sGC stimulators and activators in in vivo models of pulmonary hypertension and right ventricular hypertrophy have been carried out (Table 1.2). Basically all of these studies show that treatment with these drugs leads to a decrease in pulmonary hypertension, as well as a concomitant reduction in right ventricular hypertrophy; independent of whether treatment takes place during<sup>65,66,99,100</sup> or after hypoxia,<sup>65</sup> whether the monocrotaline rat model is used,<sup>65,66</sup> or whether an sGC stimulator<sup>65,66,99,100</sup> or and sGC activator<sup>65</sup> is employed. Additionally, sGC activators and stimulators were shown to reduce hypertension,<sup>101-105</sup> left ventricular hypertrophy,<sup>102-105</sup> and reduce left ventricular<sup>103-105</sup> and renal fibrosis<sup>101,104</sup> in models of hypertension and left ventricular hypertrophy, that is in rats with 5/6 nephrectomy,<sup>102</sup> rats with angiotensin II-induced hypertension,<sup>103</sup> rats treated with L-NAME (a NOS inhibitor),<sup>105</sup> low- and high-renin rat models of hypertension,<sup>104</sup> and Dahl salt-sensitive rats maintained on a high salt diet.<sup>101</sup> Moreover, in rats with suprarenal aortic constriction,<sup>106</sup> the sGC stimulator BAY 41-2272 was shown to reduce left ventricular fibrosis independent of blood pressure.

To sum these studies up, activators and stimulators of sGC successfully decrease hypertension, concomitant hypertrophy, as well as fibrosis. Whether these effects can also be shown in isolated right ventricular hypertrophy, independent of changes in afterload, is one of the questions this dissertation addresses.

**Table 1.2** – In vivo studies of sGC stimulators and activators in experimental models of cardiac hypertrophy

Reference	Experimental model	Intervention	Effect on hypertrophy	Afterload-dependency
Deruelle et al., <sup>99</sup> 2006	Rat hypoxia	BAY 41-2272 i.m. during exposure	↓ Pulmonary hypertension, ↓ RV hypertrophy	dependent
Dumitrascu et al., <sup>65</sup> 2006	Mouse hypoxia	BAY 41-2272, BAY 58-2667 p.o. following exposure	↓ Pulmonary hypertension, ↓ RV hypertrophy	dependent
Dumitrascu et al., <sup>65</sup> 2006	Rat MCT	BAY 41-2272, BAY 58-2667 p.o.	↓ Pulmonary hypertension, ↓ RV hypertrophy	dependent
Kalk et al., <sup>102</sup> 2006	Rat 5/6 nephrectomy	BAY 58-2667 p.o.	↓ hypertension, ↓ LV hypertrophy, ↓ LV CM diameter	dependent
Masuyama et al., <sup>103</sup> 2006	Rat Ang II induced hypertension	BAY 41-2272 p.o.	↓ Hypertension, ↓ HW, ↓ LV fibrosis	dependent
Zanfolin et al., <sup>105</sup> 2006	Rat treated w/ L-NAME (NOS inhibition)	BAY 41-2272 p.o. during exposure	↓ Hypertension, ↓ LV hypertrophy, ↓ LV fibrosis	dependent
Schermuly et al., <sup>66</sup> 2008	Mouse hypoxia	BAY 63-2521 (Riociguat) during exposure	↓ Pulmonary hypertension, ↓ RV hypertrophy	dependent
Schermuly et al., <sup>66</sup> 2008	Rat MCT	BAY 63-2521 (Riociguat)	↓ Pulmonary hypertension, ↓ RV hypertrophy	dependent
Masuyama et al., <sup>106</sup> 2009	Rat suprarenal aortic constriction	BAY 41-2272 p.o.	↓ LV fibrosis	independent
Sharkovska et al., <sup>104</sup> 2010	Rat low-renin and high-renin models of hypertension	BAY 63-2521 (Riociguat)	↓ Hypertension, ↓ LV weight, ↓ LV fibrosis, ↓ renal fibrosis	dependent
Thorsen et al., <sup>100</sup> 2010	Rat hypoxia	BAY 41-2272 p.o.	↓ Pulmonary hypertension, ↓ RV hypertrophy	dependent
Geschka et al., <sup>101</sup> 2011	Dahl salt-sensitive rats maintained on a high salt diet	BAY 63-2521 (Riociguat) p.o.	↓ Hypertension, ↓ fibrosis	dependent

i.m. indicates intramuscular; RV, right ventricular; p.o., per os; MCT, monocrotaline; LV, left ventricular; CM, cardiomyocyte; Ang II, angiotensin II; HW, heart weight; L-NAME, N<sup>ω</sup>-nitro-L-arginine methyl ester; NOS, nitric oxide synthase

### 1.2.3 Cyclic Guanosine Monophosphate

Cyclic guanosine monophosphate (cGMP) is a ubiquitous second messenger, which is formed from GTP in a reaction catalyzed by sGC and particulate guanylyl cyclase (pGC).<sup>76</sup>

cGMP can exert its effects via three distinct pathways:<sup>75</sup> it can regulate the activity of the cGMP-dependent protein kinases I and II (cGKI and cGKII); it can regulate cyclic nucleotide-gated (CNG) cation channels; and it can regulate the activity of cGMP-regulated PDEs. By interacting with PDEs which breakdown cAMP (cGMP stimulates PDE2 and inhibits PDE3), cGMP can effectively establish crosstalk to the cyclic adenosine monophosphate (cAMP) signaling cascade.<sup>75,107</sup> cGMP could also directly activate protein kinase A (PKA), a cAMP-dependent

enzyme; but whilst for the inhibition of PDE3 a concentration similar to that needed for the activation of cGK is required, the concentration required for the activation of PKA might exceed physiological levels.<sup>108</sup>

The effects of cGMP can be terminated in two ways: either by cGMP becoming degraded by PDEs, or through being transported out of the cell by multidrug resistance-associated protein 5.<sup>75</sup>

Studies in agonist-stimulated cultured cardiomyocytes and fibroblasts have shown that application of 8-bromo-cGMP, a permeable cGMP-analogue that directly activates cGK, reduces growth, hypertrophy, and de novo collagen synthesis (Table 1.3). These results lend support to the hypothesis, that activation of the NO-sGC-pathway could directly affect right ventricular hypertrophy.

**Table 1.3** – In vitro studies of cGMP analogues in experimental models of cardiac and fibroblastic hypertrophy

Reference	Experimental model	Intervention	Effect on hypertrophy
<i>Cardiomyocytes</i>			
Calderone et al., <sup>81</sup> 1998	Cultured neonatal rat ventricular myocytes, agonist-stimulated	Application of 8-bromo-cGMP	↓ growth
Horio et al., <sup>109</sup> 2000	Cultured neonatal rat ventricular myocytes, agonist-stimulated	Application of 8-bromo-cGMP	↓ growth in basal and agonist-stimulated condition
Wollert et al., <sup>82</sup> 2002	Cultured neonatal rat cardiomyocytes, agonist stimulated	Application of 8-bromo-cGMP	↓ hypertrophy
Tokudome <sup>110</sup> 2004	Cultured neonatal rat ventricular myocytes, agonist-stimulated	Application of 8-bromo-cGMP	↓ growth
<i>Fibroblasts</i>			
Cao & Gardner, <sup>83</sup> 1995	Cultured neonatal rat cardiac fibroblasts, agonist- and stretch-stimulated	Application of 8-bromo-cGMP	↓ growth
Fujisaki et al., <sup>84</sup> 1995	Cultured neonatal rat fibroblasts, agonist-stimulated	Application of 8-bromo-cGMP	↓ growth
Calderone et al., <sup>81</sup> 1998	Cultured neonatal rat ventricular fibroblasts, agonist-stimulated	Application of 8-bromo-cGMP	↓ growth
Tsuruda et al., <sup>111</sup> 2002	Cultured adult canine cardiac fibroblasts	Application of 8-bromo-cGMP	↓ de novo collagen synthesis

8-bromo-cGMP indicates 8-bromo-cyclic guanosine monophosphate

## 1.2.4 cGMP-dependent Protein Kinase

cGMP-dependent protein kinases (cGKs), also called PKGs (from protein kinase G), are the principal intracellular mediators of cGMP signals. They are serine/threonine kinases, which, upon binding of cGMP to the regulatory domain, release their cat-

alytic core from the inhibition by the N-terminus, leading to their activation and allowing the phosphorylation of target proteins.<sup>76</sup> cGKs are homodimers of two identical subunits, and two different genes code for them in mammals.<sup>112</sup>

cGK-I is located in the cytosol, widely expressed in mammalian tissues and acts a soluble intracellular modulator of  $\text{Ca}^{2+}$ . The N-terminus of cGKI is encoded by two alternatively used exons, resulting in two distinct isoforms, cGK-I $\alpha$  and cGK-I $\beta$ . The cGK-I $\alpha$  isoform is found mainly in cardiomyocytes,<sup>113</sup> fibroblasts,<sup>114</sup> vascular endothelial cells,<sup>115</sup> the lung, cerebellum, kidneys and adrenal glands,<sup>116</sup> whilst cGK-I $\beta$  is only found in the uterus.<sup>117</sup>

cGK-II is a membrane bound homodimer, which is absent from the cardiovascular system, but expressed in brain, intestine, lung, kidneys and bone.<sup>112</sup> It regulates fluid homeostasis at the cell membrane.<sup>112</sup>

cGKs regulate the activity of numerous target proteins via phosphorylation, e.g. CNG ion channels, which regulate the transmembrane  $\text{Na}^+$  and  $\text{Ca}^{2+}$  conductance, L-type  $\text{Ca}^{2+}$  channels, ATP-sensitive potassium channels sarcolemmal and sarcoplasmic  $\text{Ca}^{2+}$ -ATPases.<sup>76,116</sup> Furthermore, cGKs were also found to phosphorylate troponin I and phospholamban, thereby exerting effects on excitation-contraction coupling, Rho A, IP3 receptor-associated cGMP kinase substrate (IRAG), which regulates IP3 receptor-dependent  $\text{Ca}^{2+}$ -signaling, and regulator of G-protein signaling 2 (RGS2).<sup>76,118</sup>

Overexpression of cGK-I $\beta$  augmented the antihypertrophic effects of SNAP and 8-bromo-cGMP in agonist-induced hypertrophy in cultured cardiomyocytes.<sup>82</sup> This lends credibility to the hypothesis that one of the main mediators of NO signaling, cGK, is responsible for the antihypertrophic effects seen in stimulation of the NO pathway. Also, application of a cGK antagonist prevented the antihypertrophic effects of increased cGMP signaling caused by knockdown of PDE5, emphasizing the crucial role cGK is playing in that mechanism.<sup>119</sup>

**Table 1.4** – In vitro studies of stimulated/inhibited cGK in experimental models of cardiac hypertrophy

Reference	Experimental model	Intervention	Effect on hypertrophy
<i>In vitro studies</i>			

Continued on next page

Table 1.4 – continued from previous page

Reference	Experimental model	Intervention	Effect on hypertrophy
Wollert et al., <sup>82</sup> 2002	Neonatal rat cardiomyocytes stimulated with PE	Application of SNAP or 8-bromo-cGMP during overexpression of cGK-1 $\beta$	Overexpression of cGK-1 $\beta$ enhances antihypertrophic effects of SNAP and 8-bromo-cGMP
Zhang et al., <sup>119</sup> 2008	Neonatal and adult rat cardiomyocytes, agonist-stimulated + PDE5 knock-down with shRNA	Application of cGK antagonist	Antihypertrophic effects of PDE5 knockdown blocked by cGK antagonist

PE indicates phenylephrine; SNAP, S-Nitroso-N-acetylpenicillamine; 8-bromo-cGMP, 8-bromo-cyclic guanosine monophosphate; cGK, cyclic guanosine kinase; PDE, phosphodiesterase

### 1.2.5 Phosphodiesterases

Phosphodiesterases (PDEs) hydrolyze cAMP and cGMP to AMP and GMP to terminate their action. PDEs are organized into 11 families, which are encoded by 20 genes, yielding more than 50 different PDE isoforms.<sup>120</sup> PDEs 5, 6 and 9 are specific for cGMP, PDEs 1, 2, 3, 10 and 11 can break down both cAMP and cGMP, and PDEs 4, 7 and 8 are cAMP-specific.<sup>120</sup> PDEs 1, 2, 3, 5 and 9 have been found to be expressed in the heart.<sup>120</sup> As mentioned above, cGMP-signaling can initiate crosstalk to the cAMP-signaling cascade by regulating the activities of PDEs 2 and 3.<sup>75,107</sup>

PDE5 is widely distributed throughout the body, and three PDE5 isoforms do exist.<sup>76</sup> PDE5 contains a phosphorylation site and two allosteric cGMP-binding sites, as well as a portion of the dimerization domain.<sup>121</sup> The carboxy-terminal part of the enzyme locates the catalytic domain which contains two Zn<sup>2+</sup>-binding motifs, and a cGMP substrate binding site.<sup>121</sup> PDE5 is specifically localized at the Z-bands of cardiomyocytes, underscoring the role it might play in myocardial contraction.<sup>76</sup>

PDE5 has been implicated in right ventricular hypertrophy, as it is upregulated in the right ventricle from patients with pulmonary hypertension, as well as in a rat model of right ventricular hypertrophy.<sup>122</sup> Furthermore, it is also implicated in left ventricular failure, being upregulated in this condition;<sup>36</sup> this is in contrast to its low expression levels in resting cardiomyocytes of either the left or the right ventricle.<sup>119</sup> This has made PDE5 an interesting target for pharmacological manipulation to probe into its role in right ventricular hypertrophy.

Studies carried out in cultured cardiomyocytes employing pharmacological inhibition<sup>83,109</sup> or genetic knockdown of PDE5,<sup>119</sup> demonstrate that decreasing PDE5 activity, and thereby increasing cGMP-signaling, reduces basal and agonist-induced hypertrophy. Vice versa overexpression of PDE5 augments agonist-induced hypertrophy.<sup>119</sup>

Studies carried out in the left ventricle came to the unambiguous result that increasing cGMP-signaling by inhibiting PDE5 activity reduces left ventricular hypertrophy and increases left ventricular function,<sup>25,123</sup> whilst a reduction in cGMP-signaling by a cardiomyocyte-specific overexpression of PDE5 increases left ventricular hypertrophy and reduces its function.<sup>124,125</sup> The antihypertrophic effects of sildenafil can be assumed to directly affect the left ventricle, as the transverse aortic constriction (TAC) model was employed, which exposes the left ventricle to a constantly increased afterload, making the model afterload-independent.

Studies performed in the right heart are rather ambiguous. Two studies, which were afterload-dependent (rat monocrotaline and rat hypoxia model) show a reduction in right ventricular hypertrophy and an increased right ventricular systolic function,<sup>26,100</sup> whilst two studies which employed the PAB model showed an increase in right ventricular hypertrophy, accompanied either by an improvement in right ventricular function,<sup>126</sup> or no change in function.<sup>26</sup> Apparently the decrease in afterload led to a decrease in right ventricular hypertrophy by sildenafil treatment, but sildenafil appears not to be antihypertrophic in the right ventricle per se. This is in stark contrast to the left ventricle, where sildenafil treatment has repeatedly been shown to exert antihypertrophic effects. Whether these differences are a result of inherent differences between the left and the right ventricle, due to species differences, differences in banding strength or something else, still needs to be determined.

To determine whether the differences seen between the left and right ventricle might be species-dependent, I will assess the effects of sildenafil treatment in pulmonary artery banded mice in this dissertation.

**Table 1.5** – In vitro and in vivo studies of stimulating/inhibiting PDE in experimental models of cardiac hypertrophy

Reference	Experimental model	Intervention	Effect on hypertrophy	Afterload-dependency
<i>In vitro studies</i>				
Cao & Gardner, <sup>83</sup> 1995	Cultured neonatal rat cardiac fibroblasts, agonist-stimulated	ANP (+/- non-selective and PDE5-selective PDE inhibitor)	PDE inhibitors augment ANP effects	
Horio et al., <sup>109</sup> 2000	Cultured neonatal rat ventricular myocytes, agonist-stimulated	Application of cGMP-specific PDE inhibitor	↓ growth in basal and agonist-stimulated condition	
Zhang et al., <sup>119</sup> 2008	Neonatal and adult rat cardiomyocytes, agonist-stimulated	PDE5 knockdown with shRNA	↓ agonist-induced hypertrophy	
Zhang et al., <sup>119</sup> 2008	Neonatal and adult rat cardiomyocytes, agonist-stimulated	Overexpression of PDE5	↑ agonist-induced hypertrophy	
Miller et al., <sup>127</sup> 2009	Neonatal and adult rat cardiomyocytes, agonist-stimulated	Pharmacological inhibition of PDE1	↓ agonist-induced hypertrophy	
<i>In situ studies</i>				
Nagendran et al., <sup>122</sup> 2007	Isolated hypertrophied hearts in Langendorff preparation and isolated cardiomyocytes from MCT rats	Application of sildenafil	Acutely ↑ contractility in RV and isolated cardiomyocytes	
<i>In vivo studies</i>				
<i>Left heart</i>				
Takimoto et al., <sup>25</sup> 2005	Mouse TAC (moderate)	Sildenafil p.o.	Prevention + reversal of LV hypertrophy, ↑ LV function	independent
Nagayama et al., <sup>123</sup> 2009	Mouse TAC (severe)	Sildenafil p.o.	Stop LV hypertrophy, ↑ LV function	independent
Pokreisz et al., <sup>124</sup> 2009	Mouse myocardial infarction	PDE5 CM-specific overexpression	↑ LV hypertrophy, ↑ LV function	independent
Adamo et al., <sup>128</sup> 2010	Mdx mouse model of Duchenne muscular dystrophy	Sildenafil p.o.	Reversal of age associated cardiomyopathy	
Zhang et al., <sup>125</sup> 2010	Mouse TAC	PDE5 overexpression CM-specific (Medium and high overexpression)	Dose-dependently ↑ LV hypertrophy, ↓ LV function	independent
<i>Right heart</i>				
Andersen et al., <sup>126</sup> 2008	Rat PAB	Sildenafil p.o.	↑ RV hypertrophy, but ↑ RV function	independent
Miller et al., <sup>127</sup> 2009	Rat, chronic isoproterenol-induced hypertrophy	siRNA downregulation of PDE1	↓ RV hypertrophy	
Schäfer et al., <sup>26</sup> 2009	Rat MCT	Sildenafil p.o.	↓ RV hypertrophy, ↑ function	dependent
Schäfer et al., <sup>26</sup> 2009	Rat PAB	Sildenafil p.o.	↑ RV hypertrophy, ↔ RV function	independent
Thorsen et al., <sup>100</sup> 2010	Rat Hypoxia	Sildenafil p.o.	↓ Pulmonary hypertension, ↓ RV hypertrophy	dependent

ANP indicates atrial natriuretic peptide; PDE, phosphodiesterase; cGMP, cyclic guanosine monophosphate; shRNA, short hairpin RNA; MCT, monocrotaline; RV, right ventricular; TAC, transverse aortic constriction; LV, left ventricular; PAB, pulmonary artery banding; CM, cardiomyocyte; siRNA, short interfering RNA

## 1.2.6 Riociguat

### 1.2.6.1 Discovery

The first sGC stimulator which was discovered was the indazole derivative YC-1.<sup>129,130</sup> YC-1 is able to activate sGC in a NO-independent, but heme-dependent manner. It moderately ( $\sim 10$ -fold) increases sGCs activity, with an increase in potency from  $0.5 \mu\text{M}$  to  $60 \mu\text{M}$ ; YC-1 increases sGCs maximum reaction rate ( $V_{max}$ ) by  $\sim 40\%$ , and reduces its affinity for GTP ( $K_m$ ) 3- to 5-fold.<sup>131,132</sup> The advantages of YC-1 were its potent anti-aggregatory activity, owing to its inhibiting effects on PDE, in addition to its stimulatory effects on sGC, resulting in both anti-thrombotic as well as vasodilatory effects.<sup>133</sup>

The desire for increased specificity and potency towards sGC led to the development of the two compounds BAY 41-2272 and BAY 41-8543, which both contain a pyrazolopyridinyl pyrimide core, with YC-1 acting as a lead structure.<sup>134</sup> The two compounds have an around 100-fold increased specificity and potency towards sGC compared to YC-1, but were both not further developed, as BAY 41-2272 alters the activity of cytochrome P450 isoenzymes, and BAY 41-8543 had unfavorable pharmacokinetics.<sup>135</sup>

Riociguat (BAY 63-2521) was developed based on BAY 41-2272 and BAY 41-8543, lacking their adverse drug metabolism and pharmacokinetic profile. It increases the activity of sGC in vitro by up to 73-fold, and up to 122-fold in the presence of NO.<sup>134</sup> Moreover, riociguat is currently employed in two Phase 3 clinical trials investigating its vasodilatory effects in PAH and CTEPH.<sup>135</sup>

### 1.2.6.2 Mechanism of Action

Riociguat belongs to the class of sGC stimulators, this implies that it depends on the reduced heme-group of sGC, and loses its activity upon oxidation of the heme group.<sup>135</sup> This is in contrast to sGC activators, which are able to activate sGC independently of the redox-state of the heme moiety.<sup>136</sup> Riociguat stimulates the native sGC directly and increases its sensitivity to low levels of NO.<sup>135</sup>

The molecular mechanisms of sGC stimulation by riociguat are still unknown,

but studies suggest that sGC stimulators might act by binding to the allosteric nucleotide-binding site in the catalytic domain of sGC.<sup>135</sup>

## 1.2.7 Sildenafil

### 1.2.7.1 Discovery

Sildenafil, a pyrazolopyrimidine, was discovered by Pfizer in an effort to find a selective inhibitor for PDE5.<sup>137</sup> It was shown to have a very good potency (IC<sub>50</sub> of 3.5 nM against human platelet-derived PDE5), as well as a high selectivity over PDEs 1-4 and 7-11.<sup>137</sup> The selectivity over PDE6 is only about 10-fold,<sup>137</sup> and visual disturbances can occur at very high doses of sildenafil, owing to the presence of PDE6 in the eye. In 1989, sildenafil (then UK-92,480) was selected as a candidate drug to enter clinical development for cardiovascular indications, and entered clinical trials in 1991.<sup>138</sup> In 1993 further development for cardiovascular indications was halted,<sup>137</sup> due to the drug's short half-life (~4 hours)<sup>139</sup> and its demonstrated interaction with nitrates. Notably, a common side-effect reported in clinical trials was that of penile erections.<sup>140</sup> In 1993 the first clinical proof-of-concept study was carried out with sildenafil in erectile dysfunction, which proved to be a success,<sup>140</sup> and sildenafil was approved by the Federal Drug Administration (FDA) and the European Medicine Evaluation Agency (EMA) as Viagra® as the first oral treatment for erectile dysfunction in 1998 .

Recently (2005), sildenafil has been also approved for the treatment of pulmonary arterial hypertension.<sup>137</sup> PDE5 is upregulated in the lungs of patients with pulmonary hypertension, and preclinical and clinical studies have shown its effectiveness in reducing pulmonary vascular resistance.<sup>137</sup>

### 1.2.7.2 Mechanism of Action

Sildenafil has a similar structure as cGMP and acts as a competitive inhibitor of PDE5, effectively increasing the levels of cGMP. The increased levels of cGMP in the corpus cavernosum in the penis lead to smooth muscle relaxation and vasodilation, increasing the inflow of blood into the penis, resulting in penile erection.<sup>140</sup> Likewise,

sildenafil reduces pulmonary vascular resistance by causing smooth muscle relaxation and vasodilation.

### 1.3 Rationale

Right heart failure is distinctly different from left heart failure and is a prevalent mechanism of cardiovascular collapse.<sup>2</sup> A new treatment strategy is to directly target the right heart and its pathological remodeling process.<sup>36</sup> As the disruption of the NO-sGC-cGMP pathway has been implicated in the pathogenesis of cardiovascular diseases,<sup>75</sup> this work investigated the effects of pharmacological stimulation of this pathway on right ventricular hypertrophy and function in the murine PAB model. The two drugs sildenafil and riociguat were employed. Prior to the treatment study, a staging study was carried out to assess the time-course of effects taking place in the right ventricle after banding, so as to determine the most efficient time-points for the commencement and termination of treatment. Magnetic resonance imaging (MRI) was employed as the primary means to assess the functional consequences of the banding procedure and of drug treatment, as it forms the gold standard of cardiac functional assessment.<sup>36</sup> Additionally, histological analysis of the right ventricle was performed to evaluate the effects of banding and of treatment on right ventricular fibrosis and cardiomyocyte size.

# Chapter 2

## Materials and methods

### 2.1 Materials

#### 2.1.1 Instruments

Table 2.1 – Instruments

Device	Product name	Manufacturer
Cannula	Sterican® 26G	Braun
Clip applier	Hemoclip®	Weck
Clippers	Contura	Wella
Cold plate	Leica EG1150 C	Leica Microsystems
Data acquisition system	Powerlab 8/30	ADInstruments
Flattening table	Leica HI1220	Leica Microsystems
Hotplate	Thermoplate S	Desaga
Image analysis software	Leica QWin V3	Leica Microsystems
Ligating Clips	Hemoclip®	Weck
Magnetic hotplate stirrer	VMS-C7	VWR International GmbH
Micro scales	Atilon	Acculab
Microscope	Leica DM6000 B	Leica Microsystems
MRI analysis software	MASS® 4Mice	Medis
Object slides	Super Frost Ultra Plus®	Thermo Scientific

Continued on next page

Table 2.1 – continued from previous page

<b>Device</b>	<b>Product name</b>	<b>Manufacturer</b>
pH meter	Lab 850	SCHOTT® Instruments
Rodent ventilator	SAR-830/P Ventilator	CWE Inc.
Rodent ventilator	MiniVent Type 845	Hugo Sachs Elektronik
Rotary microtome	Leica RM2255	Leica Microsystems
Scales	EMB 1200-1	Kern
Small animal MRI	PharmaScan	Bruker BioSpin
Stereoscopic microscope	Leica M50	Leica Microsystems
Surgical instruments		Fine Science Tools GmbH
Suture	Vicryl® Plus 5-0	Ethicon
Syringe	Omnifix® -F	Braun
Tissue embedding station	Leica EG1160	Leica Microsystems
Tissue processor	Leica ASP200 S	Leica Microsystems
Vaporizer	Vapor® 2000	Dräger
Water bath	Leica HI1210	Leica Microsystems

## 2.1.2 Chemicals and reagents

Table 2.2 – Chemicals and reagents

<b>Name</b>	<b>Manufacturer</b>
Bepanthen Augen- und Nasensalbe	Bayer AG
BSA	Carl Roth GmbH + Co. KG
Citric Acid	Sigma-Aldrich Chemie GmbH
Cutasept® F	Bode Chemie Hamburg
Dako Fluorescent Mounting Medium	Dako
DAPI	Invitrogen/Life Technologies
Disodium phosphate (Na <sub>2</sub> HPO <sub>4</sub> · 2 H <sub>2</sub> O)	Carl Roth GmbH + Co. KG
Entellan®	Merck KgA

Continued on next page

Table 2.2 – continued from previous page

<b>Name</b>	<b>Manufacturer</b>
Ethanol	Carl Roth GmbH + Co. KG
Glucosteril 5%	Fresenius Kabi
Isoflurane	Baxter Deutschland GmbH
Saline	Fresenius Kabi
Lectin FITC	Sigma-Aldrich Chemie GmbH
Monopotassium phosphate (KH <sub>2</sub> PO <sub>4</sub> )	Carl Roth GmbH + Co. KG
Rimadyl (Carprofen)	Pfizer
Riociguat	Bayer AG
Roti-Histol	Roth
Sildenafil	Pfizer Deutschland GmbH
Sodium chloride (NaCl)	Carl Roth GmbH + Co. KG
Triton X 100	Carl Roth GmbH + Co. KG
Vetergesic (Buprenorphine hydrochlorid)	Braun
Xylol	Carl Roth GmbH + Co. KG

### 2.1.3 Mice

Adult male C57Bl/6J mice (21–24 g body weight) were obtained from Harlan Laboratories, Inc., Netherlands. The mice were housed under controlled temperature (21–23 °C), humidity (70 %) and lighting (7AM-7PM light, 7PM-7AM dark) conditions. Free access to food and water was provided. The experiments were approved by the Regierungspräsidium Darmstadt (B2/219, B2/244).

## 2.2 Methods

### 2.2.1 Study plans

In both studies employing MRI, the PAB operation was performed after, and on the same day as the first MRI scan, which served to record the baseline characteristics

of the mice prior to operation.

### 2.2.1.1 Staging study - MRI

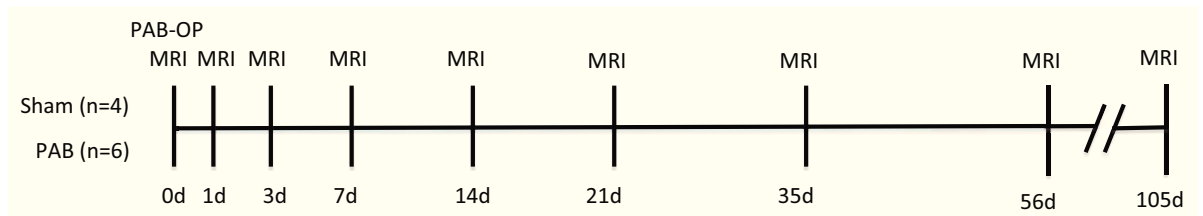


Figure 2.1 – Staging study - Study plan MRI

### 2.2.1.2 Staging study - Histology & Catheterization

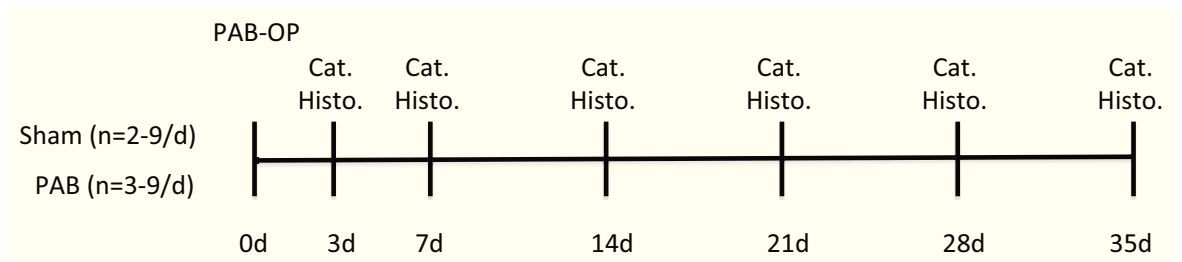


Figure 2.2 – Staging study - Study plan histology & catheterization; Cat. indicates catheterization; Histo., histology

### 2.2.1.3 Treatment study

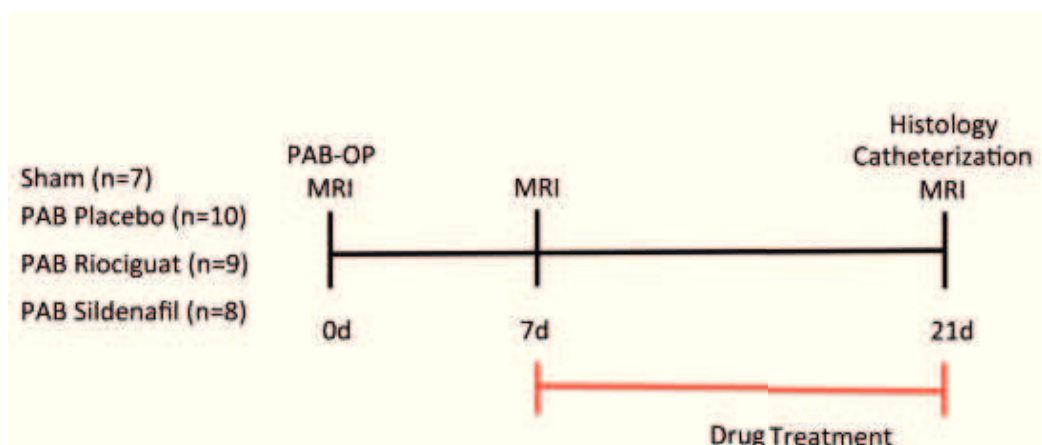
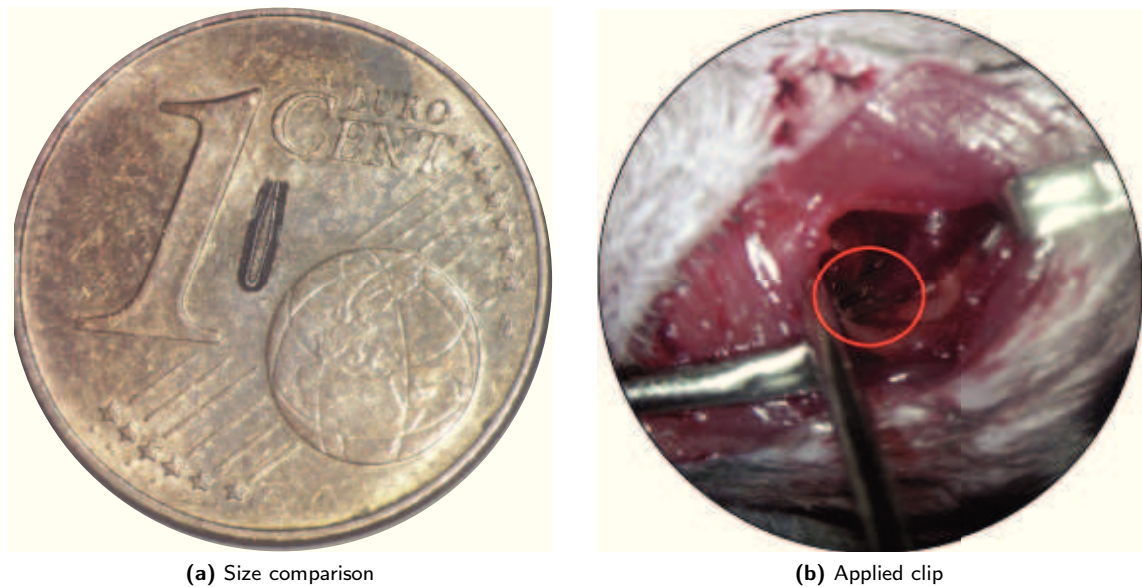


Figure 2.3 – Treatment study - Study plan



**Figure 2.4** – The titanium hemoclip used for banding of the pulmonary artery. a) Size comparison to a 1 cent coin. b) The hemoclip applied to a mouse pulmonary artery.

### 2.2.2 Pulmonary artery banding

Chronic pressure overload was induced by surgical banding of the main pulmonary artery. Mice were anesthetised using isoflurane (1.5–2.5 % v/v). Buprenorphine hydrochlorid (0.05 mg/kg bw, Vetergesic, Braun) was administered s.c. as an analgesic prior to operation. The animals were placed on a heating pad to maintain body temperature and were artificially ventilated with a rodent ventilator (MiniVent Type 845, Hugo Sachs Elektronik KG, March, Germany) using a mixture of 0.5 L/min oxygen and 1.0 L/min medical air. The rodent ventilator was set to a stroke volume of 250  $\mu$ L and 200 strokes/min. A lateral thoracotomy was performed to gain access to the pulmonary artery. The skin was shaved, and an incision made half-way between the sternum and the axilla. The pectoralis major and pectoralis minor muscles were bluntly dissected and moved to the sides to gain access to the third intercostal space, which was opened. The pericard was opened and the pulmonary artery bluntly dissected from the ascending aorta. The pulmonary artery was constricted to 350  $\mu$ m using titanium clips (Hemoclip<sup>®</sup>, Weck, Germany) and a modified, adjustable clip applier (Hemoclip<sup>®</sup>, Weck, Germany). After banding, the intercostal space was closed by attaching the ribs using a vicryl suture (Vicryl<sup>®</sup> Plus 5-0, Ethicon, Germany). The pectoralis major and pectoralis minor were returned into their original

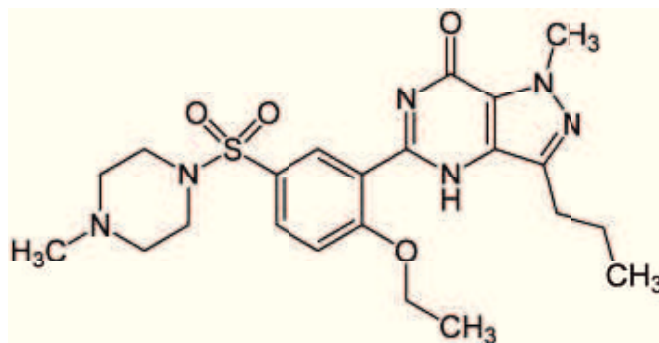


Figure 2.5 – Sildenafil - Chemical structure

position and the skin was sewn with a vicryl suture (Vicryl® Plus 5-0, Ethicon, Germany). 0.5 mL Glucosteril 5% (Fresenius Kabi, Germany) was injected s.c. to compensate for potential fluid loss. Isoflurane administration was terminated and the animals were extubated once they started regaining consciousness. The whole operation lasted for approximately 20 minutes. Carprofen (8 mg/kg/d, Rimadyl®, Pfizer) was administered via drinking water for 3 days post-operation. The sham group underwent the same procedure except that no titanium clip was applied.

## 2.2.3 Drug treatment

### 2.2.3.1 Sildenafil

Sildenafil was prepared by dissolving 0.6 g citric acid and 250 mg sildenafil in 300 ml H<sub>2</sub>O, constantly mixing the solution with a magnetic stirrer (VMS-C7, VWR International GmbH, Darmstadt, Germany), until the citric acid and sildenafil were dissolved. The drug was administered via drinking water. With mice expected to drink 3 ml/d, the treatment provided a dosage of 100 mg/kg/d. This dose was shown to yield a mean free plasma concentration of  $(10.4 \pm 2.3)$  nM.<sup>25</sup> The IC<sub>50</sub>, the amount of drug which inhibits 50% of PDE5A activity in the presence of substrate, of sildenafil is 5 to 10 nM. This is comparable to levels obtained in humans at doses of 1 mg/kg/d and reflects the nearly 100-fold higher rate of metabolism of sildenafil in mice.<sup>139</sup>

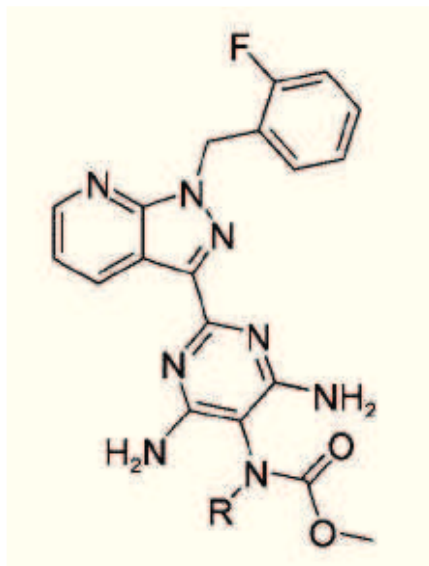


Figure 2.6 – Riociguat - Chemical structure

### 2.2.3.2 Riociguat

Riociguat was prepared by dissolving 0.75 mg riociguat in 0.25 ml 1% methylcellulose. 1% methylcellulose was prepared by dissolving 1 g methylcellulose in 100 ml H<sub>2</sub>O. 0.25 ml of the riociguat/methylcellulose solution was given to mice via oral gavage daily to provide a dose of 30 mg/kg/d.

## 2.2.4 Magnetic Resonance Imaging

Depending on the type of study, cardiac MRI was either performed on days 0 (pre-OP), 1, 3, 7, 14, 21, 35, 56 and 105 post-OP (staging study), or on days 0 (pre-OP), 7 (start of treatment) and day 21. Cardiac MRI measurements were performed on a 7.0 T Bruker PharmaScan, equipped with a 300 mT/m gradient system, using a custom-built circularly polarized birdcage resonator and the IntraGate<sup>TM</sup> self-gating tool (Bruker, Ettlingen, Germany). Mice were measured under volatile isoflurane (2.0% v/v) anesthesia delivered in an oxygen/medical air (0.5/0.5 L/min) mixture. Body temperature was maintained at 37 °C throughout the experiment. The measurement is based on the gradient echo method (repetition time = 6.2 ms; echo time = 1.6 ms; field of view = 2.20x2.20 cm; slice thickness = 1.0 mm; matrix = 128x128; repetitions = 100; resolution 0.0172 cm/pixel). The imaging plane was localized using scout images showing the sagittal and coronal view of the heart, followed by

acquisition in axial view, orthogonally to the septum of both scout scans. Multiple (9–10) contiguous axial slices were acquired for complete coverage of the left and right ventricle. MRI data was analyzed using MASS® 4Mice digital imaging software (Medis, Leiden, Netherlands).

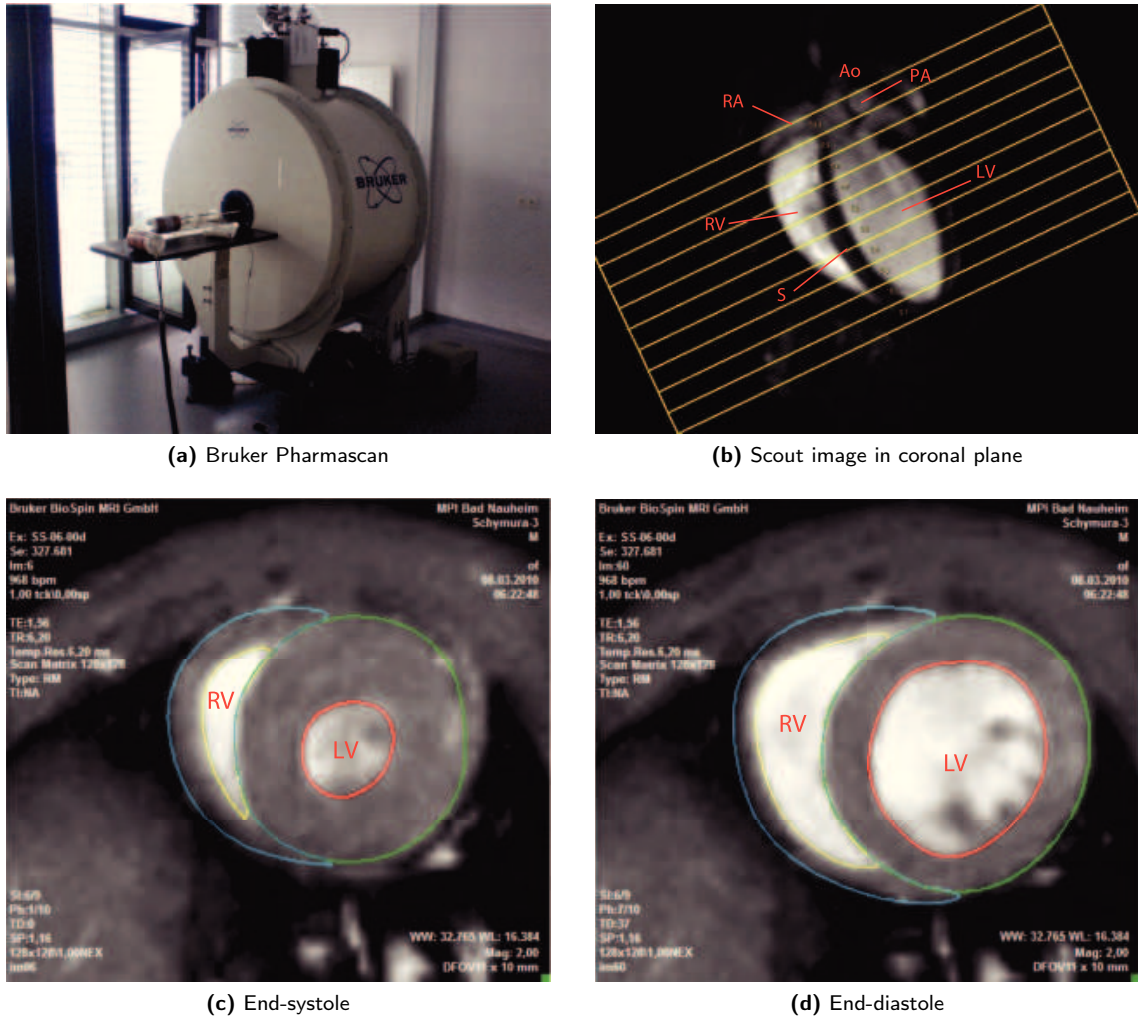


**Figure 2.7** – Bruker Pharmascan (a) and MRI images of a mouse heart before operation (b, c, d). b) Mouse heart in coronal view with a grid (yellow), depicting the axial slices which will be measured. c, d) Example of an axial slice on the mid-papillary level at end-systole and end-diastole. RA indicates right atrium; RV, right ventricle; LV, left ventricle; S, septum; PA, pulmonary artery; Ao, aorta

### 2.2.5 Analysis of MRI images

To determine the volumes of the ventricles, the MASS® 4Mice program employs the Simpson method. Simpson’s rule is based on the summation of partial volumes

( $S_N$ ) to determine the total volume ( $V_t$ ):

$$V_t = S_1 + S_2 + S_3 + \cdots + S_{N-1} + S_N \quad (2.1)$$

This method is considered to be the most accurate, as it does not depend on making geometrical assumptions.<sup>141</sup> It is possible to employ the Simpson method as the whole heart is imaged, without any interslice gaps, and by using a small slice thickness. The small slice thickness, along with the omission of interslice gaps has the further benefit of the reduction of partial volume effects. To calculate the volume, for every slice the end-systolic and end-diastolic frames had to be determined first. The slice with the largest ventricular volume was determined to be the end-diastolic frame, whilst the slice with the smallest volume was determined to be the end-systolic frame. The boundaries of the diastolic and systolic endo- and epicardial borders were then manually outlined (Fig. 2.7, p. 36). This allowed the software to calculate the end-diastolic (EDV) and end-systolic volumes (ESV) for each slice, as it was known that the slice thickness was 1 mm. The area inside the endocardial borders determined the ventricular volume, whilst the area inside the epicardial border minus the endocardial area determined the myocardial volume. To calculate the total diastolic and systolic ventricular volume, the software then summed up the calculated single slice volumes. To calculate the myocardial mass, the myocardial volume was multiplied by the specific density of myocardial tissue, which is 1.05 g/ml.

### 2.2.5.1 Calculation of derived parameters

From knowing the EDV, ESV and heart rate (HR), it is possible to derive the following standard clinical parameters:

**Stroke volume** The stroke volume (SV) is calculated by subtracting the ESV from the EDV. It is the amount of blood which is pumped out from the heart with every heartbeat, and is a parameter for the contractility and performance of the

heart.

$$SV = EDV - ESV \quad (2.2)$$

**Ejection fraction** The ejection fraction (EF) is calculated by dividing the SV by the EDV. The value reflects the relative amount of blood which is pumped out of the heart with every heartbeat. The EF, like the SV is a parameter for the contractility and performance of the heart. Right ventricular EF is the most widely accepted and used measure of right ventricular function.<sup>17</sup> Healthy patients have an EF of 60–75%, whilst an EF of 40-60% is defined as a mild contractile dysfunction, 30-40% as a modest dysfunction, and  $\leq 30\%$  as severe.

$$EF = \frac{SV}{EDV} \quad (2.3)$$

**Cardiac output** The cardiac output (CO) is the volume of blood being pumped by the heart in the time interval of one minute. It is calculated by multiplying SV with HR.

$$CO = SV \times HR \quad (2.4)$$

**Left ventricular eccentricity index** The left ventricular eccentricity index (LVEI) reflects the degree of septal flattening, which results in an abnormal LV shape. The value is calculated for both end-diastole and end-systole, in the axial plane on the mid-papillary level. It is calculated as the ratio of the length of the major axis of the LV ( $L_1$ ), which runs parallel to the septum, to the length of the minor axis of the LV ( $L_2$ ), which runs perpendicular to the septum (Fig. 2.8, p. 39). In healthy human hearts this value should approximate 1.0.

$$LVEI = \frac{L_1}{L_2} \quad (2.5)$$

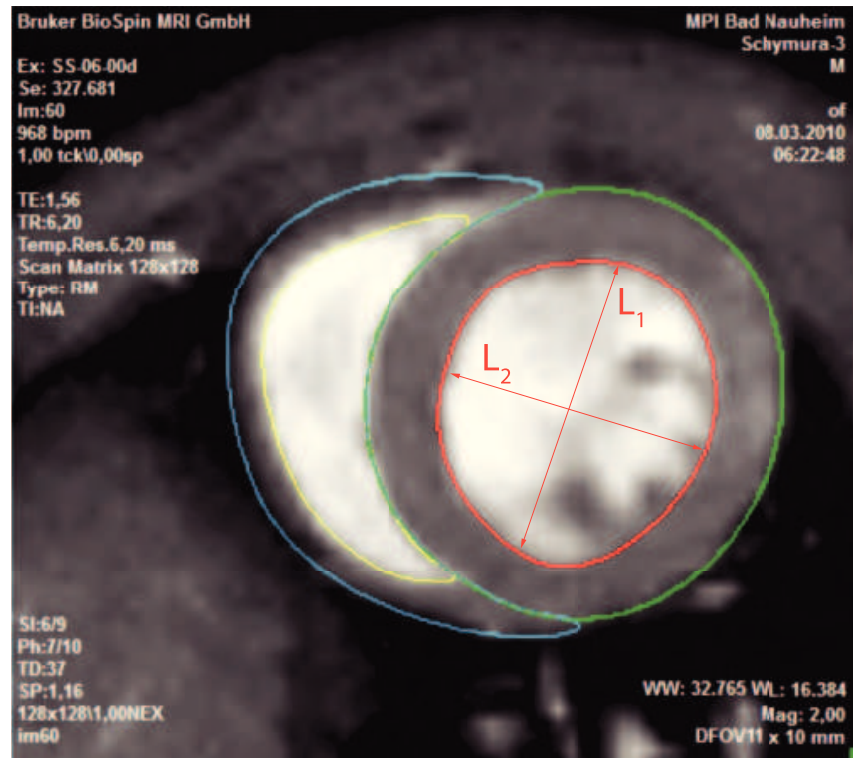


**Figure 2.8** – Measuring the length of the axes ( $L_1$ ,  $L_2$ ) for calculating the left ventricular eccentricity index

### 2.2.6 In vivo hemodynamics

21 days after PAB, mice were anesthetized using isoflurane (1.5% v/v) and placed on a heating pad throughout the measurement to maintain physiological body temperature. Heart rate and systemic blood pressure were measured by catheterizing the carotid artery. The right jugular vein was used for catheterization of the right ventricle to measure right ventricular pressure. Hemodynamic measurements were performed using a Millar microtip catheter (SPR-671, FMI, Foehr Medial Instruments GmbH, Seeheim/Ober-Beerbach, Germany) and a PowerLab 8/30 System with the Chart 7.0 Software (ADInstruments GmbH, Spechbach, Germany).

### 2.2.7 Tissue processing

After pressure measurement the animals were exsanguinated and the heart was isolated. The right ventricle was dissected from the left ventricle and septum (LV+S) and weighed to obtain the right ventricle to left ventricle plus septum ratio (RV/LV+S). For histological analysis, the right ventricle was fixed in 4%

paraformaldehyde (PFA).

## 2.2.8 Histology

The right ventricles were embedded in paraffin blocks and sections of 3  $\mu\text{m}$  were cut. The degree of interstitial fibrosis was assessed by picrosirius red staining. Using polarized light, at a 40x magnification, the amount of collagen was measured in 20–40 randomly chosen areas uniformly distributed across the histological section. The observer was blinded to treatment in each animal. The percentage of collagen was measured as the ratio of the area occupied by collagen to the total area of the section. For the assessment of cardiomyocyte diameter, transversally cut paraffin slides were stained with WGA-FITC and DAPI, which were visualized under fluorescent light (Leica DM6000 B [Leica Microsystems GmbH, Wetzlar, Germany]; DAPI: Filterblock A, excitation wavelength: 340–380 nm; WGA FITC: Filterblock I3, excitation wavelength: 450–490 nm). Per slide, 5–6 randomly chosen fields of view, uniformly distributed across the histological section, were analyzed. Only cardiomyocytes which contained a nucleus were measured. The short-axis diameter of cardiomyocytes was measured.

### 2.2.8.1 Picrosirius red staining

0.1 % picrosirius red was prepared by dissolving 200 mg sirius red (Siriusrot F3B, C.I. 35780, Niepötter Labortechnik, Germany) in 200 ml saturated picric acid (Picric acid solution 1.2 % BioChemica, Lot: 1O004669, AppliChem GmbH, Germany). The pH was fixed at 2. 1 % glacial acetic acid was prepared by dissolving 10 ml of glacial acetic acid (Essigsäure, Rotipuran® 100 %, p.a., Carl Roth GmbH + Co. KG, Germany) in dH<sub>2</sub>O. The following protocol was used to stain paraffin sections with picrosirius red:

**Table 2.3** – Picrosirius red staining protocol

Step	Solution/incubation	Remarks	Time
1	Incubation at 58 °C	Melting of paraffin	60
2	Xylol	Deparaffinization	10
3	Xylol	Deparaffinization	10
4	Xylol	Deparaffinization	10
5	99.6 % Ethanol	Rehydration	5
6	99.6 % Ethanol	Rehydration	5
7	96 % Ethanol	Rehydration	5
8	70 % Ethanol	Rehydration	5
9	dH <sub>2</sub> O	Washing	3
10	0.1 % Picrosirius Red	Staining	60
11	1 % Glacial acetic acid	Washing	0.5
12	1 % Glacial acetic acid	Washing	0.5
13	1 % Glacial acetic acid	Washing	0.5
14	dH <sub>2</sub> O	Washing	1
15	70 % Ethanol	Dehydration	5
16	96 % Ethanol	Dehydration	5
17	99.6 % Ethanol	Dehydration	5
18	Xylol	Clearing	10
19	Xylol	Clearing	10
20	Mounting and coverslip		
21	Dry at room temperature		Overnight

### 2.2.8.2 WGA-FITC staining

PBS was prepared by dissolving 1 part 10x PBS in 9 parts dH<sub>2</sub>O. 10x PBS was made up of 1.44 g/l KH<sub>2</sub>PO<sub>4</sub> (MW 136.09), 7.95 g/l Na<sub>2</sub>HPO<sub>4</sub> (MW 141.96) and 90 g/l NaCl (MW 58.44), and fixed to pH 7.4. Blocking solution (3 % BSA) was prepared by dissolving 3 g BSA and 200 µl Triton X100 in 100 ml 1x PBS. WGA-

FITC stock solution was prepared by dissolving 0.5 mg WGA-FITC (Sigma-Aldrich Chemie GmbH, Taufkirchen, Germany) in 0.5 ml 1x PBS. WGA-FITC working solution (10  $\mu\text{g}/\text{ml}$ ) was prepared by diluting 1 part WGA-FITC stock solution in 99 parts 1x PBS. DAPI stock solution (5 mg/ml) was prepared by dissolving 10 mg DAPI dihydrochloride (MW = 350.3) (Invitrogen/Life Technologies GmbH, Lot: 633921, Darmstadt, Germany) in 2 ml dH<sub>2</sub>O. DAPI working solution (500 ng/ml) was prepared by diluting one part DAPI stock solution in 9999 parts PBS. The following protocol was used to stain paraffin sections with WGA-FITC:

**Table 2.4 – WGA-FITC staining**

<b>Step</b>	<b>Solution/incubation</b>	<b>Remarks</b>	<b>Time</b>
1	Incubation at 58 °C	Melting of paraffin	60
2	Xylol	Deparaffinization	10
3	Xylol	Deparaffinization	10
4	Xylol	Deparaffinization	10
5	99.6 % Ethanol	Rehydration	5
6	99.6 % Ethanol	Rehydration	5
7	96 % Ethanol	Rehydration	5
8	70 % Ethanol	Rehydration	5
9	dH <sub>2</sub> O	Washing	3
10	PBS	Washing	5
11	Blocking solution	Blocking	60
12	PBS	Washing	5
13	PBS	Washing	5
14	PBS	Washing	5
15	PBS	Washing	5
16	WGA-FITC	Staining	60
17	PBS	Washing	5
18	PBS	Washing	5
19	PBS	Washing	5
20	DAPI	Staining	10

Continued on next page

Table 2.4 – continued from previous page

Step	Solution/incubation	Remarks	Time
21	PBS	Washing	5
22	PBS	Washing	5
23	PBS	Washing	5
24	Mounting and coverslip		

### 2.2.9 Statistics

Data were analyzed with GraphPad Prism (version 5.0c, GraphPad Software Inc.). All values are given as mean  $\pm$  SEM. Differences between groups were assessed using one-way ANOVA and repeated measures ANOVA with Bonferroni post-hoc-test for multiple comparisons. A  $p$  value of  $<0.05$  was regarded as significant. Linear regression was used to calculate missing values in the staging study to allow for repeated measures ANOVA to be carried out.

# Chapter 3

## Results

### 3.1 Staging Study

The purpose of the staging study was to characterize the time course of effects which banding is having on the murine heart. To achieve this goal, C57Bl/6 mice were randomly assigned to either sham or banding group. Then an MRI analysis of the heart was performed as described in the methods section, before surgery. The only difference in the operation procedure between the two groups was the omission of the titanium clip in sham mice. MRI analyses were subsequently performed 1, 3, 7, 14, 21, 35, 56 and 105 days after operation.

Furthermore, additional mice were operated to assess the time course of fibrosis and cardiomyocyte growth, and of right ventricular and systemic arterial pressure. For this, animals were sacrificed 3, 7, 14, 21, 28 and 35 days after operation.

#### 3.1.1 Time Course of Function and Morphology of the Banded Heart

PAB led to severe dilatation, hypertrophy, and functional impairment of the right ventricle. As a result, the left ventricle was compressed to its side and was functionally impaired as well due to interventricular interaction, reflected in severely reduced end-systolic and end-diastolic diameters, and a significantly reduced stroke volume (example of the effects of 5 weeks of banding shown in fig. 3.1, p. 45, and fig. 3.2,

p. 46). Whilst the right ventricular mass, cardiomyocyte size and fibrosis showed a progressive increase over the course of the study, the functional effects of banding could be distinguished into three phases: a rapid, initial functional impairment at day 1 after operation; a compensatory response between days 1 to 7; and a gradual decompensation following day 7. Approximately 50 days after operation, animals in the PAB group started to die, and had a median survival of 124 days. None of the sham-operated animals died during the study.

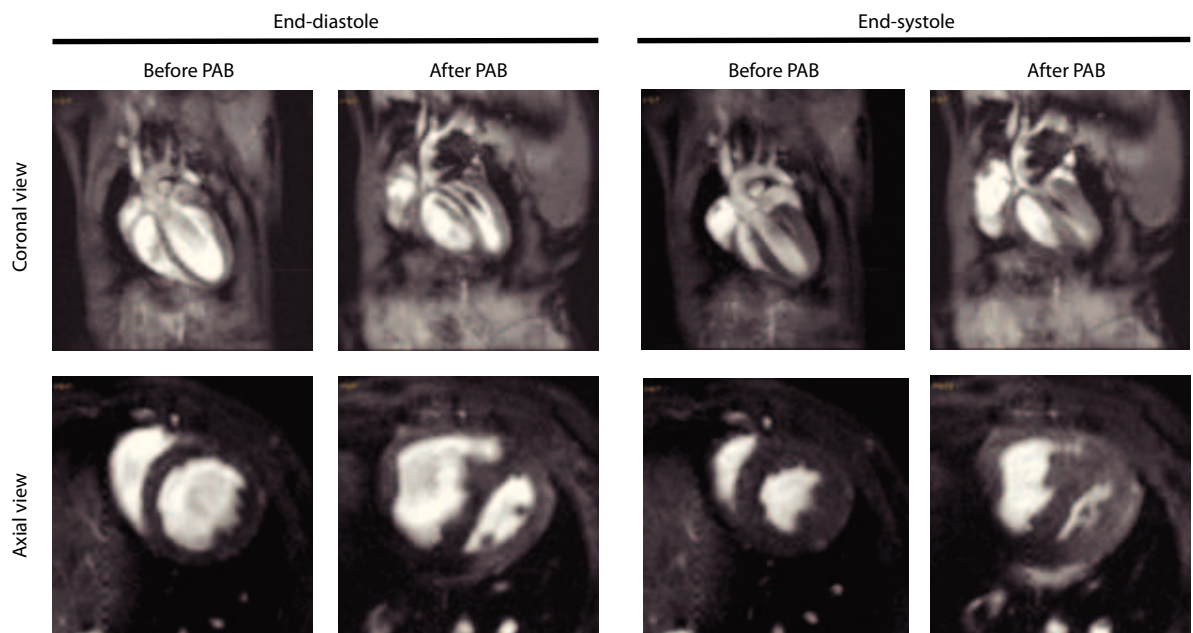


**Figure 3.1** – MRI images of a mouse heart in coronal and axial view at end-diastole and end-systole before and 5 weeks after PAB.

### 3.1.2 Right Ventricular Pressure

After banding of the pulmonary artery, the right ventricular systolic pressure increased significantly over sham-operated animals, eventually plateauing after 21 days (fig. 3.3, p. 47). The first significant difference between the banding and the sham group was apparent at day 7 (RVP<sub>sys</sub>:  $28.5 \pm 0.9$  mmHg vs.  $46.9 \pm 3.5$  mmHg [Sham vs. PAB];  $p < 0.01$ ). The pressure continues to increase until day 21, where it reaches a plateau level at about 65 mmHg. The right ventricular systolic pressure of sham-operated animals stays at a physiological level of about 28 mmHg throughout the study, making the difference between the sham and banding group highly

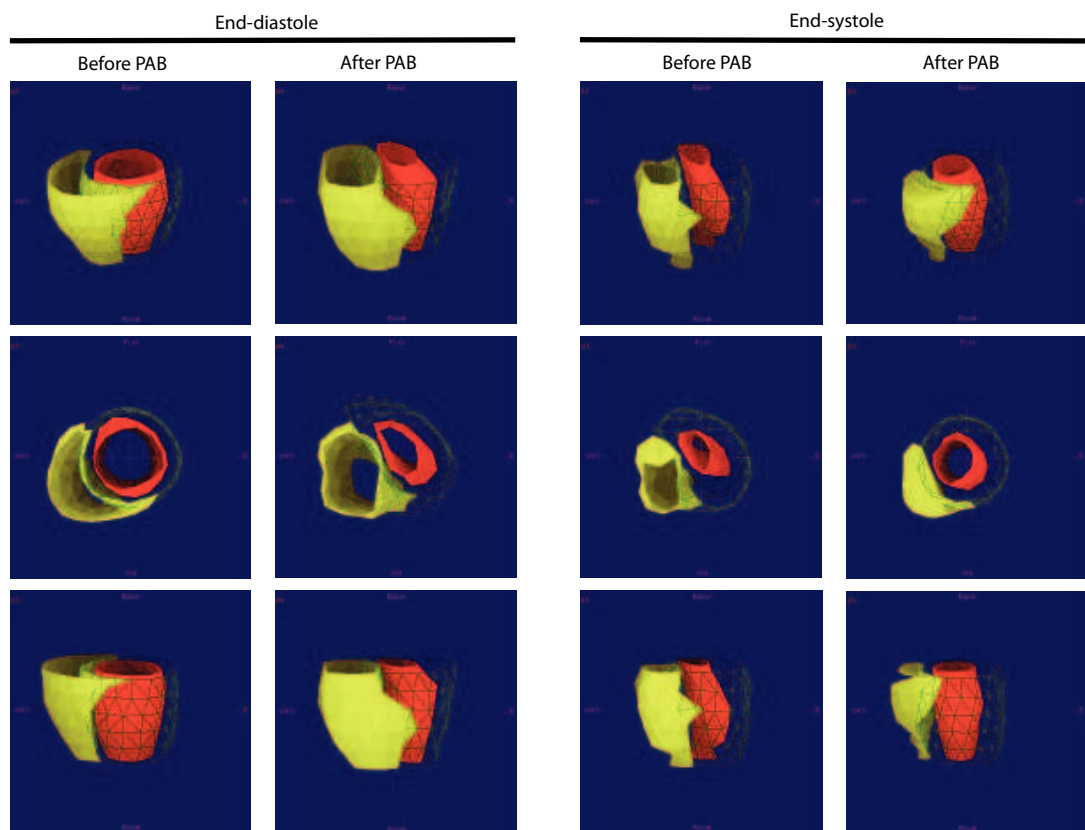


**Figure 3.2** – Three-dimensional reconstructions of the mouse heart shown in figure 3.1, before and after banding of the pulmonary artery at end-diastole and end-systole in different views. The left ventricular lumen is colored in red, the right ventricular lumen in yellow, and the left ventricular myocardium is depicted as a green grid structure.

significant ( $p < 0.001$ ).

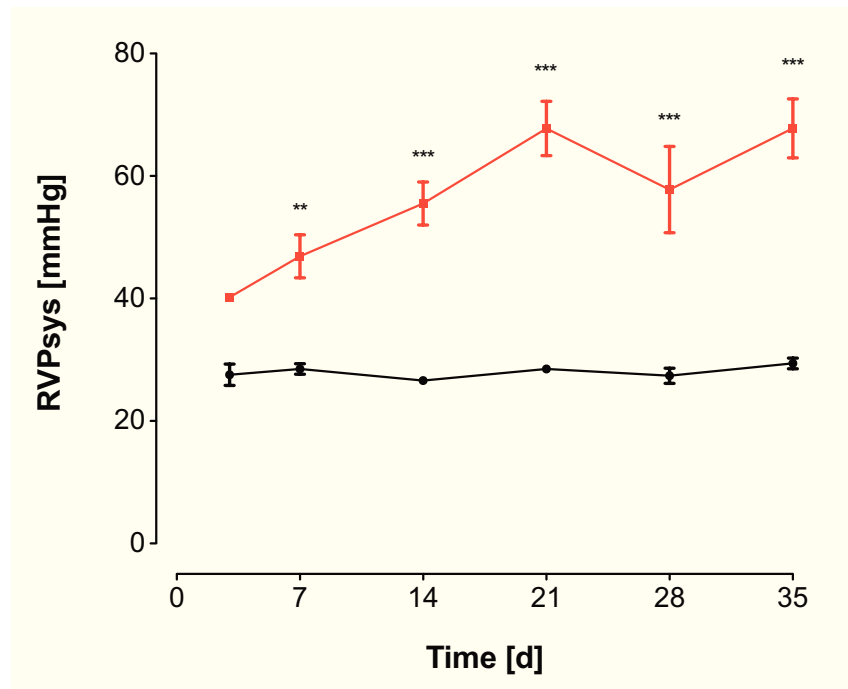


**Figure 3.3 – Effects of banding on the right ventricular systolic pressure (RVpsys, mmHg); PAB (—), sham (—); d, day. \*\*\* $p < 0.001$ , \*\* $p < 0.01$**

### 3.1.3 Right Ventricular Dilatation and Impaired Function

The end-systolic and the end-diastolic ventricular volume was significantly increased in PAB mice, as compared to sham-operated mice, reflecting right ventricular dilatation and impaired contractile function (fig. 3.4, p. 48). This is reflected in decreased stroke volume and ejection fraction in PAB animals (fig. 3.5, p. 49). The effects of banding follow a triphasic response: Both right ventricular end-diastolic and end-systolic volume initially (1 day after the banding procedure) increase significantly, i.e. the right ventricle strongly dilates and its contractile capacity is impaired (RV EDV:  $45.6 \pm 1.4 \mu\text{l}$  vs.  $63.0 \pm 3.8 \mu\text{l}$  [Sham vs. PAB],  $p < 0.05$ ; RV ESV:  $11.9 \pm 0.2 \mu\text{l}$  vs.  $38.4 \pm 5.5 \mu\text{l}$  [Sham vs. PAB];  $p < 0.001$ ). From days 3 to 7, dilatation as well as the right ventricular end-systolic volume recede back near sham values (RV EDV:  $43.4 \pm 2.6 \mu\text{l}$  vs.  $45.6 \pm 4.4 \mu\text{l}$  [Sham vs. PAB],  $p > 0.05$ ; RV ESV:  $11.1 \pm 1.5 \mu\text{l}$  vs.  $24.3 \pm 4.1 \mu\text{l}$  [Sham vs. PAB];  $p > 0.05$ ). Following day 7 until the end of the study, the right ventricle gradually dilates further, albeit the difference to the sham group

remains non-significant, and the right ventricular end-systolic volume continues to increase.

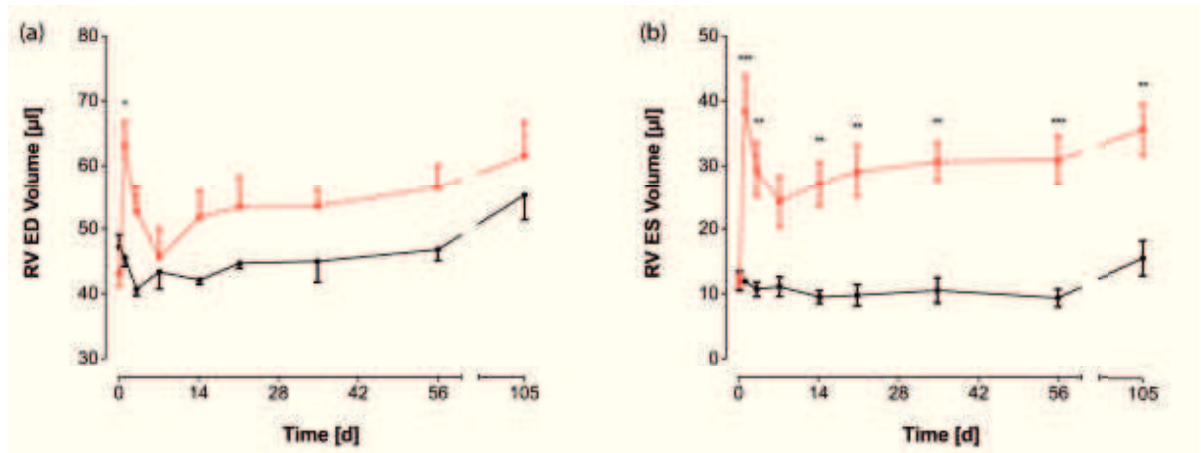


**Figure 3.4 – Effects of banding on right ventricular volumes.** (a) Right ventricular end-diastolic volume (RV ED Volume,  $\mu\text{l}$ ) (b) Right ventricular end-systolic volume (RV ES Volume,  $\mu\text{l}$ ); PAB (—), sham (—); d, day. \*\*\* $p<0.001$ , \*\* $p<0.01$ , \* $p<0.05$

This triphasic response is also expressed in the right ventricular ejection fraction, which is derived from the right ventricular end-diastolic and end-systolic volumes: after an early drop of the ejection fraction at day 1 after operation (RV EF:  $73.8 \pm 0.8 \mu\text{l}$  vs.  $40.4 \pm 5.4 \mu\text{l}$  [Sham vs. PAB],  $p<0.001$ ), the ejection fraction slightly recovers until day 7 to 14 (RV EF:  $74.7 \pm 2.3 \mu\text{l}$  vs.  $48.4 \pm 4.2 \mu\text{l}$  at day 7 [Sham vs. PAB],  $p<0.001$ ), after which it continues to decline. The phasic response for the right ventricular stroke volume is less apparent: after an initial decline until day 7, it recovers slightly until days 14 to 21, after which its slope resembles that of the control group. It is interesting to note, that the right ventricular stroke volume of the sham-operated animals also declines in the first week following operation, after which it recovers back to baseline values. Apparently this is an effect caused by the operation per se.

### 3.1.4 Right Ventricular Hypertrophy

PAB significantly increased the mass of the right ventricle, whereas there was no change in sham-operated animals (fig. 3.6, p. 49). Right ventricular weight rose rapidly after operation, becoming significantly higher three days after operation (RV Mass / Bodyweight:  $2.1 \pm 0.1 \text{ mg/g}$  vs.  $3.0 \pm 0.1 \text{ mg/g}$  [Sham vs. PAB],  $p<0.01$ ; RV

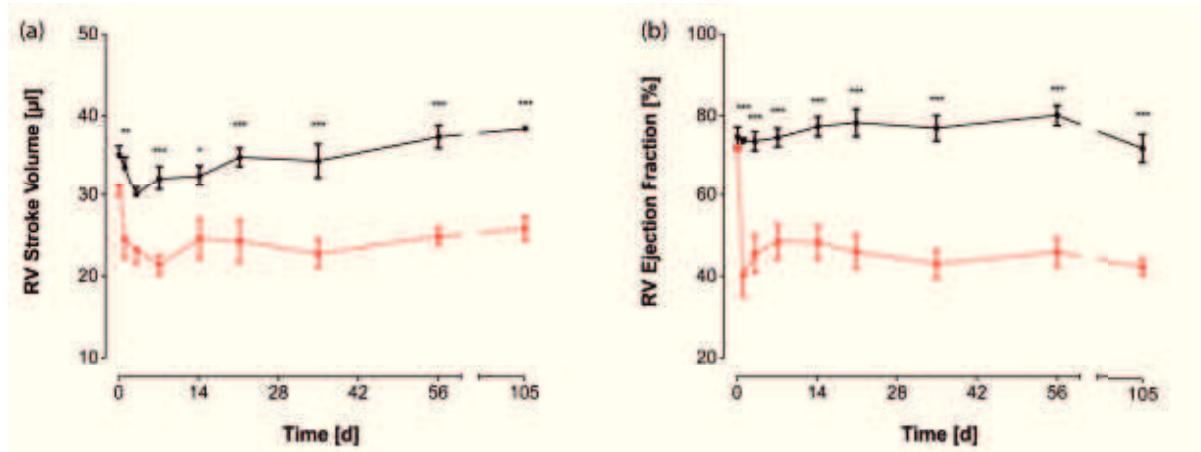


**Figure 3.5 – Effects on banding on right ventricular functional parameters.** (a) Right ventricular stroke volume (RV Stroke Volume,  $\mu\text{l}$ ) (b) Right ventricular ejection fraction (RV Ejection Fraction, %); PAB (—), sham (—); d, day. \*\*\* $p < 0.001$ , \*\* $p < 0.01$ , \* $p < 0.05$

Mass / LV Mass:  $0.6 \pm 0.0 \text{ mg/mg}$  vs.  $0.8 \pm 0.0 \text{ mg/mg}$  [Sham vs. PAB],  $p < 0.01$ ). Bodyweight did not significantly differ between both groups (tables A.1 and A.2, pp. 95 and 97). In the course of the study, the right ventricular mass to bodyweight ratio eventually reached a value of  $3.5 \pm 0.3 \text{ mg/g}$  ( $p < 0.001$  vs. Sham) at day 105, and the right ventricular weight to left ventricular weight ratio increased to  $1.1 \pm 0.1 \text{ mg/g}$  ( $p < 0.001$  vs. Sham).

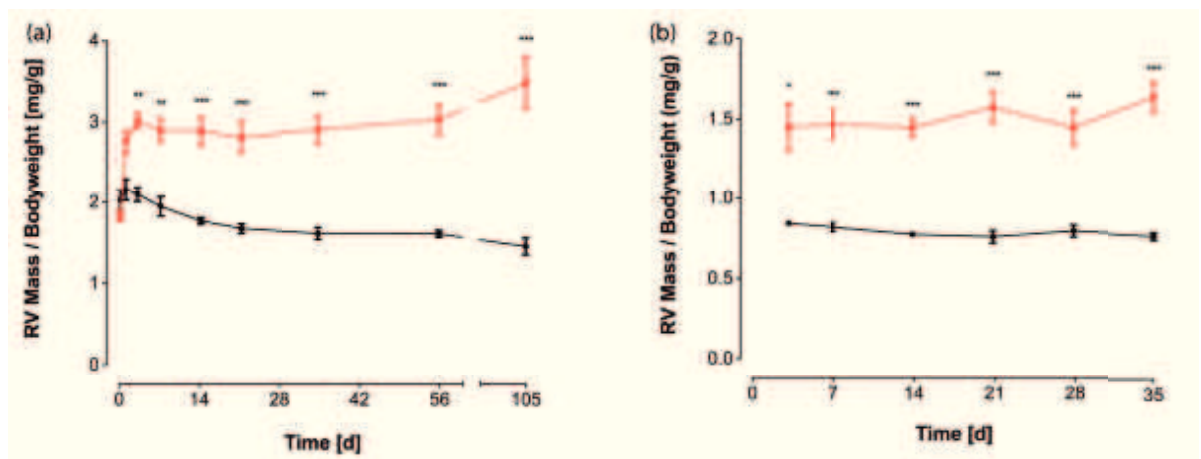


**Figure 3.6 – Effects of banding on right ventricular hypertrophy.** (a) Right ventricular mass to bodyweight ratio (RV Mass / Bodyweight,  $\text{mg/g}$ ), RV mass data derived from MRI measurements (b) as before, but RV mass data derived from harvest organ weight; PAB (—), sham (—); d, day. \*\*\* $p < 0.001$ , \*\* $p < 0.01$ , \* $p < 0.05$

There were no major difference between the left ventricular weight of the PAB and sham group (fig. 3.8, p. 50). What is apparent though, is the non-significant decrease of left ventricular weight of the banded animals: A likely explanation for this is the decreased stroke volume the left ventricle has to deal with: due to the

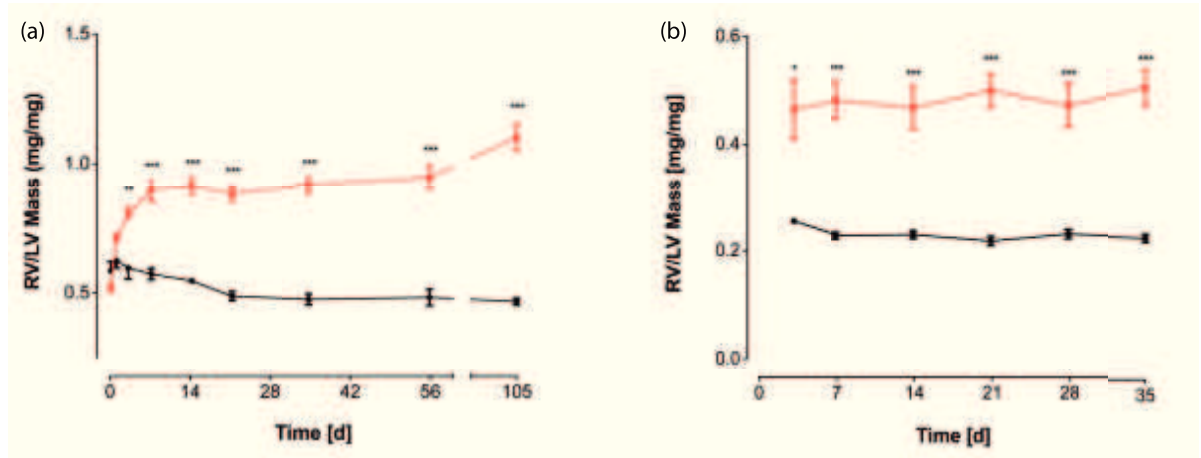


**Figure 3.7 – Effects of banding on right ventricular hypertrophy.** (a) Right ventricular mass to left ventricular mass ratio (RV/LV Mass, mg/mg), ventricular weight data derived from MRI measurements (b) as before, but ventricular weight data derived from harvest organ weights; PAB (—), sham (—); d, day. \*\*\* $p < 0.001$ , \*\* $p < 0.01$ , \* $p < 0.05$

decreased need for force production, the left ventricle adapts to the new situation by a decrease in weight.

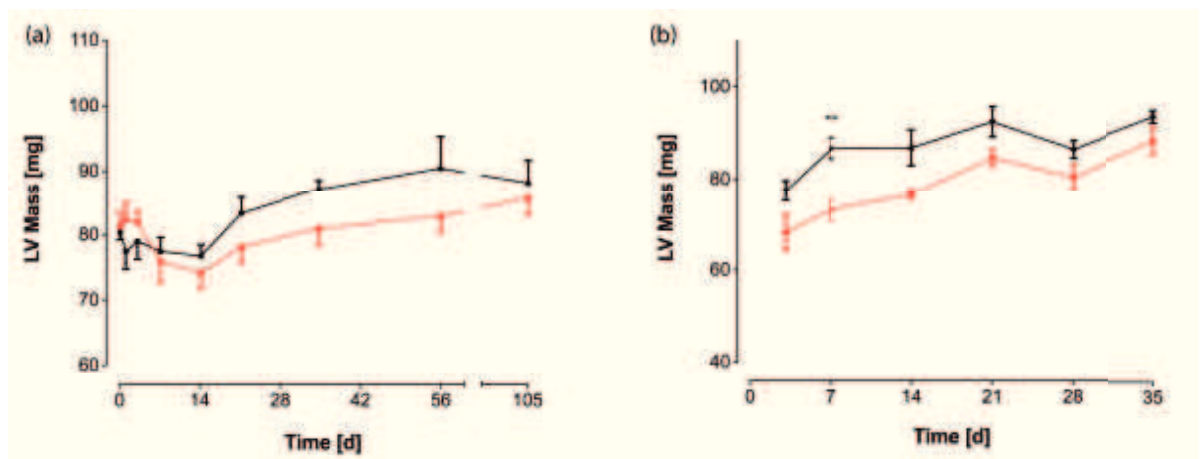


**Figure 3.8 – Effects of banding on left ventricular mass**(a) Left ventricular mass data derived from MRI measurements (LV Mass, mg) (b) as before, but LV mass data derived from harvest organ weights; PAB (—), sham (—); d, day. \*\*\* $p < 0.001$

The harvest data, shown in graph (b) in figures 3.6, 3.8 and 3.7, show the excellent agreement with the MRI data. The only apparent difference is the over-estimation of the right ventricular mass by the MRI analysis software, which is about two-fold. As this is the same for both the banding and the sham group, this does not jeopardize detecting differences between the groups, as can be seen from the figures.

### 3.1.5 Functional Impairment of the Left Ventricle

Due to interventricular interaction, PAB reduced the left-ventricular end-diastolic and end-systolic volumes, as the left heart was displaced by the dilated and hypertrophied right ventricle (fig. 3.9, p. 51). The left ventricular end-diastolic volume became significantly different from the sham group on day 7 post operation (LV EDV:  $52.1 \pm 2.7 \mu\text{l}$  vs.  $33.2 \pm 4.1 \mu\text{l}$  [Sham vs. PAB],  $p < 0.01$ ). Whilst the left ventricular end-diastolic volume of the sham group tended to increase over time, from  $55.5 \pm 2.2 \mu\text{l}$  at day 0, to  $65.8 \pm 3.8 \mu\text{l}$  at day 105), the left ventricular volume of the banding group stayed constantly low throughout the study. This is explained by the slow but steady increase in right ventricular end-diastolic volume and mass (figs. 3.4 and 3.6, pp. 48 and 49), leaving the left ventricle no room to further extend.

Although statistically not significant until day 105 (LV ESV:  $25.8 \pm 4.5 \mu\text{l}$  vs.  $11.5 \pm 2.1 \mu\text{l}$  [Sham vs. PAB],  $p < 0.05$ ), the left ventricular end-systolic volume of the PAB group stayed below the sham group throughout the study.

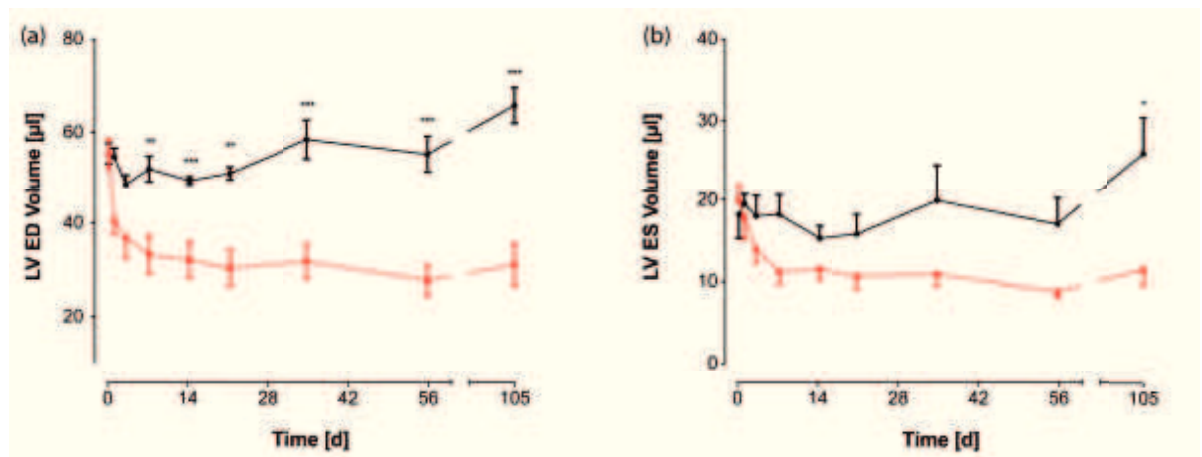


**Figure 3.9 – Effects of banding on left ventricular volumes.** (a) Left ventricular end-diastolic volume (LV ED Volume,  $\mu\text{l}$ ) (b) Left ventricular end-systolic volume (LV ES Volume,  $\mu\text{l}$ ); PAB (—), sham (—); d, day. \*\*\* $p < 0.001$ , \*\* $p < 0.01$ , \* $p < 0.05$

The impaired ability of the left ventricle to properly dilate and fill resulted in a reduced left ventricular stroke volume, whilst the left ventricular ejection fraction basically remained unchanged (fig. 3.10, p. 52). Already one day after surgery, the left ventricular stroke volume in banded animals fell to a level significantly below that of the sham group ( $35.2 \pm 1.2 \mu\text{l}$  vs.  $22.6 \pm 2.8 \mu\text{l}$  [Sham vs. PAB],  $p < 0.01$ ) and, apart from day 7, stayed significantly low until the end of the study. As can be

seen from figure 3.10 (p. 52), the left ventricular stroke volume of the sham group tended to increase over time, keeping up with the increase in bodyweight (tables A.1 and A.2, pp. 95 and 97). As the bodyweight of banded animals continued to increase as well, a constant stroke volume implies decreased end-organ perfusion.

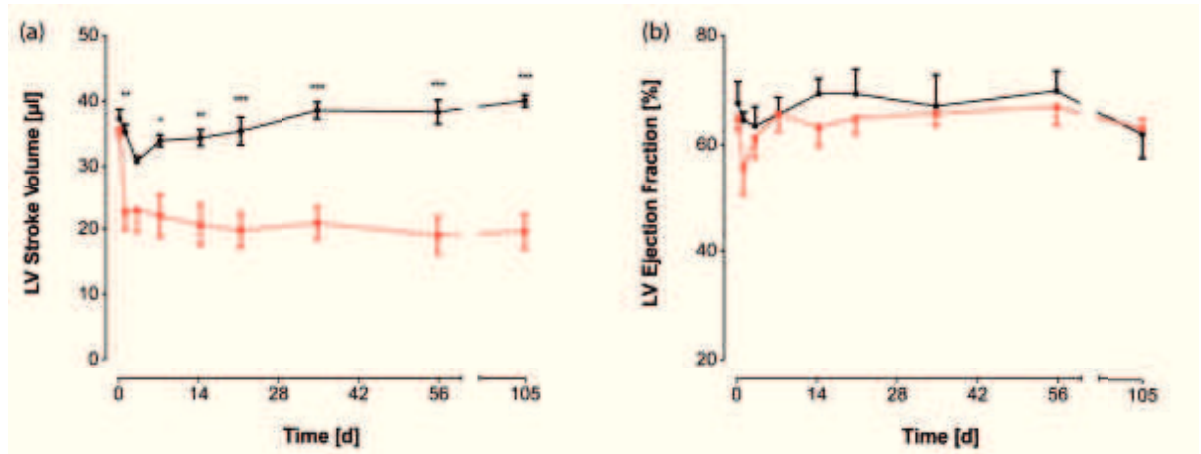


**Figure 3.10 – Effects on banding on left ventricular functional parameters.** (a) Left ventricular stroke volume (LV Stroke Volume,  $\mu\text{l}$ ) (b) Left ventricular ejection fraction (LV Ejection Fraction, %); PAB (—), sham (—); d, day. \*\*\* $p < 0.001$ , \*\* $p < 0.01$ , \* $p < 0.05$

The growth of the right ventricle leads to a compression of the left ventricle. The left ventricular eccentricity index (LVEI) is a parameter, which is a direct reflection of the amount of compression exerted on the left ventricle. In right ventricular pressure and volume overload states it was shown to increase, reflecting an abnormal bulging of the interventricular septum towards the left ventricle.<sup>142</sup> It is calculated by dividing the length of the left ventricular long axis, which runs parallel to the septum, by the length of the left ventricular short axis, which runs perpendicular to the long axis. As can be seen in figure 3.11 (p. 53), banding of the pulmonary artery leads to a rapid increase of the LVEI in systole and diastole one day after banding (LVEI ED:  $1.2 \pm 0.0$  mm/mm vs.  $1.7 \pm 0.1$  mm/mm [Sham vs. PAB],  $p > 0.05$ ; LVEI ES:  $1.3 \pm 0.0$  mm/mm vs.  $1.7 \pm 0.1$  mm/mm [Sham vs. PAB],  $p > 0.05$ ), which continues to increase and becomes statistically significant until day 105 (LVEI ED:  $1.2 \pm 0.0$  mm/mm vs.  $2.5 \pm 0.4$  mm/mm [Sham vs. PAB],  $p < 0.001$ ; LVEI ES:  $1.2 \pm 0.0$  mm/mm vs.  $3.1 \pm 0.4$  mm/mm [Sham vs. PAB],  $p < 0.001$ ), reflecting the continued growth of the right ventricle, and pressure exerted on the left ventricle.

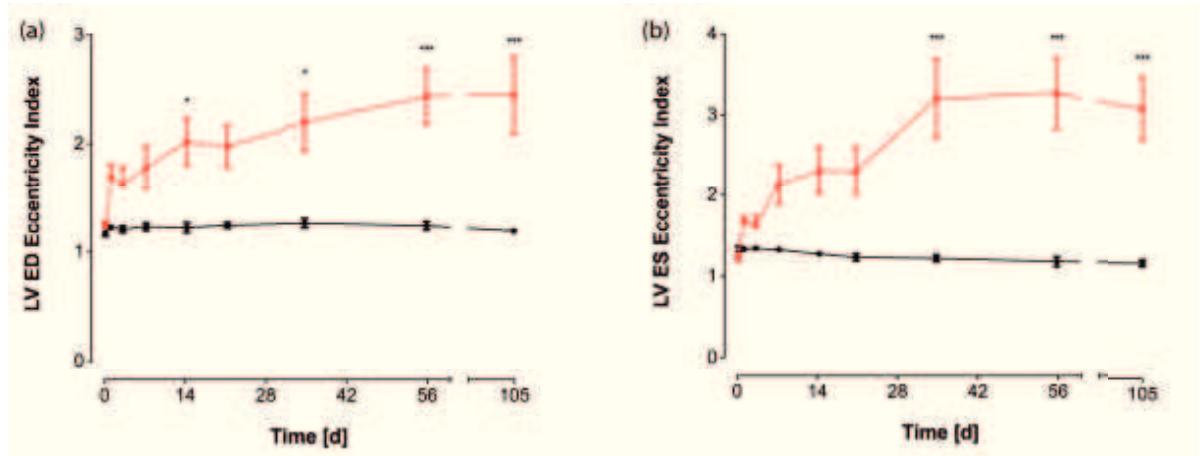


**Figure 3.11 – Effects of banding on pressure of the right ventricle exerted on the left ventricle.** (a) Left ventricular eccentricity index at end-diastole (LV ED Eccentricity Index, mm/mm) (b) Left ventricular eccentricity index at end-systole (LV ES Eccentricity Index, mm/mm); PAB (—), sham (—); d, day. \*\*\* $p < 0.001$ , \*\* $p < 0.01$ , \* $p < 0.05$

### 3.1.6 Systemic Arterial Pressure

PAB led to a decrease of the systemic arterial pressure (fig. 3.12, p. 54), which is a reflection of the decreased cardiac output (fig. 3.14, p. 55). This is especially nice to see on day 7, where the drop in left ventricular cardiac output goes hand in hand with the drop in systemic arterial pressure.

### 3.1.7 Heart Rate and Cardiac Output

Even though the heart rate non-significantly increased in banded animals (fig. 3.13, p. 54), the increase was not sufficient to compensate for the decrease in stroke volume, as the cardiac output remained decreased in banded animals throughout the study (fig. 3.14, p. 55). Nonetheless, it decreased the gap between the two curves, compared to the stroke volume curves.

After an initial drop in left ventricular cardiac output on day one post operation (LV CO:  $17.4 \pm 0.9$  ml/min vs.  $11.3 \pm 1.6$  ml/min [Sham vs. PAB],  $p > 0.05$ ), the output slightly recovers on days 3 to 7, after which it stays constantly low, become statistically significant on day 21 (LV CO:  $19.0 \pm 1.8$  ml/min vs.  $11.03 \pm 0.14$  ml/min [Sham vs. PAB],  $p < 0.05$ ) until the end of the study on day 105 (LV CO:  $18.6 \pm 2.1$  ml/min vs.  $11.1 \pm 1.5$  ml/min [Sham vs. PAB],  $p < 0.05$ ).

The right ventricular cardiac output follows a similar curve as the left ventricular

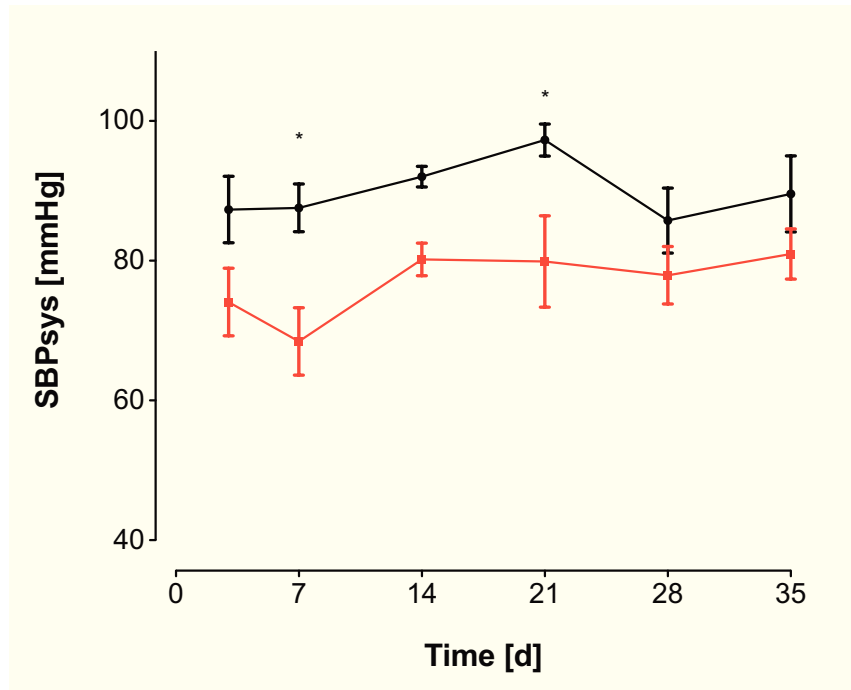


Figure 3.12 – Effects of banding on the systemic arterial pressure (SPsys, mmHg); PAB (—), sham (—); d, day. \* $p < 0.05$

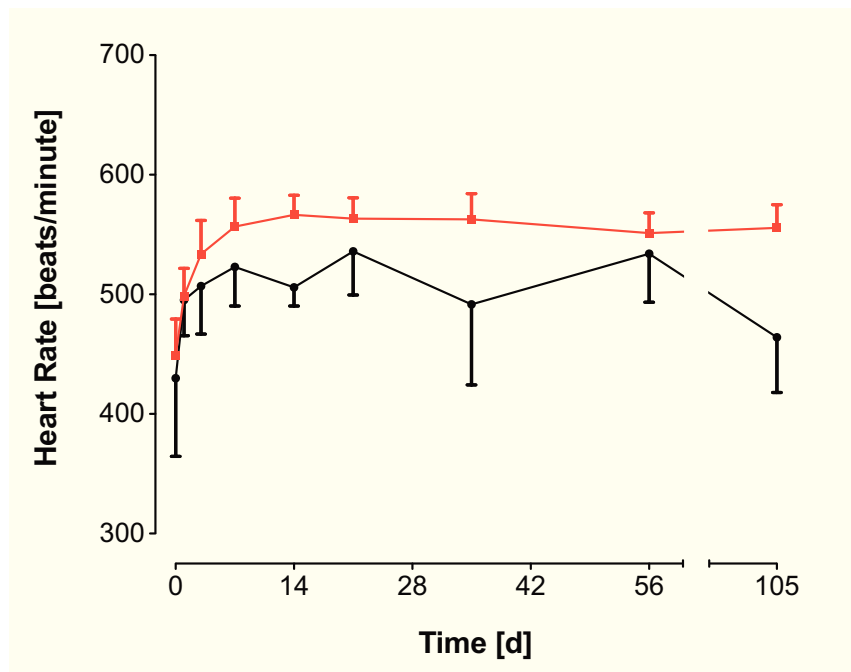
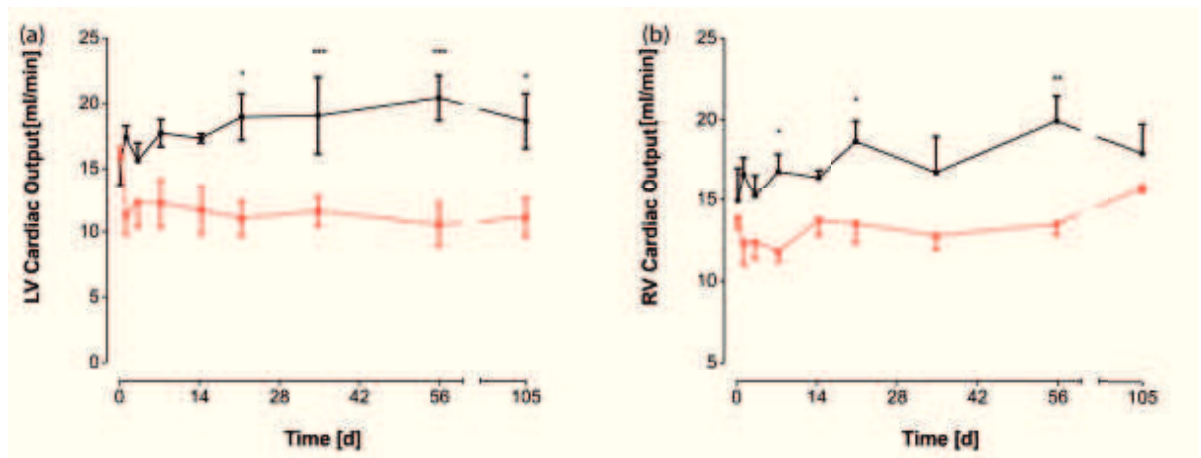


Figure 3.13 – Effects of banding on the heart rate (beats/minute). PAB (—), sham (—); d, day.

one. The major difference is, that the distance between the sham and the PAB group is smaller. This is due to the right ventricular stroke volume being higher, due to tricuspid regurgitation. In this case, right ventricular cardiac output means the total volume of blood per minute expelled out of the right ventricle, independent of whether the blood is going into the forward (to the pulmonary circulation via the pulmonary artery) or backward (to the right atrium via the tricuspid valve) direction. Therefore, the left ventricular cardiac output is the true reflection of the amount of blood the body receives.



**Figure 3.14 – Effects of banding on cardiac output.** (a) Left ventricular cardiac output (LV Cardiac Output, ml/min) (b) Right ventricular cardiac output (RV Cardiac Output, ml/min); PAB (—), sham (—); d, day. \*\*\* $p < 0.001$ , \*\* $p < 0.01$ , \* $p < 0.05$

### 3.1.8 Survival

Animals in the banded group started dying 50 days after operation, and had a median survival of 104.5 days, whilst all animals of the sham group survived the study period (fig. 3.15, p. 56).

### 3.1.9 Timecourse of Fibrosis in the Banded Heart

Whilst the collagen content of the right ventricles of the sham and PAB groups was equal 3 days after operation, at seven days there was a non-significant increase in the PAB group, which became highly significant 14 days after operation (Collagen area:  $18.6 \pm 2.1$  ml/min vs.  $11.1 \pm 1.5$  ml/min [Sham vs. PAB],  $p < 0.05$ ), and continued to increase until 21 days, when it plateaued (Collagen area:  $18.6 \pm 2.1$  ml/min vs.

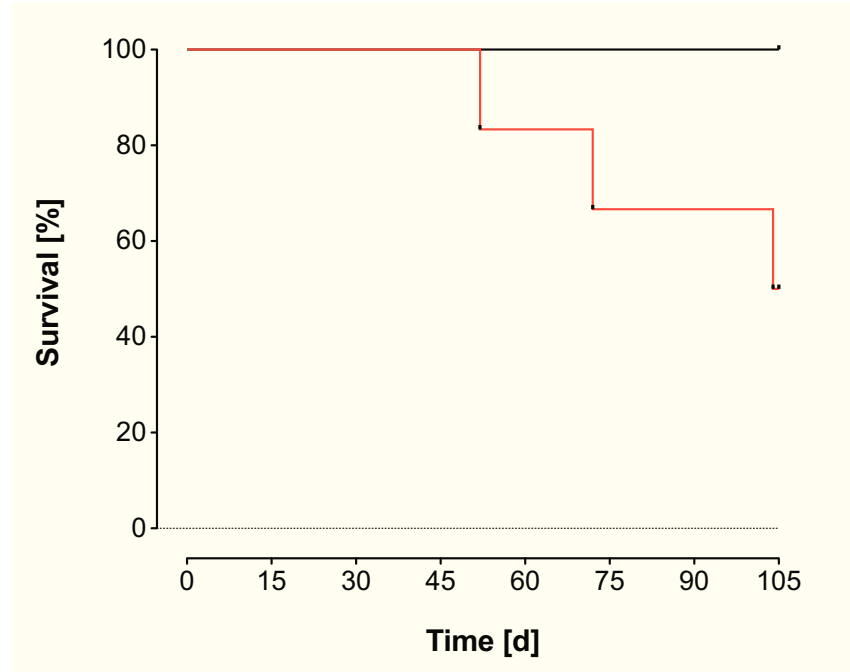


Figure 3.15 – Effects of banding on survival (%). PAB (—), sham (—); d, day.

$11.1 \pm 1.5$  ml/min [Sham vs. PAB],  $p < 0.05$ ) (fig. 3.16, p. 57). The collagen amount in the right ventricles of sham-operated was not affected by the operating procedure.

Picrosirius red specifically stains collagen red when viewed under a light microscope. When viewed under a microscope with circular polarized light, only collagen is visible, as it becomes birefringent when it has been stained with picrosirius red. A comparison of picrosirius red-stained right ventricular slices of sham and PAB animals as seen under polarized light can be found on page 58 (fig. 3.17). As can be quickly deduced from the pictures, the sham operation has no effects on right ventricular collagen content, whilst banding of the pulmonary artery leads to a gradual increase in collagen content.

### 3.1.10 Timecourse of Cardiomyocyte Size in the Banded Heart

Cardiomyocyte size, measured as the average of the diameter of individual cardiomyocytes cut transversally, was already increased in banded animals, albeit non-significantly, on day 3 after operation (CM size:  $16.1 \pm 0.3 \mu\text{m}$  vs.  $18.3 \pm 0.2 \mu\text{m}$  [Sham vs. PAB],  $p > 0.05$ ) (fig. 3.18, p. 60). The difference became significant on day 7 post-op (CM size:  $14.8 \pm 0.3 \mu\text{m}$  vs.  $18.7 \pm 0.4 \mu\text{m}$  [Sham vs. PAB],  $p < 0.001$ )

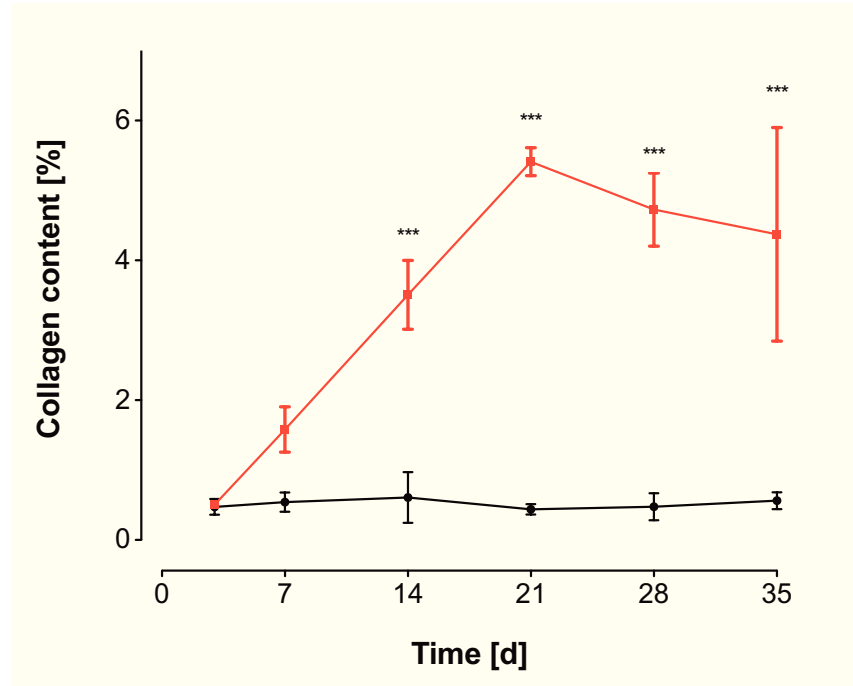


**Figure 3.16 – Effects of banding on the collagen content of the right ventricle (%).** PAB (—), sham (—); d, day. \*\*\* $p < 0.001$

and continued to increase until the end of the study.

Histological pictures comparing sham and PAB cardiomyocytes can be found in figure 3.19 (p. 61). The pictures show transversal slices of right ventricular cardiomyocytes stained with WGA-FITC (green), which specifically stains the cell membrane, and DAPI (blue), which stains the nucleus. As can be seen on the pictures, the individual cardiomyocytes of the banding group are already larger in diameter on day 3, and continue to grow until the end of the study. Furthermore, if one looks closely, but especially apparent at 4 weeks in the PAB group, one can make out streaks of collagen, which also have been stained green.

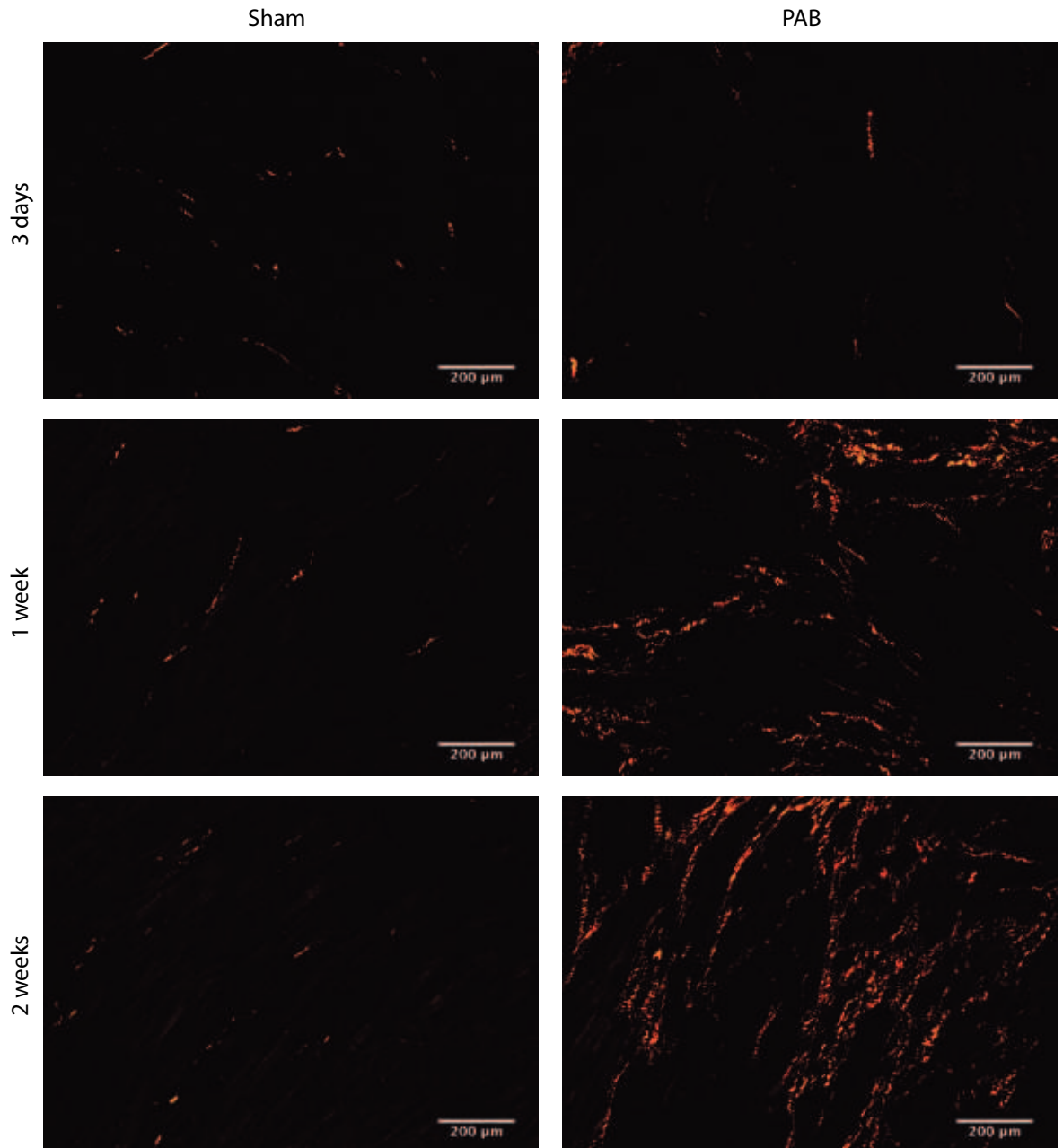


**Figure 3.17 – Effects of banding on the collagen content of the right ventricle.** Sample images showing typical stainings as they are visualized under polarized light in specimen of sectioned right ventricular hearts of banded and sham-operated mice. The time-dependent increase of the picosirius red-stained area in PAB mice can be clearly seen.

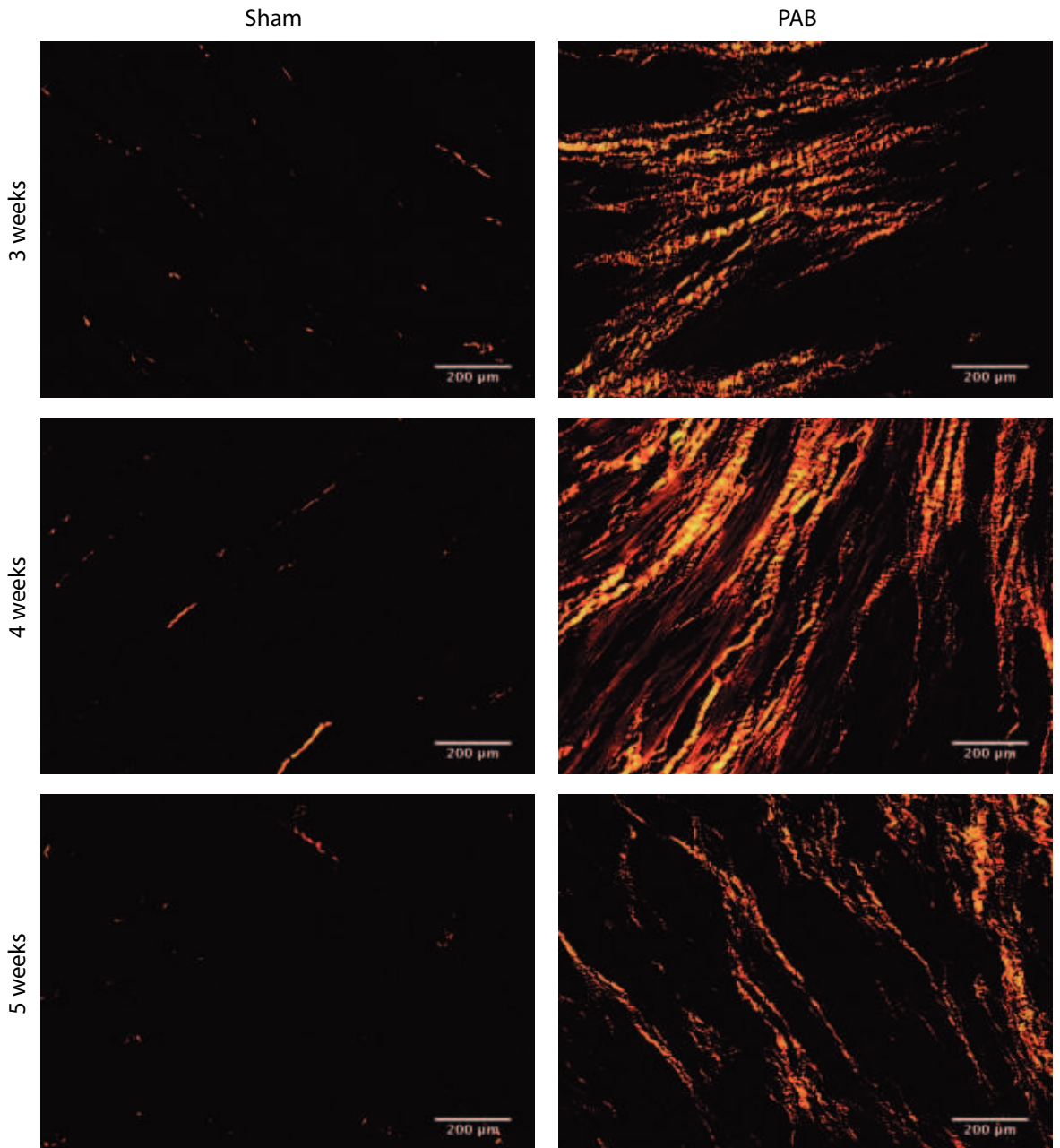
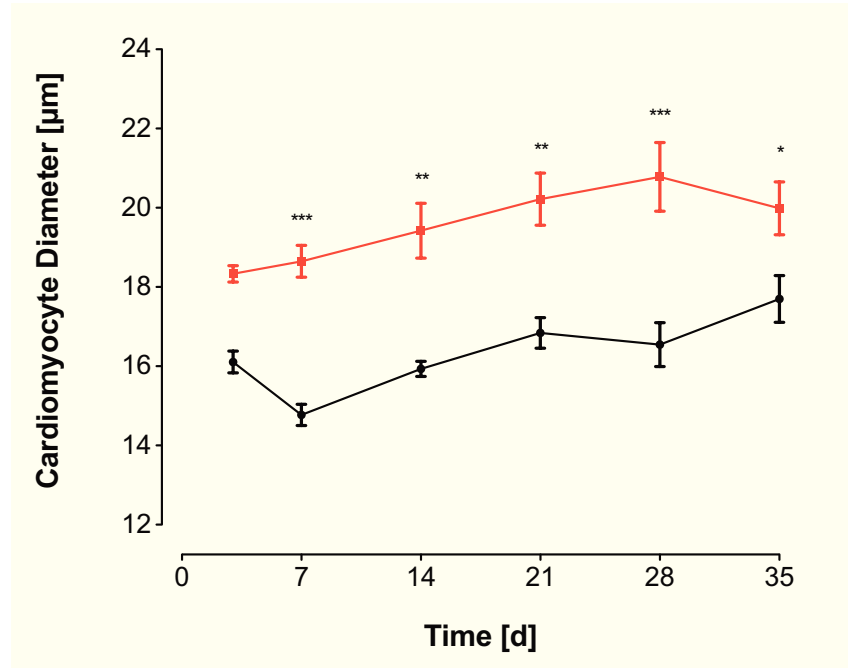


Figure 3.17 – continued



**Figure 3.18 – Effects of banding on cardiomyocyte size ( $\mu\text{m}$ ).** PAB (—), sham (—); d, day. \*\*\* $p<0.001$ , \*\* $p<0.01$ , \* $p<0.05$

## 3.2 Riociguat and Sildenafil Study

This interventional study was designed to test and compare the effects of sildenafil, a PDE5A inhibitor, and riociguat, an sGC stimulator, on right ventricular morphology and function in the pulmonary artery banding model. The hypothesis was, that intervention with these drugs ameliorates pathological right ventricular remodeling and increases right ventricular function. As could be concluded from the staging study, a major impairment of right ventricular function occurred right after operation, which was followed by a brief compensatory response lasting approximately one week. After day 7, a progressive decompensation of the right ventricle began, eventually resulting in heart failure. The study plan can be found in the materials and methods section (fig. 2.3, p. 32). Briefly, mice were operated, left to develop right ventricular dysfunction for 7 days, after which treatment started for another 14 days. 21 days after operation, mice were finally assessed and sacrificed.

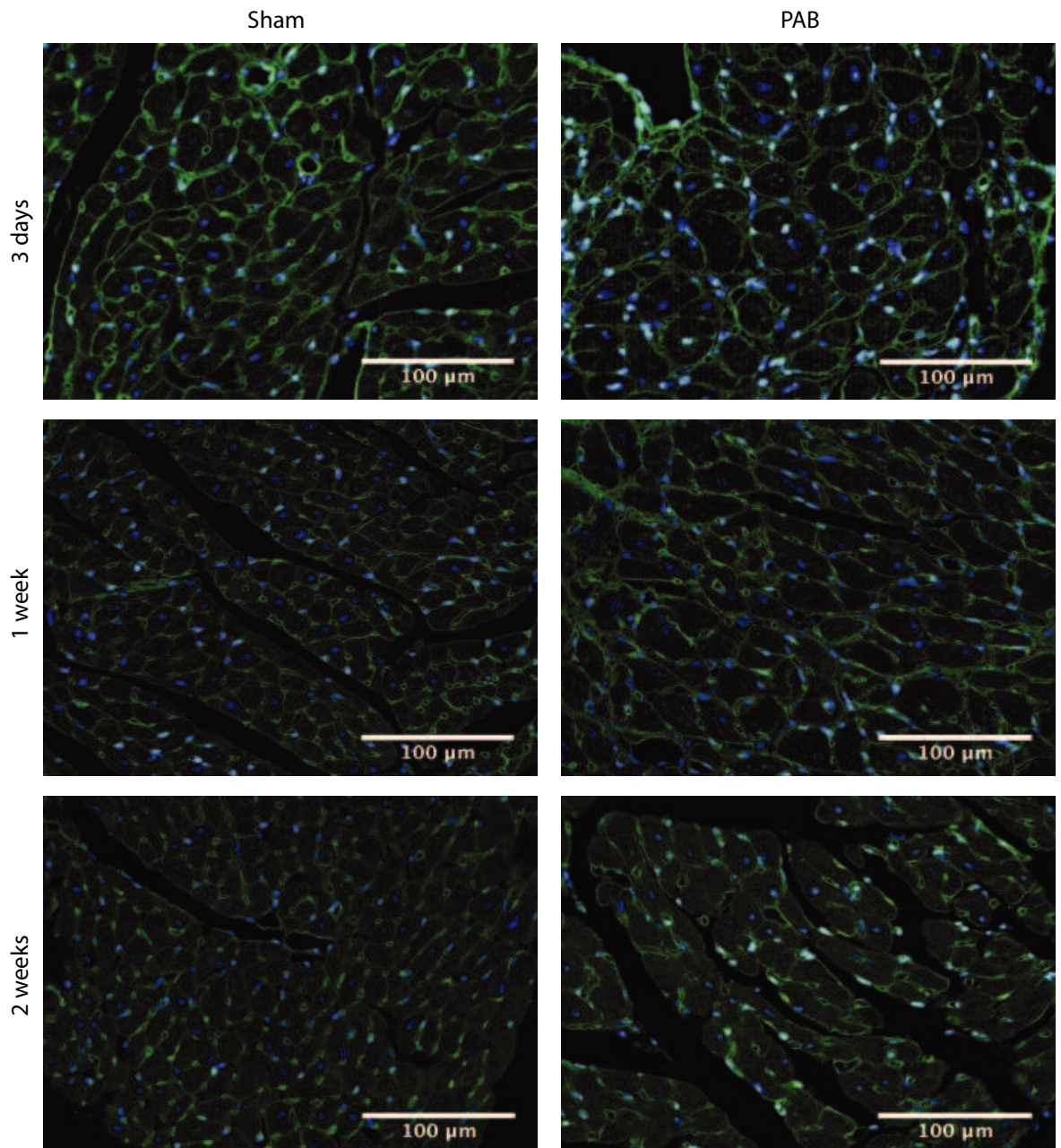


**Figure 3.19 – Effects of banding on the size of right ventricular cardiomyocytes.** Sample images showing typical stainings as they are visualized under fluorescent light in specimen of sectioned right ventricular hearts of banded and sham-operated mice. Cell membranes are stained with WGA-FITC (●), nuclei are stained with DAPI (●).

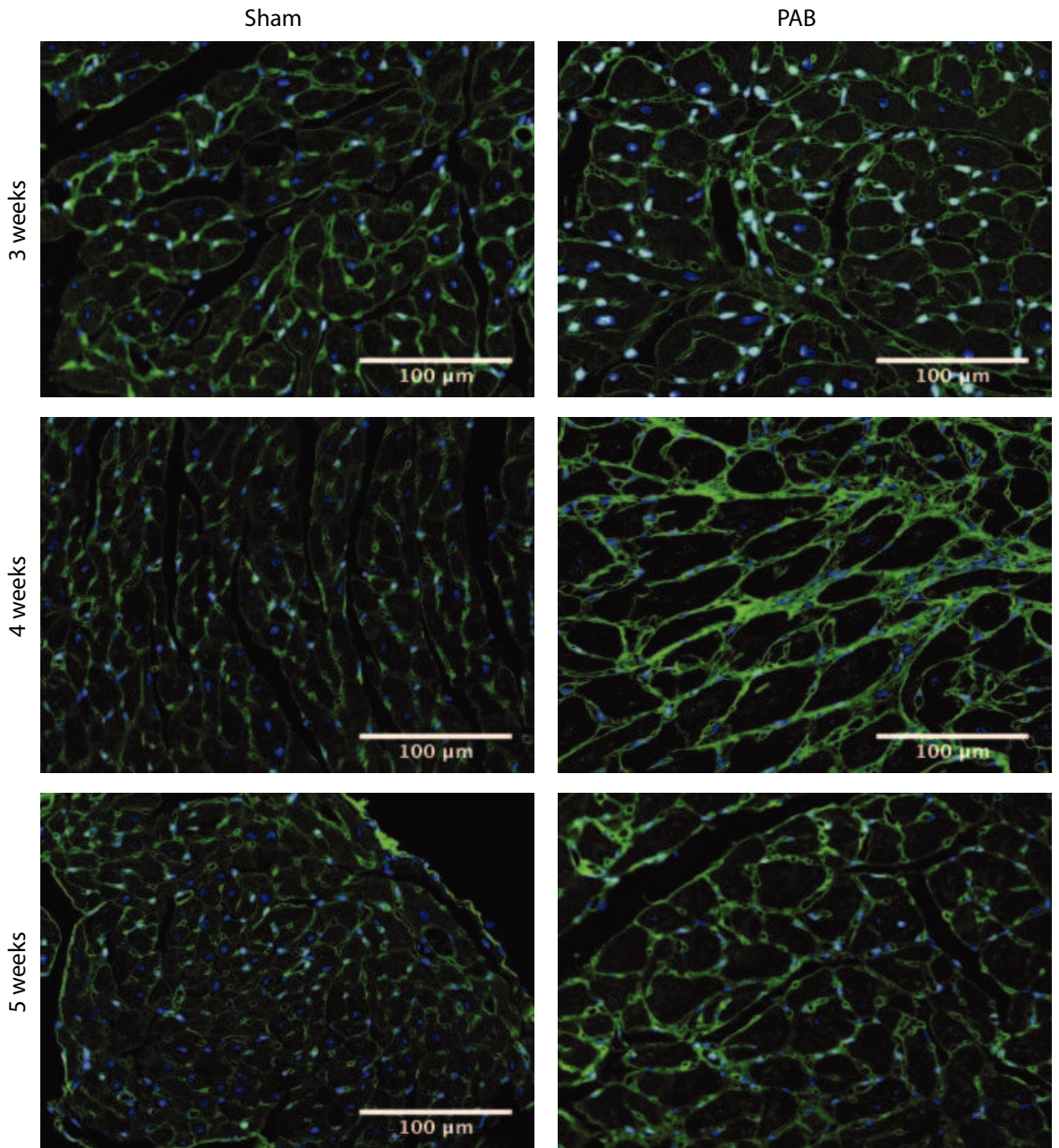
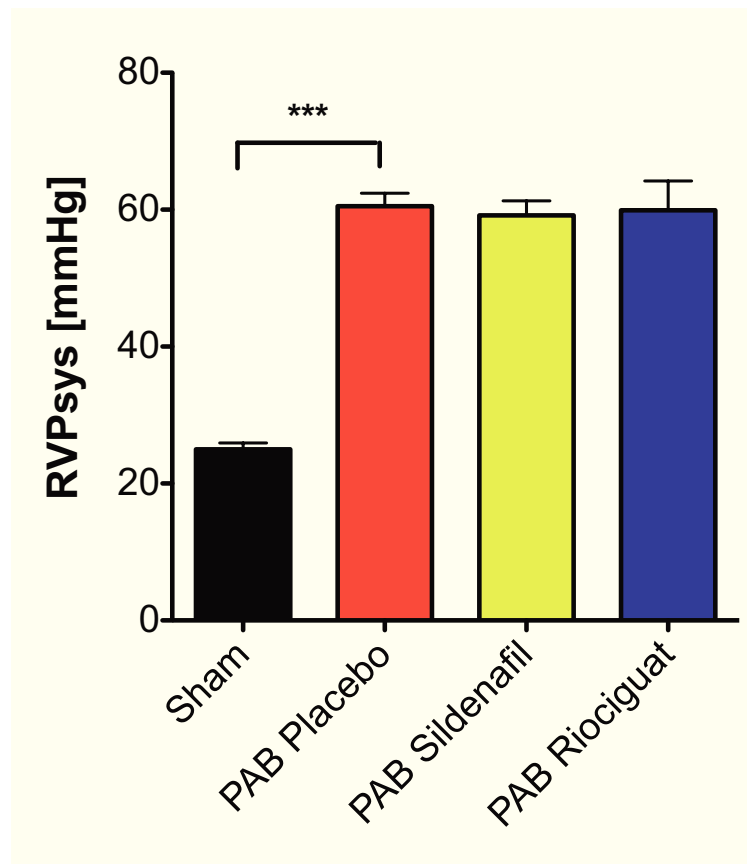


Figure 3.19 – continued

### 3.2.1 Right Ventricular Pressure

As expected, banding increased the right ventricular systolic pressure by the same amount in the placebo-, sildenafil- and riociguat-treated group (RVPsys:  $25.0 \pm 0.9$  mmHg vs.  $60.5 \pm 1.9$  mmHg vs.  $59.2 \pm 2.1$  mmHg vs.  $59.9 \pm 4.3$  mmHg [Sham vs. placebo vs. sildenafil vs. riociguat],  $p < 0.001$  for Sham vs. Placebo). This reflects the reliability of the method to reproducibly constrict the pulmonary artery to a predefined extent (fig. 3.20, p. 63).



**Figure 3.20** – Effects of sildenafil and riociguat on right ventricular systolic pressure (RVPsys, mmHg) in banded mice. Banding increased RVPsys ( $p < 0.001$ ), and drug treatment did not have any effects on RVPsys. \*\*\* $p < 0.001$

### 3.2.2 Effects on Right Ventricular Volumes and Function

PAB increased the right ventricular end-diastolic volume to the same extent in the placebo and riociguat groups at day 7 after banding (RV EDV: Placebo:  $73.3 \pm 5.2$   $\mu$ l; Riociguat:  $71.2 \pm 3.5$   $\mu$ l), and to a lesser extent in the sildenafil group (RV EDV: Sildenafil -  $59.9 \pm 3.3$   $\mu$ l,  $p < 0.05$  for placebo vs. sildenafil) (fig. 3.21, p. 64). 21

days after operation, riociguat and sildenafil led to non-significant decreases in right ventricular dilatation ( $\Delta$ RV EDV:  $-0.7 \pm 1.9 \mu\text{l}$  vs.  $-5.5 \pm 2.1 \mu\text{l}$  vs.  $-7.8 \pm 5.2 \mu\text{l}$  [Placebo vs. sildenafil vs. riociguat],  $p > 0.05$ ). Yet, comparing the 21 day values, the sildenafil group had a significantly lower right ventricular end-diastolic volume than the placebo group (RV EDV:  $72.6 \pm 4.3 \mu\text{l}$  vs.  $54.5 \pm 2.7 \mu\text{l}$  [Placebo vs. sildenafil],  $p < 0.001$ ).

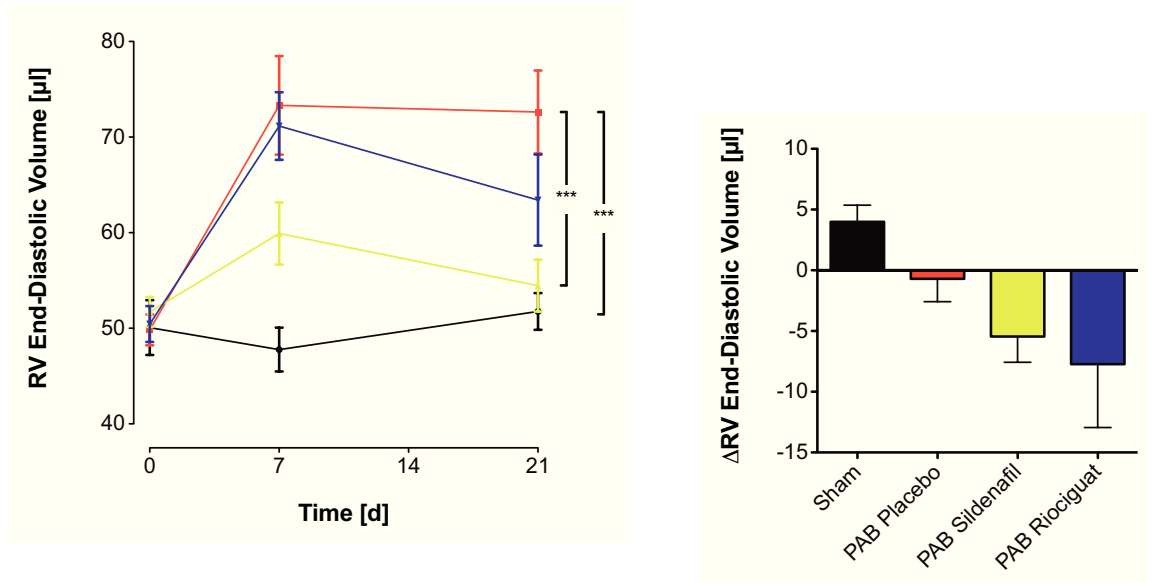


**Figure 3.21 – Effects of sildenafil and riociguat on right ventricular end-diastolic volume (RV End-Diastolic Volume,  $\mu\text{l}$ ).** (a) Time course of right ventricular end-diastolic volume from start of the study (day 0, pre-OP) until the end of the study (day 21, post-OP, post-treatment) (b) Change in right ventricular end-diastolic volume from day 7 (start of treatment) to day 21 (end of treatment). PAB (—), sham (—), sildenafil (—), riociguat (—); d, day. \*\*\* $p < 0.001$

A similar development could be observed for the right ventricular end-systolic volume (fig. 3.22, p. 65): Banding led to an elevated right ventricular end-systolic volume in banded mice, with the sildenafil group experiencing a smaller degree of increase (RV ESV:  $49.6 \pm 4.1 \mu\text{l}$  vs.  $37.0 \pm 3.5 \mu\text{l}$  vs.  $46.8 \pm 3.3 \mu\text{l}$  [Placebo vs. sildenafil vs. riociguat],  $p < 0.01$  for placebo vs. sildenafil). Sildenafil and riociguat treatment both managed to reduce these values at day 21 (RV ESV:  $47.4 \pm 3.6 \mu\text{l}$  vs.  $28.8 \pm 2.9 \mu\text{l}$  vs.  $36.0 \pm 3.4 \mu\text{l}$  [Placebo vs. sildenafil vs. riociguat];  $p < 0.001$  for placebo vs. sildenafil,  $p < 0.05$  for placebo vs. riociguat). The decrease in right ventricular end-systolic volume from day 7 to day 21 was also significant in riociguat-treated mice compared to placebo-treated mice (RV ESV:  $-2.2 \pm 1.9 \mu\text{l}$  vs.  $-10.9 \pm 3.9 \mu\text{l}$  [Placebo vs. riociguat],  $p < 0.05$ ).

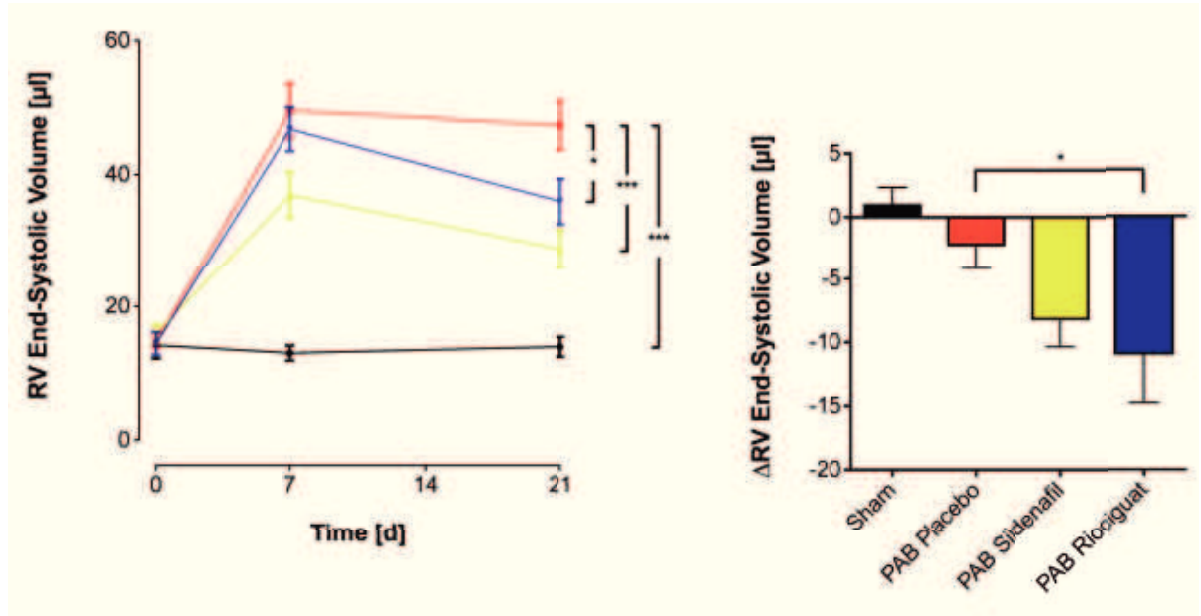


**Figure 3.22 – Effects of sildenafil and riociguat on right ventricular end-systolic volume (RV End-Systolic Volume,  $\mu\text{l}$ ).** (a) Time course of right ventricular end-systolic volume from start of the study (day 0, pre-OP) until the end of the study (day 21, post-OP, post-treatment) (b) Change in right ventricular end-systolic volume from day 7 (start of treatment) to day 21 (end of treatment). PAB (—), sham (—), sildenafil (—), riociguat (—); d, day. \*\*\* $p < 0.001$ , \*\* $p < 0.01$ , \* $p < 0.05$

The decrease in right ventricular dilatation and the reduced right ventricular end-systolic volume translated into an improved performance of the right ventricle (fig. 3.23, p. 66). Whilst the right ventricular stroke volume only marginally increased over placebo values ( $\Delta\text{RV SV}$ :  $1.5 \pm 0.7 \mu\text{l}$  vs.  $2.7 \pm 0.9 \mu\text{l}$  vs.  $3.1 \pm 1.8 \mu\text{l}$  [Placebo vs. sildenafil vs. riociguat];  $p > 0.05$ ), the right ventricular ejection fraction showed a robust increase for sildenafil and riociguat both when measured at day 21 (RV EF:  $35.4 \pm 1.7\%$  vs.  $48.2 \pm 3.3\%$  vs.  $43.7 \pm 2.2\%$  [Placebo vs. sildenafil vs. riociguat];  $p < 0.001$  for placebo vs. sildenafil,  $p < 0.05$  for placebo vs. riociguat), and when taking into account the change from start of treatment to the end of the study ( $\Delta\text{RV EF}$ :  $2.5 \pm 1.3\%$  vs.  $9.1 \pm 2.2\%$  [Placebo vs. sildenafil],  $p < 0.05$ ) (fig. 3.24, p. 66).

The operation increased the heart rate of the animals in each group to approximately the same value at day 7 (HR:  $501.5 \pm 19.6 \text{ bpm}$  vs.  $515.8 \pm 12.8 \text{ bpm}$  vs.  $507.5 \pm 14.5 \text{ bpm}$  [Placebo vs. sildenafil vs. riociguat],  $p > 0.05$ ) (fig. 3.25, p. 67). As the sham group started out with a slightly higher baseline, the increase in heart rate in the banded groups was larger. Furthermore, whilst the heart rate of the sham group returned back to baseline at day 21, the heart rate of the banded groups

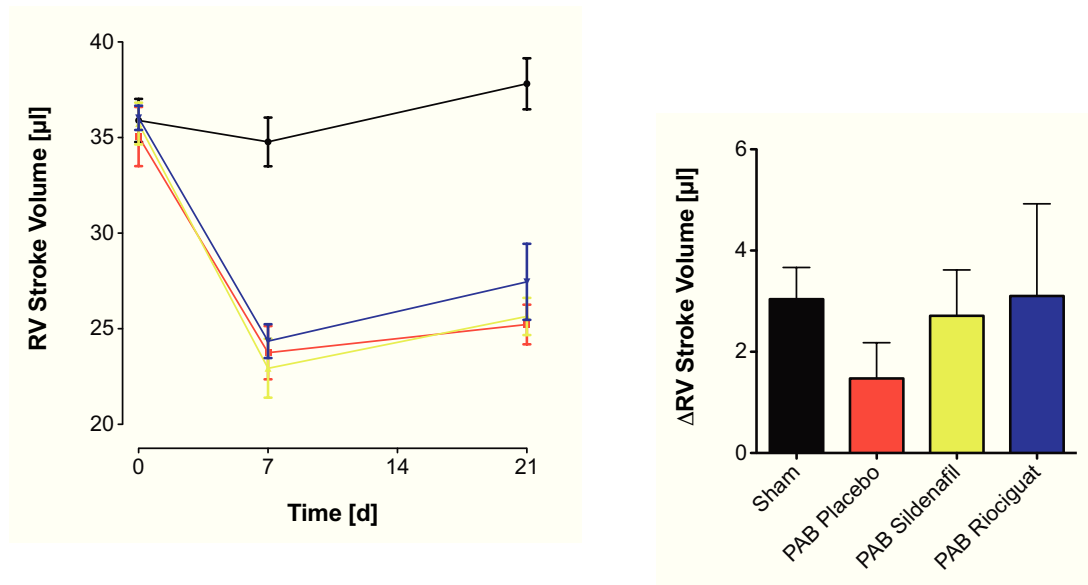


**Figure 3.23 – Effects of sildenafil and riociguat on right ventricular stroke volume (RV Stroke Volume,  $\mu\text{l}$ ).** (a) Time course of right ventricular stroke volume from start of the study (day 0, pre-OP) until the end of the study (day 21, post-OP, post-treatment) (b) Change in right ventricular stroke volume from day 7 (start of treatment) to day 21 (end of treatment). PAB (—), sham (—), sildenafil (—), riociguat (—); d, day.

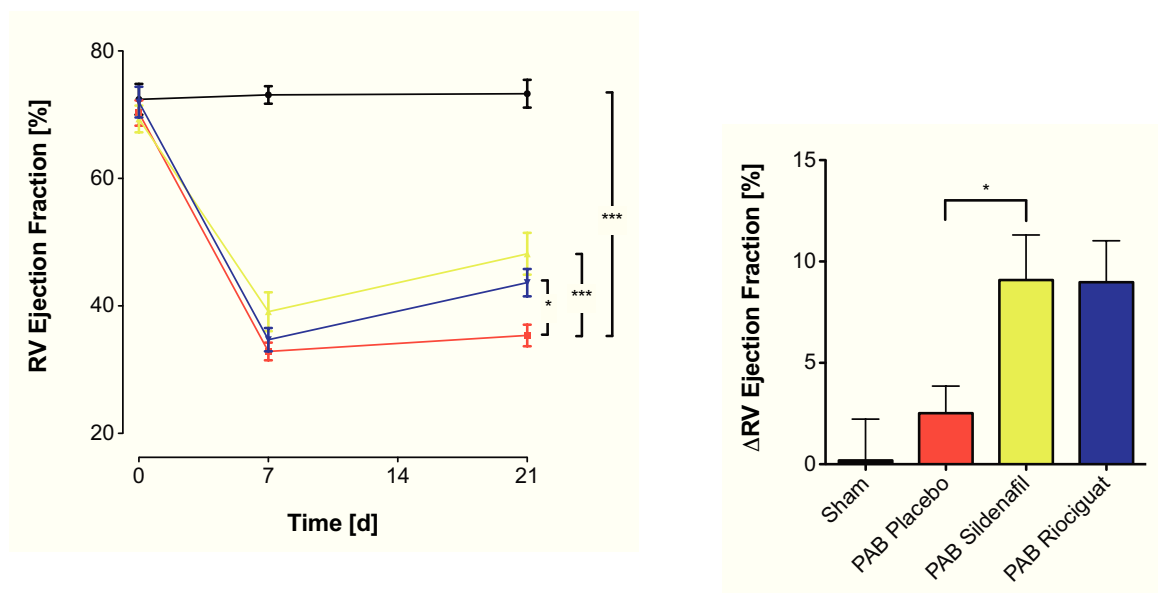


**Figure 3.24 – Effects of sildenafil and riociguat on right ventricular ejection fraction (RV Ejection Fraction, %).** (a) Time course of right ventricular ejection fraction from start of the study (day 0, pre-OP) until the end of the study (day 21, post-OP, post-treatment) (b) Change in right ventricular ejection fraction from day 7 (start of treatment) to day 21 (end of treatment). PAB (—), sham (—), sildenafil (—), riociguat (—); d, day. \*\*\* $p < 0.001$ , \* $p < 0.05$

tended to increase slightly further. This response is expected, as the heart tries to compensate for its decrease in stroke volume with an increase in beating frequency to bring the cardiac output back to normal. As can be seen from figure 3.26 (p. 68), this leads to a slight, albeit non-significant, increase in right ventricular cardiac output from day 7 to day 21 ( $\Delta$ RV CO:  $1.2 \pm 0.5$  ml/min vs.  $2.0 \pm 0.4$  ml/min vs.  $2.0 \pm 1.0$  ml/min [Placebo vs. sildenafil vs. riociguat];  $p > 0.05$ ).

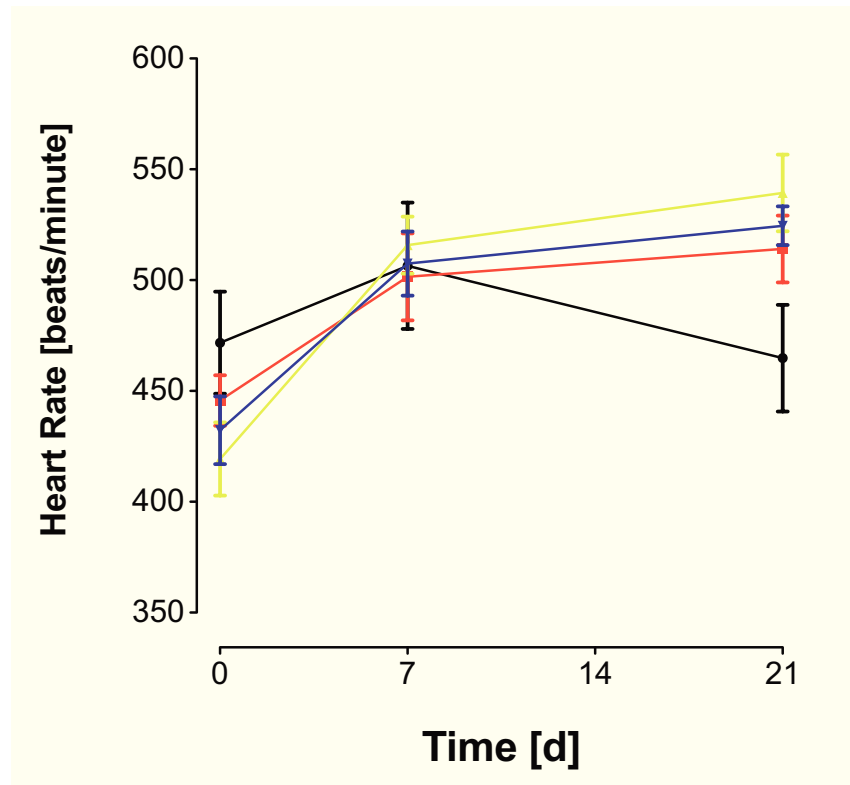


**Figure 3.25** – Effects of sildenafil and riociguat on heart rate (beats/min) in banded mice. PAB (—), sham (—), sildenafil (—), riociguat (—)

One might wonder, why the right ventricular cardiac output is larger than the left ventricular cardiac output. This is due to an inherent limitation of the method of measurement: the cardiac output is calculated as the product of stroke volume and heart rate (2.4, p. 38). As the stroke volume is calculated by subtracting the end-systolic volume from the end-diastolic volume (2.2, p. 38), the value gives no account of whether the blood is flowing into the forward or the backward direction. It is well known that right ventricular dilatation leads to tricuspid regurgitation,<sup>35</sup> i.e. blood is flowing back from the right ventricle into the right atrium when the ventricle contracts, as the tricuspid valve is not able to close sufficiently any longer.

Having used echocardiography, our group has shown this to be the case for this model as well (data not shown).

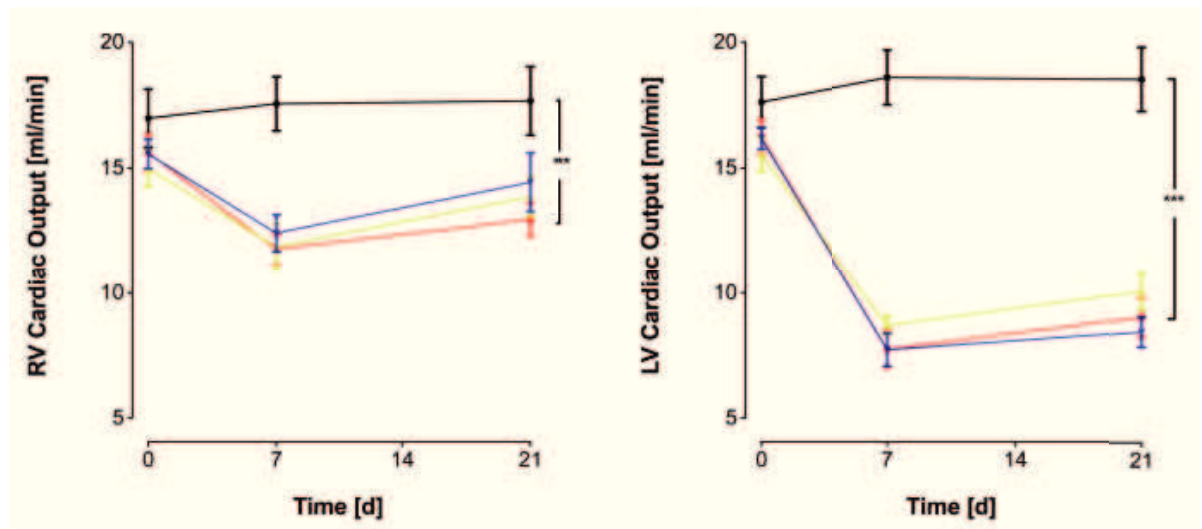


**Figure 3.26 – Effects of sildenafil and riociguat on cardiac output** (a) Time course of right ventricular cardiac output (RV Cardiac Output, ml/min) from start of the study (day 0, pre-OP) until the end of the study (day 21, post-OP, post-treatment) (b) Time course of left ventricular cardiac output (LV Cardiac Output, ml/min) from start of the study (day 0, pre-OP) until the end of the study (day 21, post-OP, post-treatment) . PAB (—), sham (—), sildenafil (—), riociguat (—); d, day. \*\*\* $p < 0.001$

### 3.2.3 Effects on Right Ventricular Hypertrophy

All banded groups showed a similar level of increase in right ventricular mass at day 7 (RV Mass:  $61.1 \pm 2.4$  mg vs.  $55.4 \pm 1.9$  mg vs.  $60.5 \pm 1.3$  mg [Placebo vs. sildenafil vs. riociguat];  $p > 0.05$ ), which was not affected by drug treatment ( $\Delta$ RV mass:  $1.3 \pm 1.5$  mg vs.  $1.7 \pm 1.7$  mg vs.  $-0.9 \pm 2.3$  mg [Placebo vs. sildenafil vs. riociguat];  $p > 0.05$ )(fig. 3.27, p. 69).

### 3.2.4 Effects on the Left Heart

Banding highly significantly reduced the left ventricular stroke volume (fig. 3.28, p. 69). As seen in the staging study, this is due to a decreased left ventricular end-diastolic volume, as the left ventricle is compressed to its side by the hypertrophied right ventricle (see also figs. 3.1 and 3.9, pp. 45 and 51). Neither treatment with riociguat, nor with sildenafil led to any significant changes in left ventricular stroke volume ( $\Delta$ LV SV:  $2.2 \pm 0.8$  ml/min vs.  $1.8 \pm 1.2$  ml/min vs.  $1.0 \pm 0.6$  ml/min [Placebo vs. sildenafil vs. riociguat];  $p > 0.05$ ).

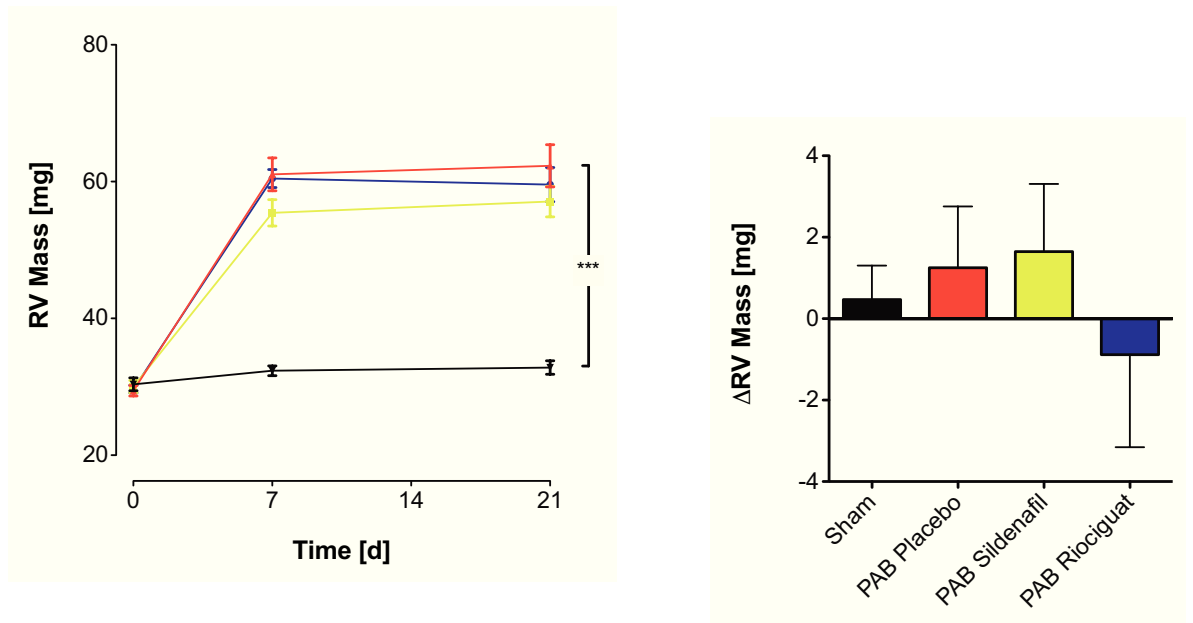


**Figure 3.27 – Effects of sildenafil and riociguat on right ventricular mass (RV Mass, mg).** (a) Time course of right ventricular mass from start of the study (day 0, pre-OP) until the end of the study (day 21, post-OP, post-treatment) (b) Change in right ventricular mass from day 7 (start of treatment) to day 21 (end of treatment). PAB (—), sham (—), sildenafil (—), riociguat (—); d, day. \*\*\* $p < 0.001$

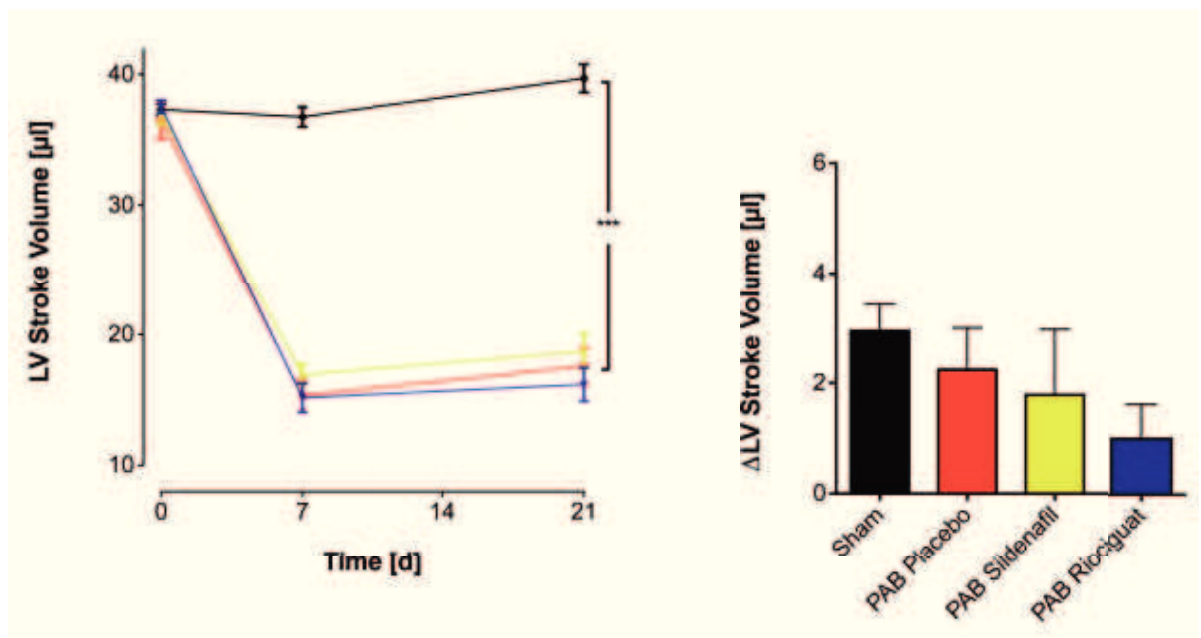


**Figure 3.28 – Effects of sildenafil and riociguat on left ventricular stroke volume (LV Stroke Volume, μl).** (a) Time course of left ventricular stroke volume from start of the study (day 0, pre-OP) until the end of the study (day 21, post-OP, post-treatment) (b) Change in left ventricular stroke volume from day 7 (start of treatment) to day 21 (end of treatment). PAB (—), sham (—), sildenafil (—), riociguat (—); d, day. \*\*\* $p < 0.001$

After an initial decrease in left ventricular mass after banding, which was already apparent in the staging study and is most likely caused by adaptive changes to the decreased left ventricular cardiac output, left ventricular mass tended to increase in sham and placebo animals, whilst it did not change in riociguat- and sildenafil-treated animals. Nonetheless, the differences were not statistically significant ( $\Delta$ LV mass:  $5.8 \pm 2.1$  mg vs.  $2.0 \pm 2.6$  mg vs.  $-0.6 \pm 1.9$  mg [Placebo vs. sildenafil vs. riociguat];  $p > 0.05$ ) (fig. 3.29, p. 70).

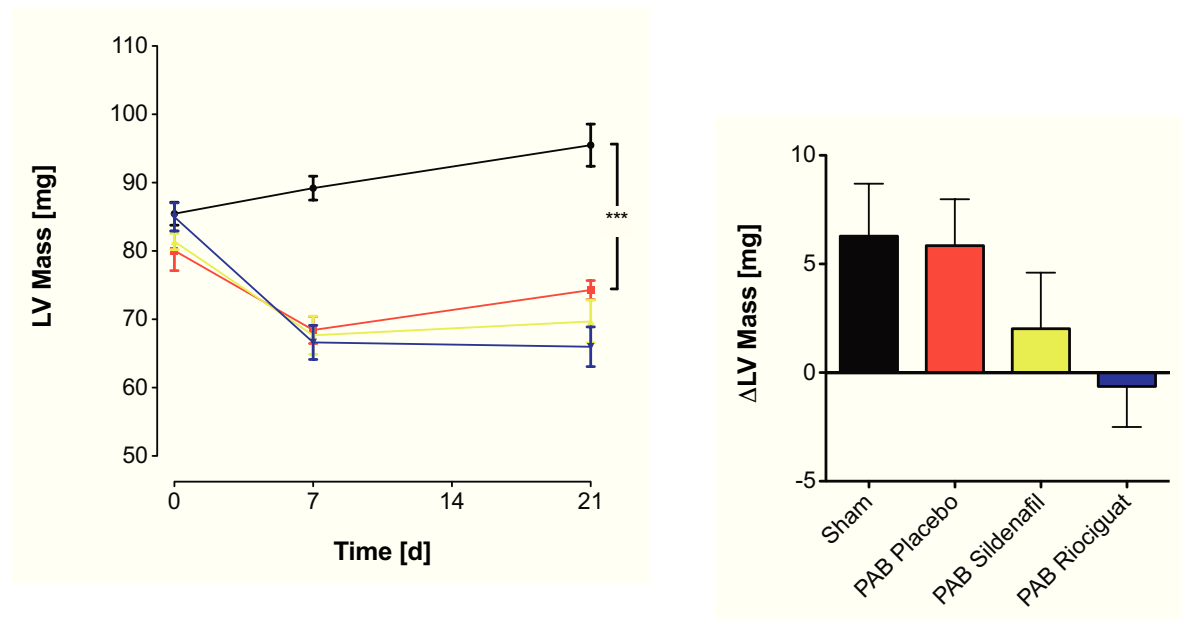


**Figure 3.29 – Effects of sildenafil and riociguat on left ventricular mass (LV Mass, mg).** (a) Time course of left ventricular mass from start of the study (day 0, pre-OP) until the end of the study (day 21, post-OP, post-treatment) (b) Change in left ventricular mass from day 7 (start of treatment) to day 21 (end of treatment). PAB (—), sham (—), sildenafil (—), riociguat (—); d, day. \*\*\* $p < 0.001$

### 3.2.5 Effects on the Systemic Arterial Pressure

Drug treatment had no effect on systemic arterial pressure (SBP<sub>sys</sub>:  $77.3 \pm 3.8$  mmHg vs.  $77.3 \pm 3.7$  mmHg vs.  $79.0 \pm 5.5$  mmHg [Placebo vs. sildenafil vs. riociguat];  $p > 0.05$ ) (fig. 3.30, p. 71). This is coherent with the finding that the left ventricular cardiac output did not change significantly.

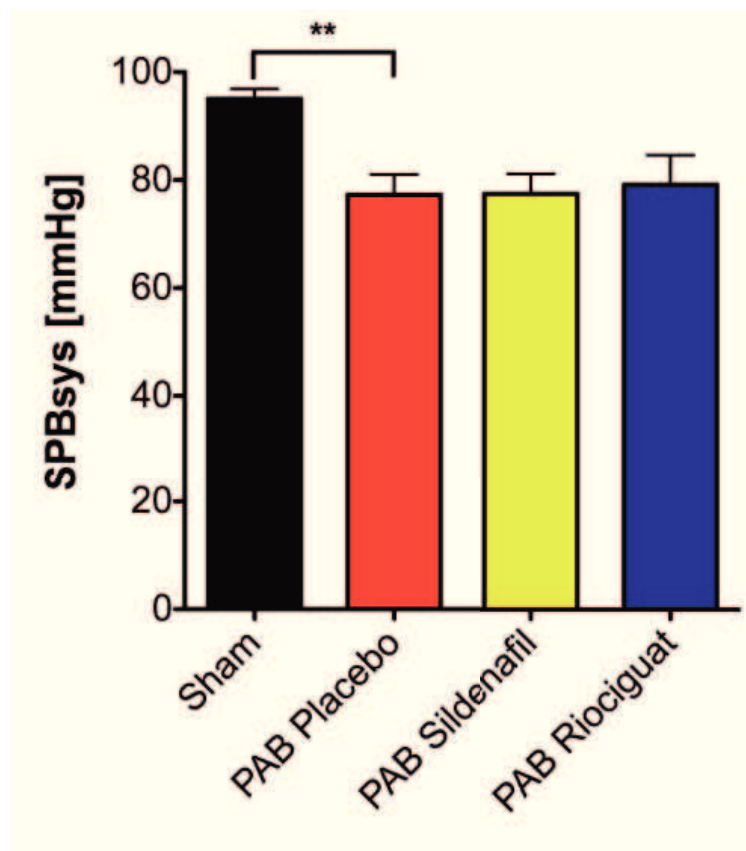
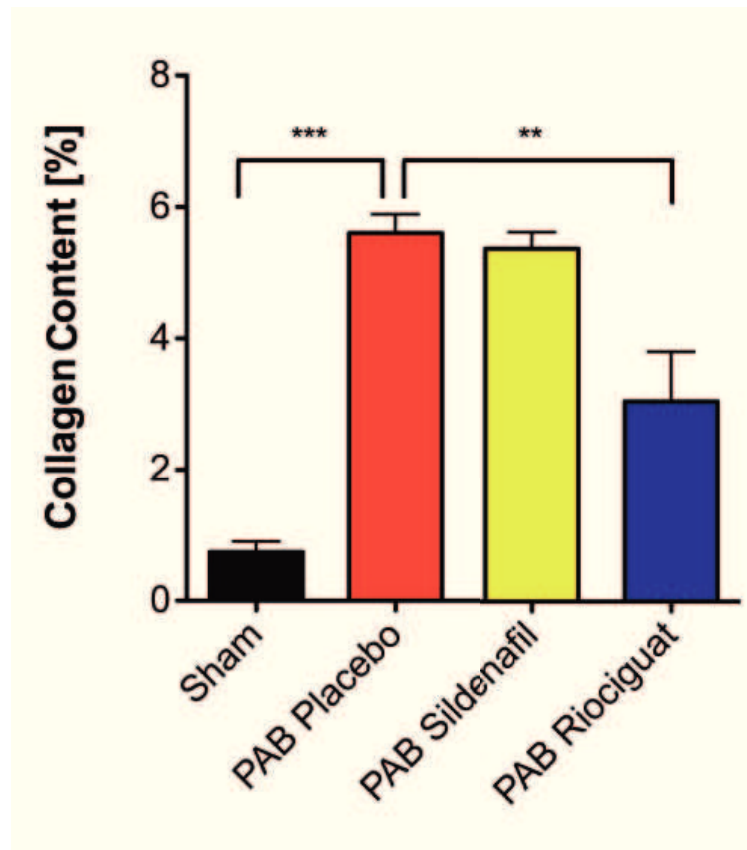


Figure 3.30 – Effects of sildenafil and riociguat on systemic arterial pressure (SBP<sub>sys</sub>, mmHg) in banded mice. Banding decreased SBP<sub>sys</sub> ( $p < 0.01$ ), and drug treatment did not have any effects on SBP<sub>sys</sub>. \*\* $p < 0.01$

### 3.2.6 Effects on Right Ventricular Fibrosis

As already noted in the staging study, banding leads to right ventricular fibrosis. The procedure increased the collagen content in placebo-treated animals to  $5.6 \pm 0.3\%$  (cf. sham:  $0.7 \pm 0.2\%$ ,  $p < 0.001$ , sham vs. placebo). Riociguat treatment significantly reduced the amount of collagen to approximately half of the placebo group (Collagen area:  $3.1 \pm 0.8\%$ ;  $p < 0.01$ , placebo vs. riociguat)(fig. 3.31, p. 72). Sildenafil did not have any measurable effect on the collagen content of the right ventricle (Collagen area:  $5.4 \pm 0.3\%$ ). Sample pictures showing typical collagen stainings are shown in figure 3.32 (p. 73). The beneficial effects of riociguat treatment on the collagen content of the right ventricle can be clearly seen in figure 3.32(d).



**Figure 3.31 – Effects of sildenafil and riociguat on the right ventricular collagen content (%) of banded mice.** Banding increased the collagen content of the right ventricle ( $p < 0.001$ ). Riociguat led to a significant reduction of the collagen content ( $p < 0.01$ ), whilst sildenafil did not show any effects. \*\*\* $p < 0.001$ , \*\* $p < 0.01$

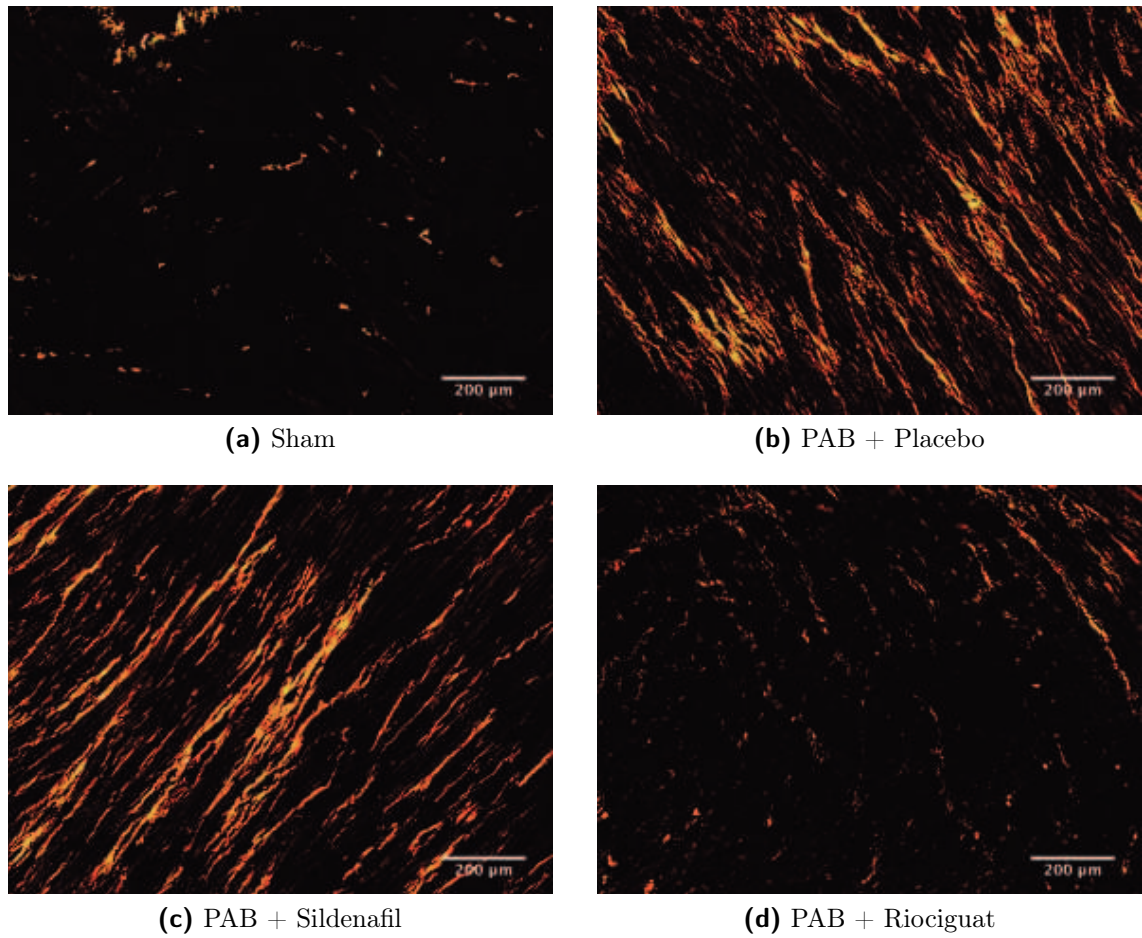


**Figure 3.32 – Effects of sildenafil and riociguat on the collagen content of the right ventricle.** Sample images showing typical stainings as they are visualized under polarized light in specimen of sectioned right ventricular hearts of (a) sham, (b) placebo-treated, (c) sildenafil-treated, and (d) riociguat-treated mice. Riociguat treatment leads to a clear reduction in the collagen content of the right ventricle.

### 3.2.7 Effects on Cardiomyocyte Size

The banding procedure increased the cardiomyocyte size in all groups, and drug treatment had no effects on cardiomyocyte hypertrophy (CM size:  $77.3 \pm 3.8$  mmHg vs.  $77.3 \pm 3.8$  mmHg vs.  $77.3 \pm 3.8$  mmHg [Placebo vs. sildenafil vs. riociguat];  $p > 0.05$ ) (figs. 3.33 and 3.34, pp. 74 and 75).

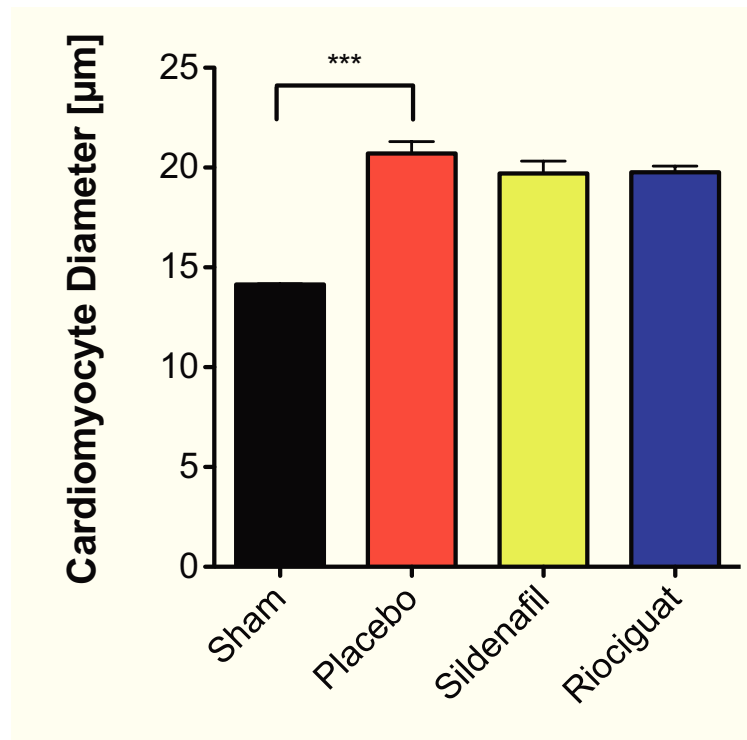


**Figure 3.33 – Effects of sildenafil and riociguat on the right ventricular cardiomyocyte diameter ( $\mu\text{m}$ ) of banded mice.** Banding increased the right ventricular cardiomyocyte diameter, whilst drug treatment had no effects. \*\*\* $p < 0.001$

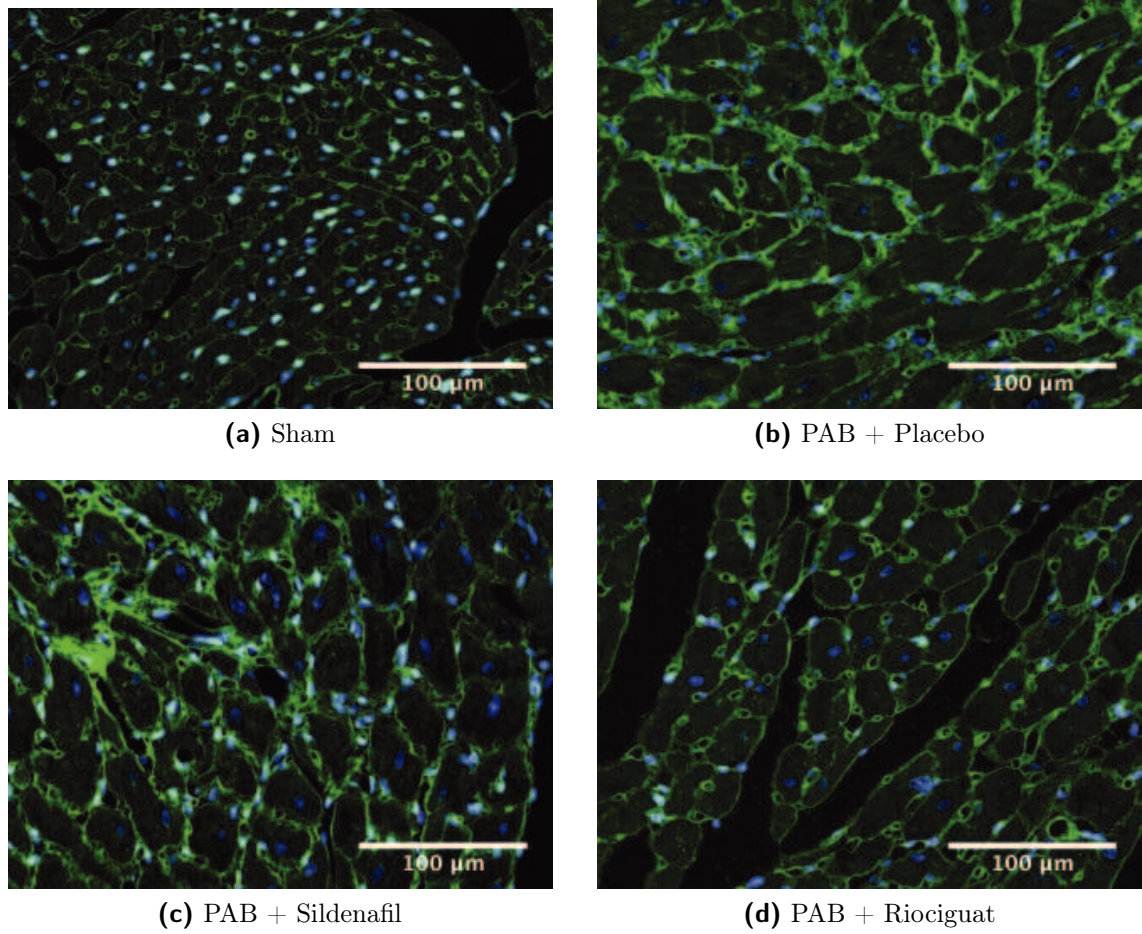


**Figure 3.34 – Effects of sildenafil and riociguat on the cardiomyocyte size of the right ventricle.** Sample images showing typical stainings as they are visualized under fluorescent light in specimen of sectioned right ventricular hearts of (a) sham, (b) placebo-treated, (c) sildenafil-treated, and (d) riociguat-treated mice. Banding increased the cardiomyocyte diameter, and drug treatment did not have any effects on this. Cell membranes are stained with WGA-FITC (●), nuclei are stained with DAPI (●).

# Chapter 4

## Discussion

This dissertation shows for the first time the temporal progress of the effects of pulmonary artery banding on several parameters of right and left ventricular function which can be derived by magnetic resonance imaging. This allows one to make a justified selection of the time points for the beginning of treatment and its termination in this model of right ventricular hypertrophy. Furthermore, for the first time the antifibrotic effects of riociguat in the right heart have been unequivocally demonstrated.

### 4.1 Staging Study

The tabular results of the staging study can be found in tables A.1 and A.2 on pages 95 and 97. The effects of banding on the right heart can be broadly classified into structural and functional changes. The structural changes, that is the growth of the right ventricle (Fig. 3.6, p. 49), the growth of its individual cardiomyocytes (Fig. 3.18, p. 60) and the increase in collagen content (Fig. 3.16, p. 57), progressively increase in the first weeks after the banding operation. After three to four weeks, the collagen content of the right ventricle appears to have plateaued, whilst the the right ventricular mass and cardiomyocyte size only very slowly continue to increase until the end of the study.

In contrast, the systolic function, represented by the right ventricular ejection fraction, resembles a triphasic response (Fig. 3.5, p. 49): after a first rapid decline

in ejection fraction one day after the banding operation, the ejection fraction recovers until days 7 to 14, after which it steadily declines. Likewise, the right ventricular end-diastolic and end-systolic volumes increase one day after operation, recover slightly until day 7, after which they continue to deteriorate, i.e. the right ventricle continues to dilate and its residual blood at systole increases (Fig. 3.4, p. 48).

The increase in right ventricular mass is unexpectedly rapid. The right heart has adapted in as little as one week to the increased resistance it has to work against, with little increase thereafter. This is also reflected functionally: the ejection fraction reached its highest values 7 to 14 days after operation. Nonetheless, individual cardiomyocytes continued to grow past week one. I assume that this is no further reaction to adapt to the banding procedure, but rather a physiological increase in cardiomyocyte size. The reason I believe this is that the cardiomyocyte size in sham-operated animals continues to grow to a similar extent (Fig. 3.18, p. 60), apparently reflecting a physiological adaptation to the continuing growth of the animals, as the animals were approximately 8 weeks of age at operation, i.e. not full-grown.

So why does the ejection fraction decline again after two weeks? If one looks at the development of the collagen content of the right heart (Fig. 3.16, p. 57), one sees that it is increasing up to 3 weeks after operation, after which it plateaus. Actually, the collagen content in banded animals is increasing by 310% from day 3 to 7, by 222% from day 7 to 14, and by a further 154% from day 14 to day 21, which is rather dramatic. The functional consequences of increased fibrosis have been well established clinically and experimentally: increased fibrosis is associated with a decreased right ventricular ejection fraction in patients with a systemic right ventricle,<sup>143</sup> with diastolic heart failure in animal models of hypertensive heart disease,<sup>144</sup> and a predictor of diastolic and systolic dysfunction during exercise in hypertrophic cardiomyopathic patients who successfully underwent operation.<sup>145</sup> Experimentally it was shown, that decreasing fibrosis leads to an improved diastolic dysfunction in dogs with tachycardia induced heart failure<sup>146</sup> and in pressure-overloaded rats.<sup>147</sup>

Collagen is the major determinant of the hearts extracellular matrix, which maintains the myocardial geometry so as to allow the individual cardiomyocytes to work in a coordinated fashion as a syncytium.<sup>35,148</sup> The major collagen isoform present in

the murine heart is collagen type I, which is also the stiffest, being around 30-times stiffer than a cardiomyocyte.<sup>148</sup>

A pathological increase in collagen leads to myocardial stiffness,<sup>149,150</sup> effectively reducing the compliance of the heart. Furthermore, fibrosis disrupts coordinated excitation-contraction coupling, which prevents the heart from working as a syncytium.<sup>144</sup> Also, exercise-induced hypertrophy is typically not accompanied by an accumulation of collagen in the myocardium.<sup>151</sup> Therefore in our staging study it appears that a certain amount of collagen increase is necessary to supply a structure for cardiomyocytes in which they can function efficiently. The increase over that certain amount on the contrary decreases the functioning of the right ventricle again, for the aforementioned reasons.

Regarding its function, the left ventricle is seriously affected by the changes occurring in the right ventricle. This is less applicable with regard to the left ventricular mass, which only diminishes relatively little in comparison to sham operated animals, and likely is a reflection of the decreased preload the left ventricle has to deal with (Fig. 3.8, p. 50). The most serious consequence is the inability of the left ventricle to expand to its original volume (Fig. 3.9, p. 51), causing a major impairment of the left ventricular stroke volume, without any change in its ejection fraction (Fig. 3.10, p. 52). The increased pressure the right ventricle exerts onto the left ventricle is well reflected in the left ventricular eccentricity index, a readout of the "compression" of the left ventricle, which increases throughout the study in banded mice, but stays constant in sham-operated animals (Fig. 3.11, p. 53).

The non-existent change in left ventricular ejection fraction is a sign that the impaired function of the left ventricle indeed is due to an interference by the right ventricle, and not an inherent impairment. The only change in left ventricular ejection fraction in banded mice occurs right after operation, most likely a reflection of the increased stress put on the heart by the banding procedure. As can be observed from figure 3.10, whilst the left ventricular stroke volume, as well as its end-diastolic volume, of the sham-operated animals increases over time, which is presumably owing to the hearts adaptation to the growth of the animals, the stroke volume of the banded animals does not increase with time, and rather tends to

further diminish. As the banded animals continue to grow as well, the probable consequence of this is a further decrease in end-organ perfusion. This poses an interesting question, which could be elucidated in future studies: is the eventual death of the animals due to heart failure, or due to organ failure? As a readout for a reduction in end-organ perfusion, the analysis of blood gas could be employed.

Even though there is a compensatory increase of heart rate in banded mice (Fig. 3.13, p. 54), this is not enough to offset the negative effects of decreased stroke volume onto the cardiac output (Fig. 3.14, p. 55). The further small increase in right ventricular stroke volume and cardiac output, which is not reflected by an increase of these parameters in the left ventricle, is a sign of increased tricuspid regurgitation, being a result of increased right ventricular dilatation and consequent extension of the tricuspid valve, allowing more blood to flow backward.

In clinical studies, several of the parameters just discussed were associated with decreased survival. Thus is the left ventricular diastolic eccentricity index associated with survival in IPAH, with patients with the highest values also having the highest event rates.<sup>152</sup> Magnetic resonance imaging studies have further shown that a large right ventricular end-diastolic volume, a low stroke volume and a reduced left ventricular end-diastolic volume are all strong predictors of mortality; a further dilatation of the right ventricle, an additional decrease of left ventricular volume, as well as a decline of left ventricular stroke volume and right ventricular ejection fraction at follow-up predict poor long-term outcome.<sup>153</sup> All of these effects were present in our study, underscoring the clinical relevance of this model.

Unequivocal evidence that this mouse model of chronic right ventricular pressure overload is in effect a model of pathological, and not compensatory hypertrophy, is the eventual death of the animals, beginning  $\sim 50$  days after operation, the median survival being 104.5 days.

## 4.2 Treatment Study

The results of the staging study had been used to determine the study plan for the treatment study. As the peak of the compensatory response was reached  $\sim 7$  days

after operation, and functional deterioration started to begin after this point, this day was chosen for the commencement of treatment. Two weeks were chosen to be the duration of treatment, drawing a consensus between the cost of drug treatment and the assumption when functional, resp. histological, treatment changes would become apparent.

The treatment was tolerated well by all animals, as none of them died during the treatment period. The banding procedure increased the right ventricular pressure in all banded groups to the same value, allowing for comparison of the groups. The results of the treatment study can be found in table A.3 on page 97.

To our surprise both drugs had no effect on right ventricular mass (Fig. 3.27, p. 69), yet both increased the systolic function of the right ventricle, reflected by an increased right ventricular ejection fraction (Fig. 3.24, p. 66). Even though right ventricular stroke volume increased as well, this increase did not reach statistical significance (Fig. 3.23, p. 66). Additionally, riociguat and sildenafil improved right ventricular diastolic dysfunction by reducing the ventricle's dilatation, albeit there was only a trend for the effects of riociguat (Fig. 3.21, p. 64). The increase in ejection fraction could be brought about by the decrease in dilatation: according to the Frank-Starling law, cardiomyocytes produce more force when stretched, so as to accommodate an increased end-diastolic volume with an increased stroke volume.<sup>154</sup> Yet, cardiomyocytes can overstretch, resulting in a decrease in force production. With the degree of dilatation seen in this model of pressure-overload, it is not unlikely that an over-stretching might have occurred. The decrease in dilatation might thus have removed these negative effects, returning the cardiomyocytes back to a level of increased force production. Also, without any change in mass, a reduction of dilatation might have shifted the heart from a state of eccentric hypertrophy towards a state of concentric hypertrophy.

One important implication from these observations can already be drawn: a reduction in pathological right ventricular hypertrophy appears not to be necessary to achieve a functional improvement of the right heart. Actually, in clinical studies it was shown that right ventricular hypertrophy was not as strongly associated with mortality as was dilatation,<sup>153</sup> underscoring the potential clinical importance of this

finding of increased function despite an unchanged right ventricular mass.

The search for a potential mechanism of the drugs beneficial effects and the knowledge of the antifibrotic potential of stimulating the NO-sGC-cGMP pathway from the literature (e.g. in the liver,<sup>155</sup> kidney<sup>104</sup>) led me to assess the drugs effects on the right ventricular collagen content. Indeed, riociguat reduced the right ventricular collagen content by nearly 50 % ( $p < 0.01$ ), whereas sildenafil did not have any effect. Thus, this study has shown for the first time a direct antifibrotic effect of riociguat in the right heart, together with a concomitant functional improvement. It was already shown in the past that a reduction in collagen content, either via an inhibition of collagen crosslinking<sup>156</sup> or by collagen degradation,<sup>157</sup> decreases myocardial and chamber stiffness. Drug intervention studies carried out in humans came to similar conclusions.<sup>158,159</sup>

A further assessment of the individual cardiomyocyte sizes showed, that banding increased cardiomyocyte size to a similar level as has been already observed in the staging study, and neither drug had any effect on this. One explanation for this finding could be the different sensitivity of cardiomyocytes and fibroblasts with regard to stimulation of the cGMP-pathway. In fact, Masuyama et al. have noted in in vitro experiments that cardiac fibroblasts show higher increases in cGMP content upon sGC stimulation than cardiac myocytes.<sup>106</sup>

The differing sensitivities of cardiac myocytes and fibroblasts can turn out to be of advantage, as an increase in cardiomyocyte size is needed to overcome the increased resistance the right heart has to work against. Hypothetically, with regard to the right ventricle, an optimal treatment would preserve its functional capacity, in part defined by the number and size of its cardiomyocytes, and ameliorate the negative consequences of pathological hypertrophy, of which one is fibrosis. Taking this into account, and the fact that exercise-induced hypertrophy occurs without any changes in myocardial collagen content, one might speculate that riociguat shifts the pathological state of the right ventricle to a more physiological one.

### 4.2.1 Riociguat

How does riociguat decrease the right hearts collagen content? Crucial for determining the mechanism would be a knowledge of the location of sGC in the right heart. Experimental problems with the immunohistochemical staining of sGC prevents me from drawing firm conclusions, forcing me to resort to knowledge of what is known from the literature. sGC has been found in rat vascular endothelial cells, rat cardiac myocytes, and human platelets.<sup>160</sup> Furthermore it was found in hepatic stellate cells, which are found in the liver and are crucially responsible for fibrotic remodeling of liver tissue,<sup>155</sup> and in rat cardiac fibroblasts.<sup>106</sup>

Regarding a potential mechanism which draws on the effects of sGC stimulation in cardiac fibroblasts, I would like to mention the results found out by Masuyama et al.<sup>103,106</sup> They employed a model of angiotensin II-induced hypertension in rats, which leads to left ventricular hypertrophy, and treated the rats with BAY41-2272, an sGC activator which exerts its effects independent of the redox state of the heme moiety of sGC. Using a dose that does not affect blood pressure and cardiac hypertrophy, BAY 41-2272 nonetheless reduced perivascular and interstitial deposition of collagen as well as transcription of type 1 collagen.<sup>103</sup> Additionally, BAY41-2272 resulted in reduced thymidine incorporation in cultured cardiac fibroblasts,<sup>103</sup> i.e. reduced fibroblast growth. In search of a potential mechanism, the same group proposed that the inhibition of fibroblast to myofibroblast transformation and the inhibition of angiotensin-converting-enzyme (ACE) are crucial factors involved in the drug's potential to reduce fibrosis.<sup>106</sup> They could show that BAY 41-2272 led to reductions of TGF- $\beta$ 1 and collagen type I expression. TGF- $\beta$ 1 is known to be an important trigger to induce the phenotypic change of fibroblasts to myofibroblasts, and myofibroblasts are known to exaggerate the production of collagen type I. Indeed, in their model a reduced transition to myofibroblasts was observed. Furthermore, BAY 41-2272 significantly reduced the activity of ACE in vivo as well as in cultured cardiac fibroblasts. As ACE also has been implicated in the transition of fibroblasts to myofibroblasts,<sup>161</sup> this mechanism might likewise be responsible for the effects observed. It has to be noted though that for the cell culture experiments, isolated cells from neonatal rats had been used. Therefore, these potential mechanisms can

only be conferred to the animal studies, if adult cells and/or cells which have been subjected to pressure-overload, behave in the same way. A similar result was found in dermal fibrosis: Beyer et al. could show that BAY 41-2272 dose-dependently inhibited collagen release in dermal fibroblasts, isolated from patients with systemic sclerosis. Furthermore, in bleomycin-induced dermal fibrosis and skin fibrosis in Tsk-1 mice, BAY 41-2272 administration reduced the number of myofibroblasts.<sup>162</sup>

Thus, the anti-fibrotic effects of sGC stimulation in the heart might be due to reduced fibroblast proliferation, together with a decreased secretion of collagen type I, as well as reduced phenotype transition to myofibroblasts.

Another mechanism of action might be owing to the effects sGC-stimulation on endothelial cells, on a process called endothelial-mesenchymal transition (EndMT). EndMT is a transformation of endothelial cells into fibroblasts. In a mouse model of pressure overload, Zeisberg et al. could show, using immunofluorescence double-labeling experiments, that banding induced EndMT. Also, the application of TGF- $\beta$ 1 to adult human coronary endothelial cells led to EndMT, which was blocked by bone morphogenic protein 7 (BMP-7). In addition, the administration of BMP7 to banded mice reduced cardiac fibrosis and the accumulation of fibroblasts.<sup>163</sup> As BAY 41-2272 was shown to reduce TGF- $\beta$ 1 levels in a mouse model of left ventricular pressure-overload,<sup>106</sup> the reduction of EndMT could also serve as a mechanism of action of the antifibrotic effects of riociguat.

Finally, the sGC activator BAY41-2272 was shown to have anti-inflammatory effects, as it reduced increased leukocyte rolling and was associated with downregulation of the adhesion molecule P-selectin in endothelial cells.<sup>164</sup> Inflammation has been associated with cardiac fibrosis,<sup>165</sup> and it was shown in rats that pressure-overload induced perivascular macrophage accumulation and fibroblast proliferation in the left heart, and blocking of macrophage invasion also inhibited fibroblast proliferation.<sup>166</sup> Therefore this might form another option on how riociguat exerts in antifibrotic effects.

To block conjectures that the functional improvement seen with riociguat is simply due to an inotropic effect, I want to mention that a study performed in a canine model of heart failure, in which no positive inotropic effects of BAY 41-2272 and

BAY 41-8543, another sGC activator, were found.<sup>167</sup>

### 4.2.2 Sildenafil

Turning to the results of the sildenafil treatment, the question arises why it increases the diastolic and systolic function of the heart (Fig. 3.24, p. 66, and fig. 3.21, p. 64). Collagen measurements yielded the result, that sildenafil treatment had no effect on this parameter, therefore another mechanism has to be responsible for the effects seen. Also, there were no changes seen in the cardiomyocyte size or the weight of the right ventricle.

Studies probing the antihypertrophic effects of sildenafil in banding models have so far been either carried out in the mouse left ventricle or, when an isolated, direct effect on the right ventricle was investigated, in the rat. In contrast to studies carried out in the left ventricle, studies in the right ventricle have actually shown an increase of right ventricular hypertrophy,<sup>26,126</sup> with either no functional changes,<sup>26</sup> or a functional improvement.<sup>126</sup> The assumption that species differences between mouse and rat might be responsible for the discrepancies seen, now becomes much less probable, as sildenafil also did not show any antihypertrophic effects in our pulmonary artery-banded mouse model.

Thus, other important differences between the right and the left ventricle must be responsible for the treatment differences seen. Amongst them are: different morphology, different loading conditions, different gene expression profiles and a different origin. Therefore, it is well possible that right ventricular cardiomyocytes respond with other signaling mechanisms to induced hypertrophy than the left ventricle. It needs to be mentioned that the field of cardiac hypertrophy has a vast range, involving several distinct signaling cascades, which are deemed to be responsible for the hypertrophy of the heart.<sup>168</sup> Thus, different signaling cascades in the right and left ventricle might be the major players in regulating hypertrophy. Therefore, the targets of increased cGMP-signaling in the right ventricle might be less involved in hypertrophic signaling than in the left ventricle. Furthermore, sildenafil can only efficiently increase cGMP levels, if sufficient levels have been produced before. So, even if the antihypertrophic signaling targets of cGMP would be the same in the

right and in the left ventricle, only if sufficient cGMP is present for their activation, a noticeable effect could be observed. A prerequisite for this would be an adequate production by cGMP producing enzymes, i.e. sGC and pGC.

Why does sildenafil then improve the function of the right ventricle? It was shown that in experimental and clinical right ventricular hypertrophy, PDE5 mRNA and protein is upregulated in cardiomyocytes, compared to healthy right ventricular myocardium.<sup>122,169</sup> Additionally, acute PDE5 inhibition by sildenafil leads to increased contractility in right ventricular trabeculae from human failing hearts, and no change in right ventricular trabeculae from nonfailing hearts.<sup>169</sup> Acute PDE5 inhibition also increases contractility in perfused Langendorff preparations and isolated cardiomyocytes in right ventricular hypertrophy, but not in the normal right ventricle.<sup>122</sup> Nagendran et al. offered an explanation for this finding: the increase in cGMP content in the hypertrophied right ventricle leads to inhibition of cGMP-sensitive PDE3, effectively increasing the content of cAMP. The positive inotropic effects of cAMP, mediated mainly by protein kinase A (PKA), are well known.<sup>170</sup> Indeed, inhibition of PKA completely inhibited the PDE5-induced inotropy.<sup>122</sup> Therefore, the functional improvement seen in banded, sildenafil-treated mice in our study might also be due to the direct positive inotropic effects of PDE5 inhibition.

Another potential mechanism which comes to mind are the vasodilatory effects of sildenafil. It is known, that right ventricular hypertrophy and increased filling pressure can impair the perfusion of the ventricle by partial occlusion of the coronary arteries. If sildenafil would exert a vasodilating effect on the coronary arteries, perfusion might be improved. This in turn might improve the function of the ventricle, owing to increased oxygen and nutrient supply.

A very recent paper, published in 2012, also probed into the improvement of right ventricular systolic function seen with sildenafil treatment. They employed the rat monocrotaline model, in which they observed a severe T-tubule loss and disorganization, as well as a blunted and dys-synchronous sarcoplasmic reticulum  $\text{Ca}^{2+}$  release. Sildenafil improved right ventricular systolic function, and concomitantly ameliorated the impairment of myocyte T-tubule integrity and  $\text{Ca}^{2+}$  handling protein and sarcoplasmic reticulum  $\text{Ca}^{2+}$  release function.<sup>171</sup> Maybe this effect underlies the

improvement seen in the PAB model as well.

## 4.3 Benefits and Limitations of the Methods

### 4.3.1 Magnetic Resonance Imaging

Magnetic resonance imaging was established in the 1970s for noninvasive measurements in humans. Due to its high cost, operational effort and little availability it is a relatively new field in rodent imaging. In the 1990s the foundation for rodent cardiac imaging was laid. The first noticeable study to be mentioned was by Rose et al. in 1994, who established a proper cardiorespiratory gating method, so as to allow the imaging of a beating rodent heart.<sup>172</sup> Owing to the rodents inherently high heart rate, which roughly ranges between 400 to 600 beats per minute, an efficient gating method is essential for obtaining images with a resolution high enough to allow for analysis. In 1997, the first study was published which assessed left ventricular mass, wall thickness and internal dimensions in a serial manner using geometric assumptions, allowing for an estimation of these parameters.<sup>173</sup> These so derived parameters proved to correlate better with autopsy data than echocardiographic data did.<sup>173</sup> Eventually Simpson's rule was applied to the measurement of the murine left ventricle in 1998, which determines the total mass and volume of the ventricle by summing up their respective partial volumes, and is deemed to be the most accurate method for measuring these parameters.<sup>174</sup> Finally, in 2002, Wiesmann et al. successfully established the feasibility of this method in the murine right ventricle.<sup>175</sup>

The advantages of magnetic resonance imaging of the heart are its high precision and reproducibility, the nonexistent need for geometrical assumptions and its non-invasiveness.<sup>17</sup> The high tissue contrast and temporal resolution enable the clear distinction between the lumen and the myocard, as well as the precise determination of the systolic and diastolic phase. The high reproducibility and non-invasiveness allow the number of animals needed for a study to be reduced, and to assess the time-course of effects, in our case the time-course of banding and that of drug treatment. Lastly, and most importantly, is the possibility to acquire images of the whole

heart, which eliminates the need for geometrical assumptions. 2D equipment, like echocardiography, rely on geometrical assumptions of the left and right ventricle. Whilst the geometrical assumptions for the left ventricle are well established, due to its spherical/elliptical form, the analysis of the right ventricle is complicated by its complex geometry and anatomically different regions, and its unpredictable morphological changes in pathologies.<sup>48</sup> Another problem with echocardiography is that the right ventricle lies posterior to the sternum, making it difficult to image. This problem is also circumvented with the use of magnetic resonance imaging. Thus it can be said, that magnetic resonance imaging is a very precise and sophisticated technique, and for these reasons it is also deemed the "gold-standard" for the determination of cardiac functional parameters.<sup>17</sup> Amongst these, the right ventricular ejection fraction is the most widely accepted and most commonly used parameter to assess right ventricular function.<sup>17</sup>

Two limitations of magnetic resonance imaging became apparent during the course of the experiments. The first is that the right ventricular stroke volume measured by magnetic resonance imaging is nearly always higher than the left ventricular stroke volume in banded animals. This owes to the fact of tricuspid regurgitation: the difference between the end-diastolic volume and the end-systolic volume depicts not the effective forward stroke volume, but both the blood that flows backwards (tricuspid regurgitation) as well as forwards (via the pulmonary artery). Nonetheless, the left ventricular stroke volume, which can be calculated unequivocally, can be used as a determination of the right one, as the blood which leaves the left ventricle, has to have reached it first. As there is no shunt in the connection from the right to the left ventricle, the left ventricular stroke volume can be assumed to be right ventricular effective forward stroke volume. Still, an increase in right ventricular stroke volume is not necessarily reflected by an increase in left ventricular stroke volume in banded animals. This is due to the fact that the left ventricle is severely limited in its capacity to dilate, as it is restricted by the size of the hypertrophied right ventricle. Thus even though the systolic function of the right ventricle might increase (e.g. under drug treatment), the increase in right ventricular stroke volume expresses itself as an increased backward-flow through the tricuspid valve, and not

as an increased cardiac output. Thus there are two possibilities of judging whether the systolic function of the right ventricle increased: one either simply takes into account the absolute increase of the right ventricular stroke volume, not minding the direction the blood goes to; or one looks at the right ventricular ejection fraction or right ventricular end-diastolic volume, as these values are alternative depictions of systolic function, independent of potential tricuspid regurgitation. Other methods to correctly judge the right ventricular cardiac output are the use of catheterization,<sup>18</sup> although this might pose to be difficult due to the small size of the murine heart; or to use Doppler-echocardiography.<sup>18</sup>

The second limitation which became apparent is that of the overestimation of the right ventricular weight by magnetic resonance imaging by a factor of  $\sim 1.5$ - to 2-fold. After it became apparent that the right ventricular weight was overestimated about 2-fold in the staging study, adjustments in the analysis of the MRI images were performed, i.e. changes in contrast/brightness, which resulted in an overestimation of about 1.5-fold in the treatment study. Yet, this does not pose a problem for the validity of the experiments, as the overestimation was the same across all groups, which becomes apparent by comparing the MRI-derived data with the data derived from organ harvesting, making the relative differences amongst the experimental groups essentially the same (Figs. 3.6 and 3.27, pp. 49 and 69).

### 4.3.2 Pulmonary Artery Banding

The first time pulmonary artery banding had been applied to mice was in 1994 by Rockman et al.,<sup>68</sup> but the scarcity of information about performing the operation hindered the replication of results by other laboratories. For the assessment of the effects of banding they employed x-ray contrast microangiography, a technique which was not investigated further, probably due to the high technical demands required and the lack of serial evaluations of mice.

The first comprehensive paper to be published which explained in detail the banding procedure was by Tarnavski et al.<sup>69</sup> They positioned a 26-gauge needle next to the pulmonary artery, after which a thread was used to tie a knot around needle and artery for constriction. The needle was removed immediately afterwards; this

resulted in a constriction of the pulmonary artery to the diameter of the 26-gauge needle. Our group resorted to the use of a modified hemoclip applier, which comes with several advantages over the use of a needle and a thread: it can be applied quickly, without having to resort to a parallel alignment of needle and pulmonary artery beforehand; as there is no needle involved, no complete constriction of the pulmonary artery takes place, which a) might lead to a rapid decompensation of the right heart, and b) lead to pathological changes different to the ones intended; it is highly reproducible due to the stability of the clip, compared to the thread, which might loosen.

The diameter of the clip was adjusted, so as to obtain right ventricular parameters similar to that of what was published by Tarnavski et al.. Whilst their mice had a right ventricular systolic pressure of  $\sim 45$  mmHg (they did not state whether this was 1 or 2 weeks after operation), our mice had a right ventricular systolic pressure of  $\sim 45$  mmHg 1 week after operation,  $\sim 55$  mmHg after 2 weeks, and  $\sim 65$  mmHg three weeks after operation; the pressure eventually stabilized at this level. Also, their right ventricular mass to bodyweight ratio was  $\sim 1.6$ , and ours was  $\sim 1.5$ .

The benefits of pulmonary artery banding are its very high post-surgical survival rate, its high reproducibility, and the similarity to severe pulmonary hypertension (in banded mice, the right ventricular systolic pressure increased to more than 45 mmHg and the right ventricular ejection fraction dropped to about 45 %). In a clinical study evaluating the right ventricular characteristics of subjects with primary pulmonary hypertension or idiopathic dilated cardiomyopathy, Quaife et al. drew the difference between a compensated and a failing heart at equal or more than 40 % right ventricular ejection fraction, and less than 40 % respectively.<sup>176</sup> This right ventricular ejection fraction is less than I have determined in my studies and could be due to different reasons: either owing to the fact that the observer is a different one; or because of differences between the murine and the human heart. Whilst the right ventricular ejection fraction in healthy patients measured by Quaife et al. was  $\sim 60$  %, it was  $\sim 75$  % in sham animals in my experiments. Taking this difference into account, the right ventricular ejection fraction, which was deemed normal (60 %), has to experience a relative decrease of more than one third to become less than

40 %. This was also the case in our model, as a reduction from 75 % to 45 % equals a relative reduction of 40 %, being well in the range of a reduction by more than one third. Also, banded animals were shown to die in the course of the staging study; as they were banded, this makes it likely that they died from right heart failure, the alternative being end-organ failure. Therefore, I assume that the characteristics of the right ventricle seen in my studies are similar to those seen clinically in severe pulmonary hypertension, resulting in a failing heart.

Frydrychowicz et al. evaluated the effects of PAB on mice using MRI.<sup>177</sup> They measured an initial right ventricular ejection fraction of 57 %, and a drop to 31 % 8 weeks after banding. The values for end-diastolic and end-systolic volumes they measured were remarkably higher than the values I measured, both for experimental and control values. The effects on right ventricular mass were not stated. Furthermore, no effects of the operation on the left ventricle could be found. The mice they used had an average weight of  $31.7 \pm 2.8$  g, being much heavier than the ones I used, which would explain the very high volume values. This difference might also account for the discrepancy between the studies, with regard to right ventricular ejection fraction and interventricular effects.

In 2003, Bär et al. performed PAB in rats to determine the time-course of specific genetic changes.<sup>178</sup> They also reported the development of the right ventricular mass over 2, 5, 10, 20 and 40 days. Interestingly, right ventricular mass in these animals increased slowly and steadily over the period of the study. This is in contrast to my study, in which the highest increase in right ventricular mass occurred rapidly after operation, followed by a slow, progressive increase. The group did not publish the banding strength they had used in the study. Nonetheless, the maximum right ventricular weight, which was reached, is in good agreement with what I have obtained (Bär et al.: 0.21 g vs. 0.39 g; Sham vs. PAB; 40 days after operation. Cf. staging study: 21 mg vs. 44 mg; Sham vs. PAB; 35 days after operation). A thorough literature search revealed a paper published in 1968 by Olivetti et al., which employed aortic constriction in rats.<sup>179</sup> In line with the results I have obtained, they too saw a rapid increase in heart weight after banding, which began to level in the course of one week after operation.

Other groups, which have performed PAB in rats report similar weight increments in the right ventricular mass to bodyweight ratio, that is a doubling, as we have.<sup>22, 180, 181</sup>

What are the potential drawbacks of pulmonary artery banding? The main culprit probably is the rapidity, with which the increased resistance is induced. This process is more reflective of a sudden increase in resistance like that experienced in pulmonary embolism, and less so in progressive diseases like COPD, in which the resistance builds up gradually over a longer period of time. For this reason, one may not assume that the changes occurring in the right heart in pulmonary artery banding are reflective of both diseases, i.e. pulmonary embolism and COPD, to the same extent, but might have different underlying genetic changes, signaling mechanisms as well as different phenotypic changes (e.g. concentric vs. eccentric hypertrophy). Nonetheless, pulmonary artery banding is the gold standard to elucidate changes and treatment effects directly in the right ventricle, without any concomitant changes in the pulmonary vasculature.<sup>69</sup>

The lack of changes in the pulmonary vasculature might form a potential drawback, as changes in the pulmonary vasculature are underlying most pathological changes in the right ventricle seen clinically. This adds additional variables which could influence gene expression patterns in the affected right heart. Yet, other rodent models of right ventricular hypertrophy that induce changes in the pulmonary vasculature, like the hypoxia or the MCT model, could also exert independent effects on the right ventricular myocardium. As one can easily conclude, all animal models have their individual advantages and disadvantages. A thoughtful combination of different models should form the most complete picture of potential treatment effects. Schermuly et al. has established the partial reversal of pulmonary hypertension and right ventricular hypertrophy in the mouse hypoxia and the rat MCT model;<sup>66</sup> together with the knowledge of the antihypertrophic effects of sildenafil seen in a model of chronic left ventricular pressure overload,<sup>25</sup> this led to the logical conclusion to probe whether these effects are also possible in the right heart, which led to the work implemented in this dissertation.

## 4.4 Clinical Relevance

Riociguat has already successfully passed Phase I and Phase II clinical trials, and is currently undergoing two Phase III trials to probe its vasodilatory effects in patients with symptomatic pulmonary arterial hypertension (PATENT-1 and -2) and chronic thromboembolic pulmonary hypertension (CHEST-1 and -2).<sup>135</sup> The knowledge of riociguat's antifibrotic effects in the right heart, together with its functional improvements, independent of changes in the pulmonary vasculature, could lead to an extension of indications the drug could be used for. As clinical safety testing has already been completed successfully and several long-term trials are ongoing, riociguat could readily be tried in proof-of-concept studies.

## 4.5 Further Experiments

A survival study employing riociguat and sildenafil could be carried, to evaluate whether the functional improvements carry over into an increased survival of the animals.

Higher doses of riociguat and sildenafil could be probed, to analyze whether they result in antihypertrophic effects, as Masuyama et al. observed in in vitro studies that cardiac fibroblasts appear to be more feasible to exert cGMP elevation than cardiac myocytes;<sup>106</sup> and if so, whether this still is associated with a functional improvement, as the resistance the right heart has to work against does not change.

Measuring cGMP levels after drug administration might shed light on whether riociguat and sildenafil treatment increase cGMP levels by the same amount, as treatment differences might owe to this. Furthermore, molecular analyses might be carried out, to look for differences between riociguat and sildenafil treatment.

Immunostaining for sGC and PDE5 in the right heart might help uncover their mechanisms of action.

In contrast to the total collagen content, the collagen type I to collagen type III ratio could be analyzed in sildenafil-treated mice. As collagen type III is more elastic than type I, this might explain the functional improvement of the ventricle, despite any change in the total amount of collagen.

Also, effects of the drugs on the heart's perfusion could be evaluated. Increased perfusion of the right heart should translate into ameliorated function, due to the better supply with oxygen and nutrients.

Lastly, one could check on the effects of drug treatment on apoptosis. Braun et al.<sup>181</sup> and Ikeda et al.<sup>182</sup> reported an increase in apoptosis markers in PAB rats; a reduction in apoptosis might improve the right heart's function as well.

## 4.6 Conclusion

This work showed for the first time the functional and morphological consequences of right ventricular pressure-overload, induced by pulmonary artery banding in the mouse, using magnetic resonance imaging. Additionally, the functional improvements in the right heart by riociguat and sildenafil treatment were demonstrated, independent of changes in the pulmonary vasculature. Finally, for the first time a direct anti-fibrotic effect of riociguat in the right heart was demonstrated.

As riociguat and sildenafil have already undergone extensive studies demonstrating their safety in pre-clinical studies, clinical studies, and from post-marketing surveillance in the case of sildenafil, the results from the experiments carried out in this work might pave the way for new indications these drugs could be employed in.

# Appendix A

## Tables

**Table A.1 – Staging Study - Results (MRI)**

Parameter	Group	Timepoint (day)									
		0	1	3	7	14	21	35	56	105	
<b>Bodyweight (g)</b>											
	Sham	23.18 ± 0.23	22.38 ± 0.35	22.25 ± 0.21	22.83 ± 0.14	23.70 ± 0.23	24.23 ± 0.31	25.65 ± 0.46	26.90 ± 0.45	28.45 ± 0.88	
	PAB	23.40 ± 0.24	21.07 ± 0.26	21.60 ± 0.50	23.43 ± 0.77	23.60 ± 0.71	24.68 ± 0.74	25.67 ± 0.58	26.00 ± 0.59	27.83 ± 0.56	
<b>Heart Rate (beats/min)</b>											
	Sham	429.89 ±65.30	495.19 ±29.81	506.92 ±40.10	522.92 ±32.60	505.83 ±15.61	535.92 ±36.40	491.61 ±67.29	533.94 ±40.53	464.10 ±46.22	
	PAB	449.16 ±30.25	498.52 ±23.16	533.72 ±28.11	556.69 ±23.75	566.51 ±16.31	563.31 ±17.42	562.70 ±21.52	551.19 ±16.98	555.57 ±19.42	
<b>Left Ventricular End Diastolic Volume (μl)</b>											
	Sham	55.48 ± 2.19	54.69 ± 1.92	48.75 ± 2.08	52.11 ± 2.74	49.63 ± 0.87	51.16 ± 1.39	58.45 ± 4.19	55.31 ± 3.83	65.78 ± 3.82	
	PAB	55.43 ± 3.20	40.48 ± 3.03	36.87 ± 4.39	33.23 ± 4.11**	32.12 ± 3.93***	30.37 ± 3.86**	31.80 ± 3.72***	27.74 ± 3.27***	31.10 ± 4.51***	
<b>Left Ventricular End Systolic Volume (μl)</b>											
	Sham	18.18 ± 2.90	19.46 ± 1.24	17.99 ± 2.53	18.17 ± 2.44	15.27 ± 1.51	15.78 ± 2.43	19.90 ± 4.63	17.00 ± 3.21	25.77 ± 4.54	
	PAB	19.79 ± 2.27	17.90 ± 2.80	13.97 ± 1.72	11.20 ± 1.50	11.51 ± 1.35	10.64 ± 1.56	10.92 ± 1.44	8.73 ± 0.78	11.53 ± 2.05*	
<b>Left Ventricular Stroke Volume (μl)</b>											
	Sham	37.29 ± 1.39	35.22 ± 1.21	30.76 ± 0.76	33.95 ± 0.88	34.37 ± 1.23	35.38 ± 2.14	38.56 ± 1.25	38.32 ± 1.82	40.01 ± 0.91	
	PAB	35.63 ± 1.13	22.59 ± 2.81**	22.90 ± 3.41	22.03 ± 3.25*	20.61 ± 3.22**	19.73 ± 2.68***	20.87 ± 2.50***	19.00 ± 2.88***	19.57 ± 2.66***	
<b>Left Ventricular Ejection Fraction (%)</b>											
	Sham	67.60 ± 3.91	64.48 ± 1.48	63.45 ± 3.53	65.57 ± 3.06	69.30 ± 2.77	69.30 ± 4.52	67.08 ± 5.68	69.82 ± 3.69	61.60 ± 4.43	
	PAB	64.88 ± 2.24	55.88 ± 5.65	61.30 ± 3.83	65.65 ± 3.17	63.23 ± 3.54	64.82 ± 2.93	65.79 ± 2.37	66.99 ± 3.47	62.61 ± 1.86	
<b>Left Ventricular Cardiac Output (ml/min)</b>											
	Sham	15.81 ± 2.11	17.39 ± 0.90	15.62 ± 1.35	17.73 ± 1.05	17.34 ± 0.35	18.97 ± 1.78	19.07 ± 2.95	20.42 ± 1.72	18.64 ± 2.10	
	PAB	15.89 ± 0.80	11.30 ± 1.55	12.30 ± 1.94	12.21 ± 1.88	11.67 ± 1.87	11.03 ± 1.36*	11.60 ± 1.16***	10.58 ± 1.69***	11.10 ± 1.50*	
<b>Left Ventricular Mass (mg)</b>											
	Sham	80.37 ± 1.10	77.48 ± 2.74	79.02 ± 2.75	77.47 ± 2.15	76.77 ± 1.74	83.34 ± 2.49	87.20 ± 1.40	90.45 ± 4.91	88.19 ± 3.52	
	PAB	81.25 ± 2.32	82.29 ± 2.71	81.96 ± 1.70	75.94 ± 3.24	74.23 ± 2.51	78.19 ± 2.53	81.03 ± 2.70	82.88 ± 2.54	85.75 ± 2.63	
<b>Right Ventricular End Diastolic Volume (μl)</b>											
	Sham	47.15 ± 1.93	45.57 ± 1.37	40.71 ± 1.00	43.35 ± 2.62	42.08 ± 0.66	44.67 ± 0.82	44.97 ± 3.24	46.78 ± 1.66	55.19 ± 3.83	
	PAB	43.16 ± 2.09	63.03 ± 3.77*	52.58 ± 4.12	45.60 ± 4.42	51.69 ± 4.23	53.36 ± 4.93	53.46 ± 2.68	56.48 ± 3.63	61.48 ± 5.29	
<b>Right Ventricular End Systolic Volume (μl)</b>											
	Sham	11.98 ± 1.49	11.92 ± 0.22	10.71 ± 1.13	11.10 ± 1.49	9.51 ± 1.00	9.77 ± 1.66	10.52 ± 1.97	9.35 ± 1.36	15.50 ± 2.74	
	PAB	11.97 ± 0.91	38.43 ± 5.51***	29.29 ± 4.31**	24.26 ± 4.06	27.06 ± 3.59**	29.06 ± 4.07**	30.67 ± 3.04**	30.82 ± 3.78***	35.41 ± 4.07**	
<b>Right Ventricular Stroke Volume (μl)</b>											
	Sham	35.16 ± 1.18	33.65 ± 1.30	30.01 ± 0.92	32.24 ± 1.53	32.57 ± 1.28	34.90 ± 1.15	34.45 ± 2.08	37.43 ± 1.38	38.44 ± 0.11	
	PAB	31.19 ± 1.31	24.61 ± 2.40**	23.28 ± 1.75	21.34 ± 1.24***	24.59 ± 2.46*	24.29 ± 2.65***	22.79 ± 1.73***	24.86 ± 1.14***	25.85 ± 1.49***	

Continued on next page

Table A.1 – continued from previous page

Parameter	Group	Timepoint (day)									
		0	1	3	7	14	21	35	56	105	
<b>Right Ventricular Ejection Fraction (%)</b>											
	Sham	74.78 ± 2.45	73.79 ± 0.75	73.78 ± 2.35	74.65 ± 2.25	77.36 ± 2.41	78.27 ± 3.35	76.99 ± 3.16	80.10 ± 2.49	71.79 ± 3.52	
	PAB	72.42 ± 1.07	40.41 ± 5.38***	45.51 ± 4.67***	48.42 ± 4.24***	48.24 ± 4.21***	46.04 ± 4.11***	43.02 ± 3.51***	45.93 ± 3.56***	42.61 ± 2.10***	
<b>Right Ventricular Cardiac Output (ml/min)</b>											
	Sham	14.95 ± 2.08	16.64 ± 1.03	15.23 ± 1.33	16.81 ± 1.07	16.43 ± 0.46	18.67 ± 1.26	16.76 ± 2.21	19.93 ± 1.51	17.85 ± 1.82	
	PAB	13.87 ± 0.66	12.31 ± 1.35	12.38 ± 1.02	11.79 ± 0.61*	13.75 ± 0.98	13.53 ± 1.25*	12.77 ± 0.90	13.51 ± 0.71**	15.75 ± 0.28	
<b>Right Ventricular Mass (mg)</b>											
	Sham	46.89 ± 2.82	48.24 ± 2.61	46.67 ± 1.76	44.39 ± 2.57	41.89 ± 0.96	40.60 ± 1.91	41.32 ± 1.31	43.17 ± 0.52	41.24 ± 2.59	
	PAB	42.74 ± 1.67	57.98 ± 2.52	65.13 ± 2.32**	67.71 ± 3.07***	67.74 ± 3.28***	68.97 ± 3.53***	74.28 ± 3.54***	78.56 ± 4.75***	95.11 ± 7.18***	
<b>Right Ventricular Mass / Bodyweight (mg/g)</b>											
	Sham	2.02 ± 0.13	2.16 ± 0.14	2.10 ± 0.09	1.95 ± 0.12	1.77 ± 0.04	1.67 ± 0.06	1.61 ± 0.07	1.61 ± 0.04	1.45 ± 0.10	
	PAB	1.83 ± 0.07	2.76 ± 0.14	3.02 ± 0.10**	2.90 ± 0.14**	2.89 ± 0.17***	2.82 ± 0.19***	2.91 ± 0.17***	3.03 ± 0.18***	3.49 ± 0.32***	
<b>Right Ventricular Mass / Left Ventricular Mass (mg/mg)</b>											
	Sham	0.58 ± 0.04	0.62 ± 0.03	0.60 ± 0.04	0.57 ± 0.02	0.55 ± 0.01	0.49 ± 0.02	0.47 ± 0.02	0.48 ± 0.03	0.47 ± 0.01	
	PAB	0.53 ± 0.03	0.70 ± 0.02	0.80 ± 0.03**	0.90 ± 0.05***	0.91 ± 0.03***	0.88 ± 0.03***	0.92 ± 0.04***	0.95 ± 0.05***	1.10 ± 0.05***	
<b>Left Ventricular End-Diastolic Eccentricity Index (mm/mm)</b>											
	Sham	1.17 ± 0.03	1.22 ± 0.01	1.20 ± 0.03	1.23 ± 0.03	1.22 ± 0.05	1.24 ± 0.03	1.26 ± 0.04	1.24 ± 0.04	1.19 ± 0.00	
	PAB	1.24 ± 0.04	1.69 ± 0.12	1.62 ± 0.17	1.78 ± 0.20	2.02 ± 0.22*	1.98 ± 0.20	2.20 ± 0.27*	2.44 ± 0.26***	2.45 ± 0.36***	
<b>Left Ventricular End-Systolic Eccentricity Index (mm/mm)</b>											
	Sham	1.28 ± 0.09	1.33 ± 0.02	1.34 ± 0.02	1.33 ± 0.02	1.28 ± 0.02	1.23 ± 0.04	1.22 ± 0.04	1.18 ± 0.06	1.17 ± 0.04	
	PAB	1.26 ± 0.08	1.67 ± 0.06	1.61 ± 0.12	2.13 ± 0.25	2.31 ± 0.29	2.30 ± 0.30	3.20 ± 0.49***	3.27 ± 0.44***	3.08 ± 0.39***	

\*p&lt;0.05, \*\*p&lt;0.01, \*\*\*p&lt;0.001; Sham vs. PAB

**Table A.2 – Staging Study - Results (Harvest)**

Parameter	Group	Timepoint (day)					
		3	7	14	21	28	35
<b>Bodyweight (g)</b>							
	Sham	23.60 ± 0.00	24.19 ± 0.70	25.83 ± 0.53	26.62 ± 0.34	25.20 ± 0.51	27.23 ± 0.33
	PAB	21.83 ± 0.93	23.80 ± 0.66	26.47 ± 0.28	26.75 ± 0.24	26.04 ± 0.46	26.94 ± 0.26
<b>Systolic Blood Pressure (mmHg)</b>							
	Sham	87.33 ± 4.77	87.57 ± 3.42	92.03 ± 1.47	97.28 ± 2.30	85.76 ± 4.65	89.57 ± 5.44
	PAB	74.08 ± 4.84	68.45 ± 4.83*	80.18 ± 2.33	79.89 ± 6.53*	77.92 ± 4.11	80.96 ± 3.59
<b>Right Ventricular Systolic Blood Pressure (mmHg)</b>							
	Sham	27.55 ± 1.74	28.50 ± 0.86	26.60 ± 0.34	28.49 ± 0.64	27.39 ± 1.24	29.40 ± 0.88
	PAB	40.20 ± 0.68	46.89 ± 3.51**	55.51 ± 3.51***	67.76 ± 4.42***	57.77 ± 7.05***	67.79 ± 4.81***
<b>Left Ventricular Mass (mg)</b>							
	Sham	77.45 ± 2.25	86.75 ± 2.27	86.83 ± 3.90	92.46 ± 3.27	86.50 ± 1.91	93.26 ± 1.34
	PAB	68.18 ± 3.91	73.06 ± 2.24***	76.58 ± 1.13	84.63 ± 1.85	80.48 ± 2.56	87.94 ± 2.93
<b>Right Ventricular Mass (mg)</b>							
	Sham	19.85 ± 0.25	19.71 ± 0.69	19.95 ± 0.39	20.18 ± 1.11	19.91 ± 0.98	20.88 ± 0.63
	PAB	31.23 ± 1.75	34.68 ± 1.94***	35.78 ± 2.78***	42.05 ± 2.33***	37.38 ± 2.40***	44.10 ± 2.73***
<b>Right Ventricular Mass / Bodyweight (mg/g)</b>							
	Sham	0.84 ± 0.01	0.82 ± 0.03	0.77 ± 0.01	0.76 ± 0.04	0.80 ± 0.04	0.77 ± 0.02
	PAB	1.45 ± 0.15*	1.47 ± 0.09***	1.45 ± 0.06***	1.57 ± 0.10***	1.45 ± 0.11***	1.64 ± 0.10***
<b>Right Ventricular Mass / Left Ventricular Mass (mg/mg)</b>							
	Sham	0.26 ± 0.01	0.23 ± 0.01	0.23 ± 0.01	0.22 ± 0.01	0.23 ± 0.01	0.23 ± 0.01
	PAB	0.47 ± 0.06*	0.48 ± 0.04***	0.47 ± 0.04***	0.50 ± 0.03***	0.47 ± 0.04***	0.50 ± 0.03***
<b>Right Ventricular Mass / Tibia Length (mg/mm)</b>							
	Sham	1.29 ± 0.02	1.25 ± 0.05	1.26 ± 0.01	1.26 ± 0.07	1.27 ± 0.07	1.26 ± 0.04
	PAB	2.02 ± 0.13	2.23 ± 0.13***	2.38 ± 0.09***	2.62 ± 0.15***	2.30 ± 0.15***	2.65 ± 0.16***
<b>Right Ventricular Cardiomyocyte Diameter (µm)</b>							
	Sham	16.11 ± 0.28	14.77 ± 0.27	15.93 ± 0.19	16.84 ± 0.39	16.54 ± 0.56	17.70 ± 0.59
	PAB	18.33 ± 0.21	18.65 ± 0.40***	19.42 ± 0.69**	20.22 ± 0.66**	20.78 ± 0.87***	19.99 ± 0.67*
<b>Right Ventricular Collagen Content (%)</b>							
	Sham	0.47 ± 0.03	0.54 ± 0.05	0.61 ± 0.11	0.44 ± 0.02	0.48 ± 0.07	0.56 ± 0.05
	PAB	0.50 ± 0.05	1.58 ± 0.32	3.51 ± 0.50***	5.41 ± 0.20***	4.73 ± 0.52***	4.37 ± 1.53***

\*p<0.05, \*\*p<0.01, \*\*\*p<0.001; Sham vs. PAB

**Table A.3 – Treatment Study - Results**

Parameter	Experimental Group				
	Sham	PAB	Sildenafil	Riociguat	
<b>Bodyweight (g)</b>					
	0	24.79 ± 0.42	23.55 ± 0.48	23.53 ± 0.27	23.78 ± 0.31
	7	25.23 ± 0.34	22.93 ± 0.61 <sup>†</sup>	22.47 ± 0.66	22.34 ± 0.52
	21	26.34 ± 0.34	24.52 ± 0.40	22.58 ± 1.12*	23.26 ± 0.39
	21-7	1.11 ± 0.32	1.59 ± 0.45	0.11 ± 0.89	0.93 ± 0.35

Continued on next page

Table A.3 – continued from previous page

Parameter	Experimental Group			
	Sham	PAB	Sildenafil	Riociguat
Heart Rate (beats/min)				
0	471.77 ±23.00	445.69 ±1.43	419.28 ±16.49	432.26 ±15.28
7	506.47 ±28.52	501.49 ±19.60	515.78 ±12.84	507.50 ±14.47
21	464.80 ±24.04	514.06 ±15.12	539.31 ±17.31	524.52 ± 8.76
21-7	-41.67 ±25.92	12.57 ±18.11	23.53 ±11.32	17.02 ±13.78
Systolic Blood Pressure (mmHg)				
21	95.06 ± 1.84	77.26 ± 3.80 <sup>††</sup>	77.33 ± 3.72	79.04 ± 5.47
Right Ventricular Systolic Blood Pressure (mmHg)				
21	24.98 ± 0.94	60.53 ± 1.87 <sup>†††</sup>	59.19 ± 2.10	59.90 ± 4.28
Left Ventricular End Diastolic Volume (μl)				
0	60.09 ± 2.28	59.37 ± 1.77	61.88 ± 1.82	60.14 ± 2.37
7	59.90 ± 1.80	25.89 ± 2.76 <sup>†††</sup>	27.25 ± 1.28	23.83 ± 1.89
21	64.18 ± 1.92	27.87 ± 1.98 <sup>†††</sup>	27.57 ± 1.94	25.57 ± 2.45
21-7	4.28 ± 0.51	1.98 ± 2.08	0.31 ± 1.49	1.75 ± 1.56
Left Ventricular End Systolic Volume (μl)				
0	22.79 ± 2.00	22.86 ± 1.22	24.79 ± 1.75	22.61 ± 2.22
7	23.15 ± 1.86	10.56 ± 1.86 <sup>†††</sup>	12.65 ± 2.55	8.66 ± 0.87
21	24.50 ± 2.09	10.30 ± 0.82 <sup>†††</sup>	8.86 ± 0.62	9.40 ± 1.52
21-7	1.35 ± 0.71	-0.26 ± 1.89	-3.79 ± 2.07	0.74 ± 1.34
Left Ventricular Stroke Volume (μl)				
0	37.31 ± 0.45	36.51 ± 1.43	37.08 ± 0.93	37.54 ± 0.50
7	36.75 ± 0.75	15.33 ± 1.18 <sup>†††</sup>	16.92 ± 0.81	15.16 ± 1.10
21	39.69 ± 1.08	17.57 ± 1.42 <sup>†††</sup>	18.70 ± 1.38	16.17 ± 1.27
21-7	2.94 ± 0.49	2.24 ± 0.75	1.78 ± 1.19	1.01 ± 0.62

Continued on next page

Table A.3 – continued from previous page

Parameter	Experimental Group			
	Sham	PAB	Sildenafil	Riociguat
Left Ventricular Ejection Fraction (%)				
0	62.49 ± 1.88	61.49 ± 1.65	60.24 ± 2.00	62.98 ± 2.17
7	61.67 ± 2.08	61.19 ± 2.89	62.27 ± 1.81	63.97 ± 1.35
21	62.14 ± 2.32	62.87 ± 1.67	67.78 ± 0.81	64.13 ± 2.53
21-7	0.47 ± 0.90	1.68 ± 3.58	5.51 ± 2.23	0.17 ± 2.46
Left Ventricular Cardiac Output (ml/min)				
0	17.63 ± 1.01	16.26 ± 0.69	15.52 ± 0.65	16.18 ± 0.42
7	18.60 ± 1.08	7.75 ± 0.74 <sup>†††</sup>	8.69 ± 0.39	7.73 ± 0.65
21	18.51 ± 1.28	9.04 ± 0.77 <sup>†††</sup>	10.08 ± 0.74	8.45 ± 0.60
21-7	-0.09 ± 0.92	1.29 ± 0.43	1.39 ± 0.59	0.73 ± 0.26
Left Ventricular Mass (mg)				
0	85.46 ± 1.67	80.05 ± 2.91	81.39 ± 1.19	84.99 ± 2.06
7	89.21 ± 1.75	68.44 ± 1.97 <sup>†††</sup>	67.66 ± 2.79	66.63 ± 2.50
21	95.49 ± 3.08	74.29 ± 1.40 <sup>†††</sup>	69.68 ± 3.13	65.99 ± 2.91*
21-7	6.28 ± 2.41	5.84 ± 2.14	2.02 ± 2.57	-0.64 ± 1.86
Right Ventricular End Diastolic Volume (μl)				
0	50.07 ± 2.87	49.83 ± 1.62	51.71 ± 1.57	50.45 ± 1.88
7	47.77 ± 2.29	73.32 ± 5.16 <sup>†††</sup>	59.92 ± 3.25*	71.16 ± 3.54
21	51.76 ± 1.92	72.62 ± 4.34 <sup>†††</sup>	54.46 ± 2.72 <sup>***</sup>	63.41 ± 4.77
21-7	3.99 ± 1.37	-0.70 ± 1.88	-5.46 ± 2.12	-7.75 ± 5.21
Right Ventricular End Systolic Volume (μl)				
0	14.17 ± 2.00	14.78 ± 1.05	15.98 ± 1.34	14.41 ± 1.71
7	12.99 ± 1.14	49.57 ± 4.06 <sup>†††</sup>	36.99 ± 3.45 <sup>**</sup>	46.80 ± 3.30
21	13.94 ± 1.48	47.40 ± 3.64 <sup>†††</sup>	28.82 ± 2.85 <sup>***</sup>	35.96 ± 3.44*
21-7	0.95 ± 1.39	-2.18 ± 1.93	-8.17 ± 2.18	-10.85 ± 3.88*

Continued on next page

Table A.3 – continued from previous page

Parameter	Experimental Group			
	Sham	PAB	Sildenafil	Riociguat
Right Ventricular Stroke Volume ( $\mu$ l)				
0	35.90 $\pm$ 1.13	35.05 $\pm$ 1.54	35.73 $\pm$ 1.09	36.04 $\pm$ 0.64
7	34.77 $\pm$ 1.28	23.75 $\pm$ 1.39 <sup>†††</sup>	22.93 $\pm$ 1.54	24.35 $\pm$ 0.88
21	37.81 $\pm$ 1.33	25.22 $\pm$ 1.03 <sup>†††</sup>	25.64 $\pm$ 0.97	27.46 $\pm$ 1.99
21-7	3.04 $\pm$ 0.63	1.47 $\pm$ 0.70	2.71 $\pm$ 0.91	3.10 $\pm$ 1.82
Right Ventricular Ejection Fraction (%)				
0	72.42 $\pm$ 2.41	70.27 $\pm$ 1.98	69.34 $\pm$ 2.09	71.98 $\pm$ 2.41
7	73.11 $\pm$ 1.37	32.85 $\pm$ 1.39 <sup>†††</sup>	39.09 $\pm$ 3.05	34.70 $\pm$ 1.82
21	73.30 $\pm$ 2.18	35.37 $\pm$ 1.69 <sup>†††</sup>	48.18 $\pm$ 3.27 <sup>***</sup>	43.65 $\pm$ 2.15*
21-7	0.19 $\pm$ 2.04	2.52 $\pm$ 1.33	9.09 $\pm$ 2.22*	8.98 $\pm$ 2.05
Right Ventricular Cardiac Output (ml/min)				
0	16.99 $\pm$ 1.16	15.61 $\pm$ 0.74	14.98 $\pm$ 0.71	15.56 $\pm$ 0.58
7	17.56 $\pm$ 1.07	11.77 $\pm$ 0.60 <sup>†††</sup>	11.87 $\pm$ 0.94	12.41 $\pm$ 0.74
21	17.67 $\pm$ 1.36	12.96 $\pm$ 0.65 <sup>†††</sup>	13.87 $\pm$ 0.77	14.44 $\pm$ 1.17
21-7	0.11 $\pm$ 0.80	1.19 $\pm$ 0.49	2.00 $\pm$ 0.44	2.03 $\pm$ 0.96
Right Ventricular Mass (mg)				
0	30.37 $\pm$ 0.94	29.43 $\pm$ 0.77	30.02 $\pm$ 0.89	29.67 $\pm$ 0.56
7	32.35 $\pm$ 0.71	61.06 $\pm$ 2.41 <sup>†††</sup>	55.44 $\pm$ 1.93	60.46 $\pm$ 1.31
21	32.82 $\pm$ 0.99	62.31 $\pm$ 3.09 <sup>†††</sup>	57.09 $\pm$ 2.23	59.57 $\pm$ 2.50
21-7	0.47 $\pm$ 0.83	1.25 $\pm$ 1.50	1.65 $\pm$ 1.66	-0.88 $\pm$ 2.27
Right Ventricular Mass / Bodyweight (mg/g)				
0	1.23 $\pm$ 0.04	1.25 $\pm$ 0.03	1.28 $\pm$ 0.04	1.25 $\pm$ 0.03
7	1.28 $\pm$ 0.03	2.67 $\pm$ 0.11 <sup>†††</sup>	2.48 $\pm$ 0.11	2.72 $\pm$ 0.10
21	1.25 $\pm$ 0.04	2.55 $\pm$ 0.14 <sup>†††</sup>	2.56 $\pm$ 0.10	2.56 $\pm$ 0.11
21-7	-0.04 $\pm$ 0.04	-0.12 $\pm$ 0.09	0.07 $\pm$ 0.15	-0.16 $\pm$ 0.10

Continued on next page

Table A.3 – continued from previous page

Parameter	Experimental Group			
	Sham	PAB	Sildenafil	Riociguat
Right Ventricular Mass / Left Ventricular Mass (mg/mg)				
0	0.36 ± 0.01	0.37 ± 0.01	0.37 ± 0.01	0.35 ± 0.01
7	0.36 ± 0.01	0.90 ± 0.04 <sup>†††</sup>	0.83 ± 0.04	0.91 ± 0.03
21	0.34 ± 0.01	0.84 ± 0.04 <sup>†††</sup>	0.83 ± 0.03	0.91 ± 0.04
21-7	-0.02 ± 0.01	-0.06 ± 0.02	0.00 ± 0.03	0.00 ± 0.04
Left Ventricular End-Diastolic Eccentricity Index (mm/mm)				
0	1.14 ± 0.02	1.13 ± 0.01	1.14 ± 0.01	1.16 ± 0.02
7	1.12 ± 0.01	2.40 ± 0.16 <sup>†††</sup>	2.32 ± 0.04	2.52 ± 0.13
21	1.14 ± 0.02	2.58 ± 0.13 <sup>†††</sup>	2.31 ± 0.12	2.65 ± 0.20
21-7	0.01 ± 0.02	0.18 ± 0.13	-0.01 ± 0.13	0.13 ± 0.10
Left Ventricular End-Systolic Eccentricity Index (mm/mm)				
0	1.18 ± 0.03	1.15 ± 0.03	1.18 ± 0.02	1.18 ± 0.03
7	1.15 ± 0.03	2.64 ± 0.26 <sup>†††</sup>	2.54 ± 0.13	2.74 ± 0.12
21	1.19 ± 0.02	3.16 ± 0.16 <sup>†††</sup>	2.63 ± 0.14*	3.16 ± 0.37
21-7	0.04 ± 0.03	0.52 ± 0.34	0.09 ± 0.11	0.42 ± 0.34
Right Ventricular Collagen Area (%)				
21	0.74 ± 0.16	5.61 ± 0.28 <sup>†††</sup>	5.37 ± 0.25	3.05 ± 0.76**
Right Ventricular Cardiomyocyte Diameter (μm)				
21	14.15 ± 0.03	20.70 ± 0.60 <sup>†††</sup>	19.70 ± 0.62	19.76 ± 0.31

\*p<0.05, \*\*p<0.01, \*\*\*p<0.001; PAB vs. Sildenafil / Riociguat

†p<0.05, ††p<0.01, †††p<0.001; PAB vs. Sham

# Bibliography

- [1] M. K. Davies and A. Hollman, "William Harvey (1578-1657)," *Heart*, vol. 76, no. 1, pp. 11–2, 1996.
- [2] N. F. Voelkel, R. A. Quaife, L. A. Leinwand, R. J. Barst, M. D. McGoon, D. R. Meldrum, J. Dupuis, C. S. Long, L. J. Rubin, F. W. Smart, Y. J. Suzuki, M. Gladwin, E. M. Denholm, and D. B. Gail, "Right ventricular function and failure - Report of a National Heart, lung, and Blood Institute working group on cellular and molecular mechanisms of right heart failure," *Circulation*, vol. 114, no. 17, pp. 1883–1891, 2006.
- [3] A. C. P. Bakos, "The Question of the Function of the Right Ventricular Myocardium - an Experimental Study," *Circulation*, vol. 1, no. 4, pp. 725–732, 1950.
- [4] A. Kagan, "Dynamic responses of the right ventricle following extensive damage by cauterization," *Circulation*, vol. 5, no. 6, pp. 816–23, 1952.
- [5] I. Starr, W. A. Jeffers, and R. H. Meade, "The absence of conspicuous increments of venous pressure after severe damage to the right ventricle of the dog, with a discussion of the relation between clinical congestive failure and heart disease," *American Heart Journal*, vol. 26, no. 3, pp. 291–301, 1943.
- [6] F. Fontan and E. Baudet, "Surgical repair of tricuspid atresia," *Thorax*, vol. 26, no. 3, pp. 240–&, 1971.
- [7] D. N. Ross and Somervil.J, "Correction of pulmonary atresia with a homograft aortic valve," *Lancet*, vol. 2, no. 7479, pp. 1446–&, 1966.
- [8] F. Haddad, P. Couture, C. Tousignant, and A. Y. Denault, "The right ventricle in cardiac surgery, a perioperative perspective: II. Pathophysiology, clinical importance, and management," *Anesthesia and analgesia*, vol. 108, no. 2, pp. 422–33, 2009.
- [9] R. M. Sade and A. R. Castaneda, "Dispensable right ventricle," *Surgery*, vol. 77, no. 5, pp. 624–631, 1975.
- [10] S. A. Furey, H. A. Zieske, and M. N. Levy, "The essential function of the right ventricle," *American Heart Journal*, vol. 107, no. 2, pp. 404–410, 1984.

- [11] J. N. Cohn, N. H. Guiha, M. I. Broder, and C. J. Limas, "Right ventricular infarction - clinical and hemodynamic features," *American Journal of Cardiology*, vol. 33, no. 2, pp. 209–214, 1974.
- [12] B. J. Baker, M. M. Wilen, C. M. Boyd, H. Dinh, and J. A. Franciosa, "Relation of Right Ventricular Ejection Fraction to Exercise Capacity in Chronic Left-Ventricular Failure," *American Journal of Cardiology*, vol. 54, no. 6, pp. 596–599, 1984.
- [13] J. F. Polak, B. L. Holman, J. Wynne, and W. S. Colucci, "Right ventricular ejection fraction - an indicator of increased mortality in patients with congestive heart-failure associated with coronary-artery disease," *Journal of the American College of Cardiology*, vol. 2, no. 2, pp. 217–224, 1983.
- [14] M. Zehender, W. Kasper, E. Kauder, M. Schonhaler, A. Geibel, M. Olschewski, and H. Just, "Right ventricular infarction as an independent predictor of prognosis after acute inferior myocardial-infarction," *New England Journal of Medicine*, vol. 328, no. 14, pp. 981–988, 1993.
- [15] S. R. Mehta, J. W. Eikelboom, M. K. Natarajan, R. Diaz, C. L. Yi, R. J. Gibbons, and S. Yusuf, "Impact of right ventricular involvement on mortality and morbidity in patients with inferior myocardial infarction," *Journal of the American College of Cardiology*, vol. 37, no. 1, pp. 37–43, 2001.
- [16] T. A. Markel, G. M. Wairiuko, T. Lahm, P. R. Crisostomo, M. Wang, C. M. Herring, and D. R. Meldrum, "The right heart and its distinct mechanisms of development, function, and failure," *Journal of Surgical Research*, vol. 146, no. 2, pp. 304–313, 2008.
- [17] F. Haddad, P. Couture, C. Tousignant, and A. Y. Denault, "The right ventricle in cardiac surgery, a perioperative perspective: I. Anatomy, physiology, and assessment," *Anesthesia and analgesia*, vol. 108, no. 2, pp. 407–21, 2009.
- [18] A. R. Hemnes and H. C. Champion, "Right heart function and haemodynamics in pulmonary hypertension," *International journal of clinical practice. Supplement*, no. 160, pp. 11–9, 2008.
- [19] M. Cecconi, E. Johnston, and A. Rhodes, "What role does the right side of the heart play in circulation?," *Critical Care*, vol. 10, 2006.
- [20] P. Zong, J. D. Tune, and H. F. Downey, "Mechanisms of oxygen demand/supply balance in the right ventricle," *Experimental biology and medicine*, vol. 230, no. 8, pp. 507–19, 2005.
- [21] C. R. Greyson, "The right ventricle and pulmonary circulation: basic concepts," *Revista espanola de cardiologia*, vol. 63, no. 1, pp. 81–95, 2010.
- [22] T. Urashima, M. Zhao, R. Wagner, G. Fajardo, S. Farahani, T. Quertermous, and D. Bernstein, "Molecular and physiological characterization of RV remodeling in a murine model of pulmonary stenosis," *American Journal*

- of Physiology-Heart and Circulatory Physiology*, vol. 295, no. 3, pp. H1351–H1368, 2008.
- [23] D. G. McFadden, A. C. Barbosa, J. A. Richardson, M. D. Schneider, D. Srivastava, and E. N. Olson, “The Hand1 and Hand2 transcription factors regulate expansion of the embryonic cardiac ventricles in a gene dosage-dependent manner,” *Development*, vol. 132, no. 1, pp. 189–201, 2005.
- [24] D. J. Garry and E. N. Olson, “A common progenitor at the heart of development,” *Cell*, vol. 127, pp. 1101–4, Dec 2006.
- [25] E. Takimoto, H. C. Champion, M. X. Li, D. Belardi, S. X. Ren, E. R. Rodriguez, D. Bedja, K. L. Gabrielson, Y. B. Wang, and D. A. Kass, “Chronic inhibition of cyclic GMP phosphodiesterase 5A prevents and reverses cardiac hypertrophy,” *Nature Medicine*, vol. 11, no. 2, pp. 214–222, 2005.
- [26] S. Schafer, P. Ellinghaus, W. Janssen, F. Kramer, K. Lustig, H. Milting, R. Kast, and M. Klein, “Chronic inhibition of phosphodiesterase 5 does not prevent pressure-overload-induced right-ventricular remodelling,” *Cardiovascular Research*, vol. 82, no. 1, pp. 30–39, 2009.
- [27] M. Kuhn, “Cardiac anti-remodelling effects of phosphodiesterase type 5 inhibitors: afterload-(in)dependent?,” *Cardiovascular Research*, vol. 82, no. 1, pp. 4–6, 2009.
- [28] WHO, “Chronic cor pulmonale: Report of an expert committee,” *Circulation*, vol. 27, no. 4, pp. 594–615, 1963.
- [29] M. Niederman and R. A. Matthay, “Cardiovascular function in secondary pulmonary hypertension,” *Heart & Lung*, vol. 15, pp. 341,351, 1986.
- [30] D. B. Badesch, H. C. Champion, M. A. Sanchez, M. M. Hoeper, J. E. Loyd, A. Manes, M. McGoon, R. Naeije, H. Olschewski, R. J. Oudiz, and A. Torbicki, “Diagnosis and assessment of pulmonary arterial hypertension,” *Journal of the American College of Cardiology*, vol. 54, no. 1 Suppl, pp. S55–66, 2009.
- [31] G. Simonneau, I. M. Robbins, M. Beghetti, R. N. Channick, M. Delcroix, C. P. Denton, C. G. Elliott, S. P. Gaine, M. T. Gladwin, Z. C. Jing, M. J. Krowka, D. Langleben, N. Nakanishi, and R. Souza, “Updated clinical classification of pulmonary hypertension,” *Journal of the American College of Cardiology*, vol. 54, no. 1 Suppl, pp. S43–54, 2009.
- [32] G. Simonneau, N. Galie, L. J. Rubin, D. Langleben, W. Seeger, G. Domenighetti, S. Gibbs, D. Lebrec, R. Speich, M. Beghetti, S. Rich, and A. Fishman, “Clinical classification of pulmonary hypertension,” in *Third World Symposium on Pulmonary Arterial Hypertension*, vol. 43, (NEW YORK), pp. 5S–12S, Elsevier Science Inc, 2004. ISI Document Delivery No.: 831QI Times Cited: 204 Cited Reference Count: 71 Suppl. S.

- [33] F. Jardin, O. Dubourg, P. Guéret, G. Delorme, and J. P. Bourdarias, “Quantitative two-dimensional echocardiography in massive pulmonary embolism: emphasis on ventricular interdependence and leftward septal displacement,” *J Am Coll Cardiol*, vol. 10, pp. 1201–6, Dec 1987.
- [34] N. Frey, H. A. Katus, E. N. Olson, and J. A. Hill, “Hypertrophy of the heart - A new therapeutic target?,” *Circulation*, vol. 109, no. 13, pp. 1580–1589, 2004.
- [35] H. J. Bogaard, K. Abe, A. V. Noordegraaf, and N. F. Voelkel, “The right ventricle under pressure cellular and molecular mechanisms of right-heart failure in pulmonary hypertension,” *Chest*, vol. 135, no. 3, pp. 794–804, 2009.
- [36] P. Pokreisz, G. Marsboom, and S. Janssens, “Pressure overload-induced right ventricular dysfunction and remodelling in experimental pulmonary hypertension: the right heart revisited,” in *Workshop on Right Ventricular Function and Pulmonary Hypertension*, vol. 9, (OXFORD), pp. H75–H84, Oxford Univ Press, 2007. ISI Document Delivery No.: 254NE Times Cited: 1 Cited Reference Count: 136 Pokreisz, Peter Marsboom, Glenn Janssens, Stefan.
- [37] B. D. Lowes, W. Minobe, W. T. Abraham, M. N. Rizeq, T. J. Bohlmeier, R. A. Quaife, R. L. Roden, D. L. Dutcher, A. D. Robertson, N. F. Voelkel, D. B. Badesch, B. M. Groves, E. M. Gilbert, and M. R. Bristow, “Changes in gene expression in the intact human heart. Downregulation of alpha-myosin heavy chain in hypertrophied, failing ventricular myocardium,” *The Journal of clinical investigation*, vol. 100, no. 9, pp. 2315–24, 1997.
- [38] J. J. Hunter and K. R. Chien, “Signaling pathways for cardiac hypertrophy and failure,” *N Engl J Med*, vol. 341, pp. 1276–83, Oct 1999.
- [39] M. Orth, K. Rasche, and G. Schultze-Werninghaus, “Chronic cor pulmonale - epidemiology, pathophysiology, and symptomatology,” *Internist*, vol. 40, no. 7, pp. 722–728, 1999.
- [40] C. V. Bourantas, H. P. Loh, T. Bragadeesh, A. S. Rigby, E. I. Lukaschuk, S. Garg, A. C. Tweddel, F. M. Alamgir, N. P. Nikitin, A. L. Clark, and J. G. Cleland, “Relationship between right ventricular volumes measured by cardiac magnetic resonance imaging and prognosis in patients with chronic heart failure,” *European Journal of Heart Failure*, vol. 13, no. 1, pp. 52–60, 2011.
- [41] A. Brieke and D. DeNofrio, “Right ventricular dysfunction in chronic dilated cardiomyopathy and heart failure,” *Coron Artery Dis*, vol. 16, pp. 5–11, Feb 2005.
- [42] W. MacNee, “Pathophysiology of cor pulmonale in chronic obstructive pulmonary disease. Part One,” *Am J Respir Crit Care Med*, vol. 150, pp. 833–52, Sep 1994.

- [43] G. E. D'Alonzo, R. J. Barst, S. M. Ayres, E. H. Bergofsky, B. H. Brundage, K. M. Detre, A. P. Fishman, R. M. Goldring, B. M. Groves, J. T. Kernis, and et al., "Survival in patients with primary pulmonary hypertension. results from a national prospective registry," *Annals of internal medicine*, vol. 115, no. 5, pp. 343–9, 1991.
- [44] F. Guarracino, C. Cariello, A. Danella, L. Doroni, F. Lapolla, C. Vullo, C. Pasquini, and M. Stefani, "Right ventricular failure: physiology and assessment," *Minerva Anesthesiol*, vol. 71, pp. 307–12, Jun 2005.
- [45] R. J. Raymond, A. L. Hinderliter, P. W. Willis, D. Ralph, E. J. Caldwell, W. Williams, N. A. Ettinger, N. S. Hill, W. R. Summer, B. de Boisblanc, T. Schwartz, G. Koch, L. M. Clayton, M. M. Jobsis, J. W. Crow, and W. Long, "Echocardiographic predictors of adverse outcomes in primary pulmonary hypertension," *Journal of the American College of Cardiology*, vol. 39, no. 7, pp. 1214–9, 2002.
- [46] S. Z. Goldhaber, "Pulmonary embolism," *Lancet*, vol. 363, no. 9417, pp. 1295–1305, 2004.
- [47] O. Sanchez, L. Trinquart, I. Colombet, P. Durieux, M. V. Huisman, G. Chatellier, and G. Meyer, "Prognostic value of right ventricular dysfunction in patients with haemodynamically stable pulmonary embolism: a systematic review," *European Heart Journal*, vol. 29, no. 12, pp. 1569–77, 2008.
- [48] J. A. Watts, M. R. Marchick, and J. A. Kline, "Right ventricular heart failure from pulmonary embolism: key distinctions from chronic pulmonary hypertension," *Journal of cardiac failure*, vol. 16, no. 3, pp. 250–9, 2010.
- [49] A. D. Renzetti, Jr, J. H. McClement, and B. D. Litt, "The Veterans Administration cooperative study of pulmonary function. 3. Mortality in relation to respiratory function in chronic obstructive pulmonary disease," *Am J Med*, vol. 41, pp. 115–29, Jul 1966.
- [50] G. A. Traver, M. G. Cline, and B. Burrows, "Predictors of mortality in chronic obstructive pulmonary disease. A 15-year follow-up study," *Am Rev Respir Dis*, vol. 119, pp. 895–902, Jun 1979.
- [51] A. P. Fishman, "State of the art: chronic cor pulmonale," *Am Rev Respir Dis*, vol. 114, pp. 775–94, Oct 1976.
- [52] V. H. Rigolin, P. A. Robiolio, J. S. Wilson, J. K. Harrison, and T. M. Bashore, "The forgotten chamber: the importance of the right ventricle," *Cathet Cardiovasc Diagn*, vol. 35, pp. 18–28, May 1995.
- [53] C. D. Vizza, J. P. Lynch, L. L. Ochoa, G. Richardson, and E. P. Trulock, "Right and left ventricular dysfunction in patients with severe pulmonary disease," *Chest*, vol. 113, pp. 576–83, Mar 1998.

- [54] A. D. Lopez and C. C. Murray, "The global burden of disease, 1990-2020," *Nature Medicine*, vol. 4, no. 11, pp. 1241-3, 1998.
- [55] C. D. Mathers and D. Loncar, "Projections of global mortality and burden of disease from 2002 to 2030," *PLoS medicine*, vol. 3, no. 11, p. e442, 2006.
- [56] C. R. Greyson, "Evaluation of right ventricular function," *Current cardiology reports*, vol. 13, no. 3, pp. 194-202, 2011.
- [57] C. L. Webb, K. J. Jenkins, P. P. Karpawich, A. F. Bolger, R. M. Donner, H. D. Allen, R. J. Barst, and Congenital Cardiac Defects Committee of the American Heart Association Section on Cardiovascular Disease in the Young, "Collaborative care for adults with congenital heart disease," *Circulation*, vol. 105, pp. 2318-23, May 2002.
- [58] H. Leonard, A. M. Barrett, J. E. Scott, and C. Wren, "The influence of congenital heart disease on survival of infants with oesophageal atresia," *Arch Dis Child Fetal Neonatal Ed*, vol. 85, pp. F204-6, Nov 2001.
- [59] A. P. Bolger, A. J. S. Coats, and M. A. Gatzoulis, "Congenital heart disease: the original heart failure syndrome," *European Heart Journal*, vol. 24, no. 10, pp. 970-976, 2003.
- [60] J. D. Hosenpud, L. E. Bennett, B. M. Keck, M. M. Boucek, and R. J. Novick, "The registry of the international society for heart and lung transplantation: seventeenth official report-2000," *J Heart Lung Transplant*, vol. 19, pp. 909-31, Oct 2000.
- [61] J. R. McMullen and G. L. Jennings, "Differences between pathological and physiological cardiac hypertrophy: novel therapeutic strategies to treat heart failure," *Clinical and experimental pharmacology & physiology*, vol. 34, no. 4, pp. 255-62, 2007.
- [62] D. A. Bluemke, R. A. Kronmal, J. A. Lima, K. Liu, J. Olson, G. L. Burke, and A. R. Folsom, "The relationship of left ventricular mass and geometry to incident cardiovascular events: the MESA (Multi-Ethnic Study of Atherosclerosis) study," *Journal of the American College of Cardiology*, vol. 52, no. 25, pp. 2148-55, 2008.
- [63] J. Mathew, P. Sleight, E. Lonn, D. Johnstone, J. Pogue, Q. Yi, J. Bosch, B. Sussex, J. Probstfield, and S. Yusuf, "Reduction of cardiovascular risk by regression of electrocardiographic markers of left ventricular hypertrophy by the angiotensin-converting enzyme inhibitor ramipril," *Circulation*, vol. 104, no. 14, pp. 1615-21, 2001.
- [64] A. Mebazaa, P. Karpati, E. Renaud, and L. Algotsson, "Acute right ventricular failure—from pathophysiology to new treatments," *Intensive care medicine*, vol. 30, no. 2, pp. 185-96, 2004.

- [65] R. Dumitrascu, N. Weissmann, H. A. Ghofrani, E. Dony, K. Beuerlein, H. Schmidt, J. P. Stasch, M. J. Gnoth, W. Seeger, F. Grimminger, and R. T. Schermuly, "Activation of soluble guanylate cyclase reverses experimental pulmonary hypertension and vascular remodeling," *Circulation*, vol. 113, no. 2, pp. 286–295, 2006.
- [66] R. T. Schermuly, J. P. Stasch, S. S. Pullamsetti, R. Middendorff, D. Muller, K. D. Schluter, A. Dingendorf, S. Hackemack, E. Kolosionek, C. Kaulen, R. Dumitrascu, N. Weissmann, J. Mittendorf, W. Klepetko, W. Seeger, H. A. Ghofrani, and F. Grimminger, "Expression and function of soluble guanylate cyclase in pulmonary arterial hypertension," *The European respiratory journal : official journal of the European Society for Clinical Respiratory Physiology*, vol. 32, no. 4, pp. 881–91, 2008.
- [67] J. Stark, C. L. Berry, and E. D. Silove, "The evaluation of materials used for pulmonary artery banding. Experimental study in piglets," *The Annals of thoracic surgery*, vol. 13, no. 2, pp. 163–9, 1972.
- [68] H. A. Rockman, S. Ono, R. S. Ross, L. R. Jones, M. Karimi, V. Bhargava, J. Ross, and K. R. Chien, "Molecular and physiological alterations in murine ventricular dysfunction," *Proceedings of the National Academy of Sciences of the United States of America*, vol. 91, no. 7, pp. 2694–2698, 1994.
- [69] O. Tarnavski, J. R. McMullen, M. Schinke, Q. Nie, S. Kong, and S. Izumo, "Mouse cardiac surgery: comprehensive techniques for the generation of mouse models of human diseases and their application for genomic studies," *Physiol Genomics*, vol. 16, pp. 349–60, Feb 2004.
- [70] R. F. Furchgott and J. V. Zawadzki, "The obligatory role of endothelial cells in the relaxation of arterial smooth muscle by acetylcholine," *Nature*, vol. 288, no. 5789, pp. 373–6, 1980.
- [71] M. Mitka, "1998 nobel prize winners are announced: three discoverers of nitric oxide activity," *JAMA*, vol. 280, p. 1648, Nov 1998.
- [72] S. Moncada, R. M. Palmer, and E. A. Higgs, "Nitric oxide: physiology, pathophysiology, and pharmacology," *Pharmacol Rev*, vol. 43, pp. 109–42, Jun 1991.
- [73] M. C. Cerra and D. Pellegrino, "Cardiovascular cGMP-generating systems in physiological and pathological conditions," *Curr Med Chem*, vol. 14, no. 5, pp. 585–99, 2007.
- [74] A. J. Hobbs, J. M. Fukuto, and L. J. Ignarro, "Formation of free nitric oxide from l-arginine by nitric oxide synthase: direct enhancement of generation by superoxide dismutase," *Proceedings of the National Academy of Sciences of the United States of America*, vol. 91, no. 23, pp. 10992–6, 1994.
- [75] O. V. Evgenov, P. Pacher, P. M. Schmidt, G. Hasko, H. H. Schmidt, and J. P. Stasch, "NO-independent stimulators and activators of soluble guanylate

- cyclase: discovery and therapeutic potential," *Nature reviews. Drug discovery*, vol. 5, no. 9, pp. 755–68, 2006.
- [76] R. H. Ritchie, J. C. Irvine, A. C. Rosenkranz, R. Patel, I. R. Wendt, J. D. Horowitz, and B. K. Kemp-Harper, "Exploiting cGMP-based therapies for the prevention of left ventricular hypertrophy: NO\* and beyond," *Pharmacol Ther*, vol. 124, pp. 279–300, Dec 2009.
- [77] K. A. Hanafy, J. S. Krumenacker, and F. Murad, "NO, nitrotyrosine, and cyclic GMP in signal transduction," *Med Sci Monit*, vol. 7, no. 4, pp. 801–19, 2001.
- [78] T. Münzel, A. Daiber, and A. Mülsch, "Explaining the phenomenon of nitrate tolerance," *Circ Res*, vol. 97, pp. 618–28, Sep 2005.
- [79] S. Dikalov, B. Fink, M. Skatchkov, D. Stalleicken, and E. Bassenge, "Formation of reactive oxygen species by pentaerythrityltetranitrate and glyceryl trinitrate in vitro and development of nitrate tolerance," *J Pharmacol Exp Ther*, vol. 286, pp. 938–44, Aug 1998.
- [80] R. P. Brandes, D. Kim, F. H. Schmitz-Winnenthal, M. Amidi, A. Gödecke, A. Mülsch, and R. Busse, "Increased nitrovasodilator sensitivity in endothelial nitric oxide synthase knockout mice: role of soluble guanylyl cyclase," *Hypertension*, vol. 35, pp. 231–6, Jan 2000.
- [81] A. Calderone, C. M. Thaik, N. Takahashi, D. L. Chang, and W. S. Colucci, "Nitric oxide, atrial natriuretic peptide, and cyclic GMP inhibit the growth-promoting effects of norepinephrine in cardiac myocytes and fibroblasts," *J Clin Invest*, vol. 101, no. 4, pp. 812–8, 1998.
- [82] K. C. Wollert, B. Fiedler, S. Gambaryan, A. Smolenski, J. Heineke, E. Butt, C. Trautwein, S. M. Lohmann, and H. Drexler, "Gene transfer of cGMP-dependent protein kinase I enhances the antihypertrophic effects of nitric oxide in cardiomyocytes," *Hypertension*, vol. 39, no. 1, pp. 87–92, 2002.
- [83] L. Cao and D. G. Gardner, "Natriuretic peptides inhibit DNA synthesis in cardiac fibroblasts," *Hypertension*, vol. 25, no. 2, pp. 227–34, 1995.
- [84] H. Fujisaki, H. Ito, Y. Hirata, M. Tanaka, M. Hata, M. Lin, S. Adachi, H. Aki-moto, F. Marumo, and M. Hiroe, "Natriuretic peptides inhibit angiotensin II-induced proliferation of rat cardiac fibroblasts by blocking endothelin-1 gene expression," *The Journal of clinical investigation*, vol. 96, no. 2, pp. 1059–65, 1995.
- [85] J. Roberts, J. D., C. T. Roberts, R. C. Jones, W. M. Zapol, and K. D. Bloch, "Continuous nitric oxide inhalation reduces pulmonary arterial structural changes, right ventricular hypertrophy, and growth retardation in the hypoxic newborn rat," *Circulation Research*, vol. 76, no. 2, pp. 215–22, 1995.

- [86] J. M. Fagan, S. E. Rex, S. A. Hayes-Licitra, and L. Waxman, "L-arginine reduces right heart hypertrophy in hypoxia-induced pulmonary hypertension," *Biochemical and biophysical research communications*, vol. 254, no. 1, pp. 100–3, 1999.
- [87] Y. Mitani, K. Maruyama, and M. Sakurai, "Prolonged administration of L-arginine ameliorates chronic pulmonary hypertension and pulmonary vascular remodeling in rats," *Circulation*, vol. 96, pp. 689–97, Jul 1997.
- [88] B. Elmedal, M. Y. de Dam, M. J. Mulvany, and U. Simonsen, "The superoxide dismutase mimetic, tempol, blunts right ventricular hypertrophy in chronic hypoxic rats," *British Journal of Pharmacology*, vol. 141, no. 1, pp. 105–13, 2004.
- [89] B. H. Jiang, J. Maruyama, A. Yokochi, M. Iwasaki, H. Amano, Y. Mitani, and K. Maruyama, "Prolonged nitric oxide inhalation fails to regress hypoxic vascular remodeling in rat lung," *Chest*, vol. 125, no. 6, pp. 2247–52, 2004.
- [90] B. E. Laursen, M. Y. Dam, M. J. Mulvany, and U. Simonsen, "Hypoxia-induced pulmonary vascular remodeling and right ventricular hypertrophy is unaltered by long-term oral L-arginine administration," *Vascular Pharmacology*, vol. 49, no. 2-3, pp. 71–76, 2008.
- [91] H. Matsuoka, M. Nakata, K. Kohno, Y. Koga, G. Nomura, H. Toshima, and T. Imaizumi, "Chronic L-arginine administration attenuates cardiac hypertrophy in spontaneously hypertensive rats," *Hypertension*, vol. 27, no. 1, pp. 14–8, 1996.
- [92] U. Zabel, M. Weeger, M. La, and H. H. Schmidt, "Human soluble guanylate cyclase: functional expression and revised isoenzyme family," *The Biochemical journal*, vol. 335 ( Pt 1), pp. 51–7, 1998.
- [93] A. Friebe, E. Mergia, O. Dangel, A. Lange, and D. Koesling, "Fatal gastrointestinal obstruction and hypertension in mice lacking nitric oxide-sensitive guanylyl cyclase," *Proceedings of the National Academy of Sciences of the United States of America*, vol. 104, no. 18, pp. 7699–7704, 2007.
- [94] U. Zabel, C. Hausler, M. Weeger, and H. H. Schmidt, "Homodimerization of soluble guanylyl cyclase subunits. Dimerization analysis using a glutathione s-transferase affinity tag," *The Journal of biological chemistry*, vol. 274, no. 26, pp. 18149–52, 1999.
- [95] J. A. Winger and M. A. Marletta, "Expression and characterization of the catalytic domains of soluble guanylate cyclase: interaction with the heme domain," *Biochemistry*, vol. 44, no. 10, pp. 4083–90, 2005.
- [96] J. Foerster, C. Harteneck, J. Malkewitz, G. Schultz, and D. Koesling, "A functional heme-binding site of soluble guanylyl cyclase requires intact N-termini of alpha 1 and beta 1 subunits," *European journal of biochemistry / FEBS*, vol. 240, no. 2, pp. 380–6, 1996.

- [97] K. G. Schmidt, O. Geyer, and T. W. Mittag, "Adenylyl and guanylyl cyclase activity in the choroid," *Experimental eye research*, vol. 78, no. 5, pp. 901–7, 2004.
- [98] J. P. Stasch, P. M. Schmidt, P. I. Nedvetsky, T. Y. Nedvetskaya, S. A. H. S. Meurer, M. Deile, A. Taye, A. Knorr, H. Lapp, H. Muller, Y. Turgay, C. Rothkegel, A. Tersteegen, B. Kemp-Harper, W. Muller-Esterl, and H. H. Schmidt, "Targeting the heme-oxidized nitric oxide receptor for selective vasodilatation of diseased blood vessels," *The Journal of clinical investigation*, vol. 116, no. 9, pp. 2552–61, 2006.
- [99] P. Deruelle, V. Balasubramaniam, A. M. Kunig, G. J. Seedorf, N. E. Markham, and S. H. Abman, "BAY 41-2272, a direct activator of soluble guanylate cyclase, reduces right ventricular hypertrophy and prevents pulmonary vascular remodeling during chronic hypoxia in neonatal rats," *Biology of the Neonate*, vol. 90, no. 2, pp. 135–144, 2006.
- [100] L. B. Thorsen, Y. Eskildsen-Helmond, H. Zibrandtsen, J. P. Stasch, U. Simonson, and B. E. Laursen, "BAY 41-2272 inhibits the development of chronic hypoxic pulmonary hypertension in rats," *European journal of pharmacology*, vol. 647, no. 1-3, pp. 147–54, 2010.
- [101] S. Geschka, A. Kretschmer, Y. Sharkovska, O. V. Evgenov, B. Lawrenz, A. Hucke, B. Hocher, and J. P. Stasch, "Soluble guanylate cyclase stimulation prevents fibrotic tissue remodeling and improves survival in salt-sensitive dahl rats," *PLoS One*, vol. 6, no. 7, p. e21853, 2011.
- [102] P. Kalk, M. Godes, K. Relle, C. Rothkegel, A. Hucke, J. P. Stasch, and B. Hocher, "No-independent activation of soluble guanylate cyclase prevents disease progression in rats with 5/6 nephrectomy," *British Journal of Pharmacology*, vol. 148, no. 6, pp. 853–9, 2006.
- [103] H. Masuyama, T. Tsuruda, J. Kato, T. Imamura, Y. Asada, J. P. Stasch, K. Kitamura, and T. Eto, "Soluble guanylate cyclase stimulation on cardiovascular remodeling in angiotensin II-induced hypertensive rats," *Hypertension*, vol. 48, no. 5, pp. 972–8, 2006.
- [104] Y. Sharkovska, P. Kalk, B. Lawrenz, M. Godes, L. S. Hoffmann, K. Wellkisch, S. Geschka, K. Relle, B. Hocher, and J. P. Stasch, "Nitric oxide-independent stimulation of soluble guanylate cyclase reduces organ damage in experimental low-renin and high-renin models," *Journal of hypertension*, vol. 28, no. 8, pp. 1666–75, 2010.
- [105] M. Zanfolin, R. Faro, E. G. Araujo, A. M. Guaraldo, E. Antunes, and G. De Nucci, "Protective effects of BAY 41-2272 (sGC stimulator) on hypertension, heart, and cardiomyocyte hypertrophy induced by chronic L-NAME treatment in rats," *Journal of cardiovascular pharmacology*, vol. 47, no. 3, pp. 391–5, 2006.

- [106] H. Masuyama, T. Tsuruda, Y. Sekita, K. Hatakeyama, T. Imamura, J. Kato, Y. Asada, J. P. Stasch, and K. Kitamura, "Pressure-independent effects of pharmacological stimulation of soluble guanylate cyclase on fibrosis in pressure-overloaded rat heart," *Hypertension Research*, vol. 32, no. 7, pp. 597–603, 2009.
- [107] T. M. Lincoln, P. Komalavilas, N. J. Boerth, L. A. MacMillan-Crow, and T. L. Cornwell, "cGMP signaling through cAMP- and cGMP-dependent protein kinases," *Adv Pharmacol*, vol. 34, pp. 305–22, 1995.
- [108] E. Butt, C. Nolte, S. Schulz, J. Beltman, J. A. Beavo, B. Jastorff, and U. Walter, "Analysis of the functional role of cGMP-dependent protein kinase in intact human platelets using a specific activator 8-para-chlorophenylthio-cGMP," *Biochem Pharmacol*, vol. 43, pp. 2591–600, Jun 1992.
- [109] T. Horio, T. Nishikimi, F. Yoshihara, H. Matsuo, S. Takishita, and K. Kangawa, "Inhibitory regulation of hypertrophy by endogenous atrial natriuretic peptide in cultured cardiac myocytes," *Hypertension*, vol. 35, no. 1 Pt 1, pp. 19–24, 2000.
- [110] T. Tokudome, T. Horio, T. Soeki, K. Mori, I. Kishimoto, S. Suga, F. Yoshihara, Y. Kawano, M. Kohno, and K. Kangawa, "Inhibitory effect of C-type natriuretic peptide (CNP) on cultured cardiac myocyte hypertrophy: interference between CNP and endothelin-1 signaling pathways," *Endocrinology*, vol. 145, no. 5, pp. 2131–40, 2004.
- [111] T. Tsuruda, G. Boerrigter, B. K. Huntley, J. A. Noser, A. Cataliotti, L. C. Costello-Boerrigter, H. H. Chen, and J. Burnett, J. C., "Brain natriuretic peptide is produced in cardiac fibroblasts and induces matrix metalloproteinases," *Circ Res*, vol. 91, no. 12, pp. 1127–34, 2002.
- [112] S. M. Lohmann, A. B. Vaandrager, A. Smolenski, U. Walter, and H. R. De Jonge, "Distinct and specific functions of cGMP-dependent protein kinases," *Trends Biochem Sci*, vol. 22, pp. 307–12, Aug 1997.
- [113] P. F. Méry, S. M. Lohmann, U. Walter, and R. Fischmeister, "Ca<sup>2+</sup> current is regulated by cyclic GMP-dependent protein kinase in mammalian cardiac myocytes," *Proc Natl Acad Sci U S A*, vol. 88, pp. 1197–201, Feb 1991.
- [114] T. Muenzel, R. Feil, A. Muelsch, S. M. Lohmann, F. Hofmann, and U. Walter, "Physiology and pathophysiology of vascular signaling controlled by cyclic guanosine 3',5'-cyclic monophosphate-dependent protein kinase," *Circulation*, vol. 108, no. 18, pp. 2172–2183, 2003.
- [115] R. Draijer, A. B. Vaandrager, C. Nolte, H. R. de Jonge, U. Walter, and V. W. van Hinsbergh, "Expression of cGMP-dependent protein kinase I and phosphorylation of its substrate, vasodilator-stimulated phosphoprotein, in human endothelial cells of different origin," *Circ Res*, vol. 77, pp. 897–905, Nov 1995.

- [116] S. P. D'Souza, M. Davis, and G. F. Baxter, "Autocrine and paracrine actions of natriuretic peptides in the heart," *Pharmacology & Therapeutics*, vol. 101, no. 2, pp. 113–129, 2004.
- [117] A. Keilbach, P. Ruth, and F. Hofmann, "Detection of cGMP dependent protein kinase isozymes by specific antibodies," *Eur J Biochem*, vol. 208, pp. 467–73, Sep 1992.
- [118] J. O. Mudd and D. A. Kass, "Tackling heart failure in the twenty-first century," *Nature*, vol. 451, no. 7181, pp. 919–28, 2008.
- [119] M. Zhang, N. Koitabashi, T. Nagayama, R. Rambaran, N. Feng, E. Takimoto, T. Koenke, B. O'Rourke, H. C. Champion, M. T. Crow, and D. A. Kass, "Expression, activity, and pro-hypertrophic effects of PDE5A in cardiac myocytes," *Cellular signalling*, vol. 20, no. 12, pp. 2231–6, 2008.
- [120] C. L. Miller and C. Yan, "Targeting cyclic nucleotide phosphodiesterase in the heart: therapeutic implications," *Journal of cardiovascular translational research*, vol. 3, no. 5, pp. 507–15, 2010.
- [121] J. D. Corbin and S. H. Francis, "Cyclic GMP phosphodiesterase-5: target of sildenafil," *J Biol Chem*, vol. 274, pp. 13729–32, May 1999.
- [122] J. Nagendran, S. L. Archer, D. Soliman, V. Gurtu, R. Moudgil, A. Haromy, C. Aubin, L. Webster, I. M. Rebeyka, D. B. Ross, P. E. Light, J. R. B. Dyck, and E. D. Michelakis, "Phosphodiesterase type 5 is highly expressed in the hypertrophied human right ventricle, and acute inhibition of phosphodiesterase type 5 improves contractility," *Circulation*, vol. 116, no. 3, pp. 238–248, 2007.
- [123] T. Nagayama, S. Hsu, M. Zhang, N. Koitabashi, D. Bedja, K. L. Gabrielson, E. Takimoto, and D. A. Kass, "Sildenafil stops progressive chamber, cellular, and molecular remodeling and improves calcium handling and function in hearts with pre-existing advanced hypertrophy caused by pressure overload," *Journal of the American College of Cardiology*, vol. 53, no. 2, pp. 207–15, 2009.
- [124] P. Pokreisz, S. Vandenwijngaert, V. Bito, A. Van den Bergh, I. Lenaerts, C. Busch, G. Marsboom, O. Gheysens, P. Vermeersch, L. Biesmans, X. Liu, H. Gillijns, M. Pellens, A. Van Lommel, E. Buys, L. Schoonjans, J. Vanhaecke, E. Verbeken, K. Sipido, P. Herijgers, K. D. Bloch, and S. P. Janssens, "Ventricular phosphodiesterase-5 expression is increased in patients with advanced heart failure and contributes to adverse ventricular remodeling after myocardial infarction in mice," *Circulation*, vol. 119, pp. 408–16, Jan 2009.
- [125] M. Zhang, E. Takimoto, S. Hsu, D. I. Lee, T. Nagayama, T. Danner, N. Koitabashi, A. S. Barth, D. Bedja, K. L. Gabrielson, Y. Wang, and D. A. Kass, "Myocardial remodeling is controlled by myocyte-targeted gene regulation of phosphodiesterase type 5," *Journal of the American College of Cardiology*, vol. 56, no. 24, pp. 2021–30, 2010.

- [126] A. Andersen, J. M. Nielsen, C. D. Peters, U. K. Schou, E. Sloth, and J. E. Nielsen-Kudsk, "Effects of phosphodiesterase-5 inhibition by sildenafil in the pressure overloaded right heart," *European Journal of Heart Failure*, vol. 10, no. 12, pp. 1158–1165, 2008.
- [127] C. L. Miller, M. Oikawa, Y. Cai, A. P. Wojtovich, D. J. Nagel, X. Xu, H. Xu, V. Florio, S. D. Rybalkin, J. A. Beavo, Y. F. Chen, J. D. Li, B. C. Blaxall, J. Abe, and C. Yan, "Role of Ca<sup>2+</sup>/calmodulin-stimulated cyclic nucleotide phosphodiesterase 1 in mediating cardiomyocyte hypertrophy," *Circulation Research*, vol. 105, no. 10, pp. 956–64, 2009.
- [128] C. M. Adamo, D. F. Dai, J. M. Percival, E. Minami, M. S. Willis, E. Patrucco, S. C. Froehner, and J. A. Beavo, "Sildenafil reverses cardiac dysfunction in the mdx mouse model of Duchenne muscular dystrophy," *Proceedings of the National Academy of Sciences of the United States of America*, vol. 107, no. 44, pp. 19079–83, 2010.
- [129] F. N. Ko, C. C. Wu, S. C. Kuo, F. Y. Lee, and C. M. Teng, "YC-1, a novel activator of platelet guanylate cyclase," *Blood*, vol. 84, pp. 4226–33, Dec 1994.
- [130] S. Yoshina, A. Tanaka, and S. C. Kuo, "[Studies on heterocyclic compounds. XXXVI. Synthesis of furo[3,2-c]pyrazole derivatives. (4) Synthesis of 1,3-diphenylfuro[3,2-c]pyrazole-5-carboxaldehyde and its derivatives (author's transl)]," *Yakugaku Zasshi*, vol. 98, pp. 272–9, Mar 1978.
- [131] J. W. Denninger, J. P. Schelvis, P. E. Brandish, Y. Zhao, G. T. Babcock, and M. A. Marletta, "Interaction of soluble guanylate cyclase with YC-1: kinetic and resonance Raman studies," *Biochemistry*, vol. 39, pp. 4191–8, Apr 2000.
- [132] J. P. Stasch, E. M. Becker, C. Alonso-Alija, H. Apeler, K. Dembowski, A. Feurer, R. Gerzer, T. Minuth, E. Perzborn, U. Pleiss, H. Schroder, W. Schroeder, E. Stahl, W. Steinke, A. Straub, and M. Schramm, "NO-independent regulatory site on soluble guanylate cyclase," *Nature*, vol. 410, no. 6825, pp. 212–215, 2001.
- [133] A. Friebe, F. Müllershausen, A. Smolenski, U. Walter, G. Schultz, and D. Koesling, "YC-1 potentiates nitric oxide- and carbon monoxide-induced cyclic GMP effects in human platelets," *Mol Pharmacol*, vol. 54, pp. 962–7, Dec 1998.
- [134] J.-P. Stasch, P. Pacher, and O. V. Evgenov, "Soluble guanylate cyclase as an emerging therapeutic target in cardiopulmonary disease," *Circulation*, vol. 123, pp. 2263–73, May 2011.
- [135] J. Mittendorf, S. Weigand, C. Alonso-Alija, E. Bischoff, A. Feurer, M. Gerisch, A. Kern, A. Knorr, D. Lang, K. Muentner, M. Radtke, H. Schirok, K. H. Schlemmer, E. Stahl, A. Straub, F. Wunder, and J. P. Stasch, "Discovery of riociguat (BAY 63-2521): a potent, oral stimulator of soluble guanylate cyclase for the treatment of pulmonary hypertension," *ChemMedChem*, vol. 4, no. 5, pp. 853–65, 2009.

- [136] J. P. Stasch, P. Schmidt, C. Alonso-Alija, H. Apeler, K. Dembowski, M. Haerter, M. Heil, T. Minuth, E. Perzborn, U. Pleiss, M. Schramm, W. Schroeder, H. Schroder, E. Stahl, W. Steinke, and F. Wunder, "NO- and haem-independent activation of soluble guanylyl cyclase: molecular basis and cardiovascular implications of a new pharmacological principle," *British Journal of Pharmacology*, vol. 136, no. 5, pp. 773–83, 2002.
- [137] H. A. Ghofrani, I. H. Osterloh, and F. Grimminger, "Sildenafil: from angina to erectile dysfunction to pulmonary hypertension and beyond," *Nature Reviews Drug Discovery*, vol. 5, no. 8, pp. 689–702, 2006.
- [138] S. F. Campbell, "Science, art and drug discovery: a personal perspective," *Clin Sci (Lond)*, vol. 99, pp. 255–60, Oct 2000.
- [139] D. K. Walker, M. J. Ackland, G. C. James, G. J. Muirhead, D. J. Rance, P. Wastall, and P. A. Wright, "Pharmacokinetics and metabolism of sildenafil in mouse, rat, rabbit, dog and man," *Xenobiotica*, vol. 29, pp. 297–310, Mar 1999.
- [140] M. Boolell, M. J. Allen, S. A. Ballard, S. Gepi-Attee, G. J. Muirhead, A. M. Naylor, I. H. Osterloh, and C. Gingell, "Sildenafil: an orally active type 5 cyclic GMP-specific phosphodiesterase inhibitor for the treatment of penile erectile dysfunction," *Int J Impot Res*, vol. 8, pp. 47–52, Jun 1996.
- [141] H. L. Wyatt, M. K. Heng, S. Meerbaum, J. D. Hestenes, J. M. Cobo, R. M. Davidson, and E. Corday, "Cross-sectional echocardiography. I. Analysis of mathematic models for quantifying mass of the left ventricle in dogs," *Circulation*, vol. 60, no. 5, pp. 1104–13, 1979.
- [142] T. Ryan, O. Petrovic, J. C. Dillon, H. Feigenbaum, M. J. Conley, and W. F. Armstrong, "An echocardiographic index for separation of right ventricular volume and pressure overload," *J Am Coll Cardiol*, vol. 5, pp. 918–27, Apr 1985.
- [143] A. Giardini, L. Lovato, A. Donti, R. Formigari, G. Oppido, G. Gargiulo, F. M. Picchio, and R. Fattori, "Relation between right ventricular structural alterations and markers of adverse clinical outcome in adults with systemic right ventricle and either congenital complete (after senning operation) or congenitally corrected transposition of the great arteries," *The American journal of cardiology*, vol. 98, no. 9, pp. 1277–82, 2006.
- [144] B. C. Berk, K. Fujiwara, and S. Lehoux, "ECM remodeling in hypertensive heart disease," *The Journal of clinical investigation*, vol. 117, no. 3, pp. 568–75, 2007.
- [145] M. Mundhenke, B. Schwartzkopff, P. Stark, H. D. Schulte, and B. E. Strauer, "Myocardial collagen type I and impaired left ventricular function under exercise in hypertrophic cardiomyopathy," *The Thoracic and cardiovascular surgeon*, vol. 50, no. 4, pp. 216–22, 2002.

- [146] T. Matsumoto, A. Wada, T. Tsutamoto, M. Ohnishi, T. Isono, and M. Kinoshita, "Chymase inhibition prevents cardiac fibrosis and improves diastolic dysfunction in the progression of heart failure," *Circulation*, vol. 107, pp. 2555–8, May 2003.
- [147] F. Kuwahara, H. Kai, K. Tokuda, M. Kai, A. Takeshita, K. Egashira, and T. Imaizumi, "Transforming growth factor-beta function blocking prevents myocardial fibrosis and diastolic dysfunction in pressure-overloaded rats," *Circulation*, vol. 106, no. 1, pp. 130–5, 2002.
- [148] R. Khan and R. Sheppard, "Fibrosis in heart disease: understanding the role of transforming growth factor-beta in cardiomyopathy, valvular disease and arrhythmia," *Immunology*, vol. 118, no. 1, pp. 10–24, 2006.
- [149] J. E. Jalil, C. W. Doering, J. S. Janicki, R. Pick, S. G. Shroff, and K. T. Weber, "Fibrillar collagen and myocardial stiffness in the intact hypertrophied rat left ventricle," *Circulation Research*, vol. 64, no. 6, pp. 1041–50, 1989.
- [150] Y. Wu, O. Cazorla, D. Labeit, S. Labeit, and H. Granzier, "Changes in titin and collagen underlie diastolic stiffness diversity of cardiac muscle," *Journal of Molecular and Cellular Cardiology*, vol. 32, no. 12, pp. 2151–62, 2000.
- [151] I. Medugorac, "Myocardial collagen in different forms of heart hypertrophy in the rat," *Research in experimental medicine. Zeitschrift fur die gesamte experimentelle Medizin einschliesslich experimenteller Chirurgie*, vol. 177, no. 3, pp. 201–11, 1980.
- [152] S. Ghio, C. Klersy, G. Magrini, A. M. D'Armini, L. Scelsi, C. Raineri, M. Passotti, A. Serio, C. Campana, and M. Viganò, "Prognostic relevance of the echocardiographic assessment of right ventricular function in patients with idiopathic pulmonary arterial hypertension," *Int J Cardiol*, vol. 140, pp. 272–8, Apr 2010.
- [153] S. A. van Wolferen, J. T. Marcus, A. Boonstra, K. M. Marques, J. G. Bronzwaer, M. D. Spreeuwenberg, P. E. Postmus, and A. Vonk-Noordegraaf, "Prognostic value of right ventricular mass, volume, and function in idiopathic pulmonary arterial hypertension," *Eur Heart J*, vol. 28, no. 10, pp. 1250–7, 2007.
- [154] E. H. Starling and M. B. Visscher, "The regulation of the energy output of the heart," *J Physiol*, vol. 62, pp. 243–61, Jan 1927.
- [155] A. Knorr, C. Hirth-Dietrich, C. Alonso-Alija, M. Harter, M. Hahn, Y. Keim, F. Wunder, and J. P. Stasch, "Nitric oxide-independent activation of soluble guanylate cyclase by BAY 60-2770 in experimental liver fibrosis," *Arzneimittel-Forschung*, vol. 58, no. 2, pp. 71–80, 2008.
- [156] S. Kato, F. G. Spinale, R. Tanaka, W. Johnson, G. Cooper, 4th, and M. R. Zile, "Inhibition of collagen cross-linking: effects on fibrillar collagen and ventricular diastolic function," *Am J Physiol*, vol. 269, pp. H863–8, Sep 1995.

- [157] J. D. Stroud, C. F. Baicu, M. A. Barnes, F. G. Spinale, and M. R. Zile, "Viscoelastic properties of pressure overload hypertrophied myocardium: effect of serine protease treatment," *American journal of physiology. Heart and circulatory physiology*, vol. 282, no. 6, pp. H2324–35, 2002.
- [158] J. Díez, R. Querejeta, B. López, A. González, M. Larman, and J. L. Martínez Ubago, "Losartan-dependent regression of myocardial fibrosis is associated with reduction of left ventricular chamber stiffness in hypertensive patients," *Circulation*, vol. 105, pp. 2512–7, May 2002.
- [159] R. Müller-Brunotte, T. Kahan, B. López, M. Edner, A. González, J. Díez, and K. Malmqvist, "Myocardial fibrosis and diastolic dysfunction in patients with hypertension: results from the Swedish Irbesartan Left Ventricular Hypertrophy Investigation versus Atenolol (SILVHIA)," *J Hypertens*, vol. 25, pp. 1958–66, Sep 2007.
- [160] E. J. Tsai, Y. Liu, N. Koitabashi, D. Bedja, T. Danner, J.-F. Jasmin, M. P. Lisanti, A. Friebe, E. Takimoto, and D. A. Kass, "Pressure-overload-induced subcellular relocalization/oxidation of soluble guanylyl cyclase in the heart modulates enzyme stimulation," *Circ Res*, vol. 110, pp. 295–303, Jan 2012.
- [161] V. V. Petrov, R. H. Fagard, and P. J. Lijnen, "Transforming growth factor-beta(1) induces angiotensin-converting enzyme synthesis in rat cardiac fibroblasts during their differentiation to myofibroblasts," *J Renin Angiotensin Aldosterone Syst*, vol. 1, pp. 342–52, Dec 2000.
- [162] C. Beyer, N. Reich, S. C. Schindler, A. Akhmetshina, C. Dees, M. Tomcik, C. Hirth-Dietrich, G. von Degenfeld, P. Sandner, O. Distler, G. Schett, and J. H. W. Distler, "Stimulation of soluble guanylate cyclase reduces experimental dermal fibrosis," *Ann Rheum Dis*, Feb 2012.
- [163] E. M. Zeisberg, O. Tarnavski, M. Zeisberg, A. L. Dorfman, J. R. McMullen, E. Gustafsson, A. Chandraker, X. Yuan, W. T. Pu, A. B. Roberts, E. G. Neilson, M. H. Sayegh, S. Izumo, and R. Kalluri, "Endothelial-to-mesenchymal transition contributes to cardiac fibrosis," *Nat Med*, vol. 13, pp. 952–61, Aug 2007.
- [164] A. Ahluwalia, P. Foster, R. S. Scotland, P. G. McLean, A. Mathur, M. Perretti, S. Moncada, and A. J. Hobbs, "Antiinflammatory activity of soluble guanylate cyclase: cGMP-dependent down-regulation of P-selectin expression and leukocyte recruitment," *Proc Natl Acad Sci U S A*, vol. 101, pp. 1386–91, Feb 2004.
- [165] A. Nicoletti and J. B. Michel, "Cardiac fibrosis and inflammation: interaction with hemodynamic and hormonal factors," *Cardiovasc Res*, vol. 41, pp. 532–43, Mar 1999.
- [166] F. Kuwahara, H. Kai, K. Tokuda, M. Takeya, A. Takeshita, K. Egashira, and T. Imaizumi, "Hypertensive myocardial fibrosis and diastolic dysfunction: another model of inflammation?," *Hypertension*, vol. 43, pp. 739–45, Apr 2004.

- [167] G. Boerrigter and J. C. Burnett, "Nitric oxide-independent stimulation of soluble guanylate cyclase with BAY 41-2272 in cardiovascular disease," *Cardiovascular Drug Reviews*, vol. 25, no. 1, pp. 30–45, 2007.
- [168] N. Frey and E. N. Olson, "Cardiac hypertrophy: The good, the bad and the ugly," *Annual Review of Physiology*, vol. 65, pp. 45–79, 2003.
- [169] X. Shan, M. P. Quaile, J. K. Monk, B. French, T. P. Cappola, and K. B. Margulies, "Differential expression of PDE5 in failing and nonfailing human myocardium," *Circ Heart Fail*, vol. 5, pp. 79–86, Jan 2012.
- [170] H. P. Rang, *Pharmacology*. New York: Churchill Livingstone, 4th ed. (usa ed.) ed., 2001.
- [171] Y.-P. Xie, B. Chen, P. Sanders, A. Guo, Y. Li, K. Zimmerman, L.-C. Wang, R. M. Weiss, I. M. Grumbach, M. E. Anderson, and L.-S. Song, "Sildenafil prevents and reverses transverse-tubule remodeling and Ca(2+) handling dysfunction in right ventricle failure induced by pulmonary artery hypertension," *Hypertension*, vol. 59, pp. 355–62, Feb 2012.
- [172] S. E. Rose, S. J. Wilson, F. O. Zelaya, S. Crozier, and D. M. Doddrell, "High resolution high field rodent cardiac imaging with flow enhancement suppression," *Magnetic resonance imaging*, vol. 12, no. 8, pp. 1183–90, 1994.
- [173] F. M. Siri, L. A. Jelicks, L. A. Leinwand, and J. M. Gardin, "Gated magnetic resonance imaging of normal and hypertrophied murine hearts," *The American journal of physiology*, vol. 272, no. 5 Pt 2, pp. H2394–402, 1997.
- [174] J. Ruff, F. Wiesmann, K. H. Hiller, S. Voll, M. von Kienlin, W. R. Bauer, E. Rommel, S. Neubauer, and A. Haase, "Magnetic resonance microimaging for noninvasive quantification of myocardial function and mass in the mouse," *Magnetic resonance in medicine : official journal of the Society of Magnetic Resonance in Medicine / Society of Magnetic Resonance in Medicine*, vol. 40, no. 1, pp. 43–8, 1998.
- [175] F. Wiesmann, A. Frydrychowicz, J. Rautenberg, R. Illinger, E. Rommel, A. Haase, and S. Neubauer, "Analysis of right ventricular function in healthy mice and a murine model of heart failure by in vivo MRI," *American Journal of Physiology-Heart and Circulatory Physiology*, vol. 283, no. 3, pp. H1065–H1071, 2002.
- [176] R. A. Quaife, D. Lynch, D. B. Badesch, N. F. Voelkel, B. D. Lowes, A. D. Robertson, and M. R. Bristow, "Right ventricular phenotypic characteristics in subjects with primary pulmonary hypertension or idiopathic dilated cardiomyopathy," *Journal of cardiac failure*, vol. 5, no. 1, pp. 46–54, 1999.
- [177] A. Frydrychowicz, M. Spindler, E. Rommel, G. Ertl, A. Haase, S. Neubauer, and F. Wiesmann, "Functional assessment of isolated right heart failure by high resolution in-vivo cardiovascular magnetic resonance in mice," *Journal of Cardiovascular Magnetic Resonance*, vol. 9, no. 3, pp. 623–627, 2007.

- [178] H. Baer, J. Kreuzer, A. Cojoc, and L. Jahn, "Upregulation of embryonic transcription factors in right ventricular hypertrophy," *Basic Research in Cardiology*, vol. 98, no. 5, pp. 285–294, 2003.
- [179] K. G. Nair, A. F. Cutilletta, R. Zak, T. Koide, and M. Rabinowitz, "Biochemical correlates of cardiac hypertrophy. I. Experimental model; changes in heart weight, RNA content, and nuclear RNA polymerase activity," *Circ Res*, vol. 23, pp. 451–62, Sep 1968.
- [180] M. J. Faber, M. Dalinghaus, I. M. Lankhuizen, K. Bezstarosti, D. H. W. Dekkers, D. J. Duncker, W. A. Helbing, and J. M. J. Lamers, "Proteomic changes in the pressure overloaded right ventricle after 6 weeks in young rats: Correlations with the degree of hypertrophy," in *6th Siena Meeting on From Genome to Proteome*, vol. 5, (WEINHEIM), pp. 2519–2530, Wiley-V C H Verlag Gmbh, 2005. ISI Document Delivery No.: 943OP Times Cited: 23 Cited Reference Count: 48.
- [181] M. U. Braun, P. Szalai, R. H. Strasser, and M. M. Borst, "Right ventricular hypertrophy and apoptosis after pulmonary artery banding: regulation of PKC isozymes," *Cardiovascular Research*, vol. 59, no. 3, pp. 658–667, 2003.
- [182] S. Ikeda, M. Hamada, and K. Hiwada, "Cardiomyocyte apoptosis with enhanced expression of P53 and Bax in right ventricle after pulmonary arterial banding," *Life Sci*, vol. 65, no. 9, pp. 925–33, 1999.

# Appendix B

## Declaration

I declare that I have completed this dissertation single-handedly without the unauthorized help of a second party and only with the assistance acknowledged therein. I have appropriately acknowledged and referenced all text passages that are derived literally from or are based on the content of published or unpublished work of others, and all information that relates to verbal communications. I have abided by the principles of good scientific conduct laid down in the charter of the Justus Liebig University of Giessen in carrying out the investigations described in the dissertation.

# Appendix C

## Acknowledgements

I would like to thank Prof. Dr. Werner Seeger for offering me the opportunity to undertake my dissertation in his department, and his remarkable provision of constructive criticism, ideas, and enthusiasm for my project. Furthermore, I wish to thank my supervisors. Prof. Dr. Ralph Schermuly and Prof. Dr. Siebert, for the competent supervision and productive discussions about this project. Especially I want to thank Prof. Dr. Schermuly for enabling me to visit national and international congresses, which was an impressive experience. Additionally, I would also like to thank Dr. Astrid Wietelmann for giving me the time and opportunity to use the MRI.

It was a true pleasure to work in the Schermuly group, and I want to thank all its members, as well as the members of the Voswinkel and Morty group, for the good time I had there. I want to especially thank Drs. Wiebke Janssen and Kirsten Szelepusa, and Uta Eule, for their invaluable support they gave me in conducting in project - your help was very much appreciated! I also want to thank the members of the animal facility for always having taken good care for my animals, particularly Tanja Enders, for doing great work and having always been extraordinarily reliable. Furthermore, I wish to thank the organisers of the IMPRS and GGL for having allowed me to take part in these great programs, whose full potential has not been exhausted yet. Finally, my thanks go out to one of the most fascinating characters I had the pleasure to meet during my PhD studies: Peter Rauschkolb. Thank your very much for just being yourself, you made my time at the institute so much more pleasing - Dude, you rock!

To all the members of Wat Puttabenjapon, especially Klaus, Josef and Jonathan, as well as Dr. Alfred Weil, I send out my warmest wishes. It is great to know and walk the path with you - you are true kalyana mittas.

Finally, I thank my family for being of constant support to me, without you, all of this would not have been possible. Thank you, mom and dad, for always having been there when I needed you. Thank you, Vicky and Robin, for bringing so much happiness into my life.

**Der Lebenslauf wurde aus der elektronischen  
Version der Arbeit entfernt.**

**The curriculum vitae was removed from the  
electronic version of the paper.**